

OFFICE OF CIVILIAN RADIOACTIVE WASTE MANAGEMENT

1. QA: QA

SPECIAL INSTRUCTION SHEET

Page: 1 of: 1

*Complete Only Applicable Items***This is a placeholder page for records that cannot be scanned or microfilmed**2. Record Date
01/29/2001

3. Accession Number

MOL. 20010220.0060

4. Author Name(s)
SRETEN MASTILOVIC5. Author Organization
N/A6. Title
VERTICAL DROP OF 21-PWR WASTE PACKAGE ON UNYIELDING SURFACE7. Document Number(s)
CAL-UDC-ME-0000128. Version
009. Document Type
REPORT10. Medium
OPTIC/PAPER11. Access Control Code
PUB12. Traceability Designator
DC # 2704313. Comments
THIS IS A ONE-OF-A-KIND DOCUMENT DUE TO THE COLORED GRAPHS ENCLOSED AND CAN BE LOCATED THROUGH THE RPC

OFFICE OF CIVILIAN RADIOACTIVE WASTE MANAGEMENT CALCULATION COVER SHEET

1. QA: QA

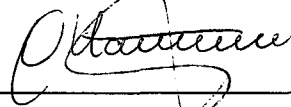
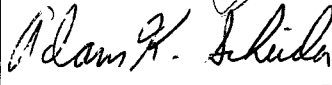
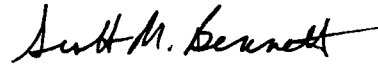
Page: 1 Of: 21

2. Calculation Title
Vertical Drop of 21-PWR Waste Package on Unyielding Surface

3. Document Identifier (including Revision Number)
CAL-UDC-ME-000012 REV 00

4. Total Attachments
3

5. Attachment Numbers - Number of pages in each
I-23, II-7, III (electronic media attachment, see Remarks)

	Print Name	Signature	Date
6. Originator	Sreten Mastilovic		01/25/01
7. Checker	Adam Scheider		JAN 25, 2001
8. Lead	Scott M. Bennett		01/29/01

9. Remarks
Attachment III is an electronic media attachment (compact disc) containing the ANSYS V5.4 and LS-DYNA V950 electronic files. The file names, file dates and times, and file sizes are listed in Section 8 of this document.

Attachment III (compact disc) is moved from REV 00B to REV 00 of this document.

Revision History

10. Revision No.	11. Description of Revision
00	Initial issue

CONTENTS

	Page
1. PURPOSE.....	4
2. METHOD	4
3. ASSUMPTIONS.....	4
4. USE OF COMPUTER SOFTWARE AND MODELS	7
4.1 SOFTWARE.....	7
4.2 SOFTWARE ROUTINES	7
4.3 MODELS	7
5. CALCULATION	8
5.1 MATERIAL PROPERTIES	8
5.1.1 Calculations for True Measures of Ductility.....	10
5.1.2 Calculations for Tangent Moduli	12
5.1.3 Effect of Change of Elongation at $T = 316\text{ }^{\circ}\text{C}$ on Material Properties	13
5.1.4 Decrease of Velocity of Stress Waves due to Increase of Material Density.....	14
5.2 CALCULATION FOR IMPACT VELOCITY	14
5.3 MASS AND GEOMETRIC DIMENSIONS OF 21-PWR FUEL ASSEMBLY.....	15
5.3.1 Calculation for Density of 21-PWR Fuel Assembly.....	15
5.4 FINITE ELEMENT REPRESENTATION	15
6. RESULTS.....	17
7. REFERENCES	19
8. ATTACHMENTS.....	21

TABLES

	Page
1. Tangent moduli at three different temperatures	13
2. Maximum Stress Intensity in OS and IS for Three Different Temperatures	17
3. Stress Intensity in Non-dimensional Form in OS and IS for Three Different Temperatures	17
4. Stress Intensity in Non-dimensional Form for Two Different Approaches Concerning Change of Elongation with Temperature	18
5. Attachment III: File Directories, Names, Dates, Times, and Sizes	21

1. PURPOSE

The objective of this calculation is to determine the structural response of a 21-PWR (pressurized-water reactor) Waste Package (WP) subjected to the 2-m vertical drop on an unyielding surface at three different temperatures. The scope of this calculation is limited to reporting the calculation results in terms of stress intensities in two different WP components. The information provided by the sketches (Attachment I) is that of the potential design of the type of WP considered in this calculation, and all obtained results are valid for that design only. This calculation is associated with the waste package design and is performed by the Waste Package Design Section in accordance with the technical work plan for *Waste Package Design Description for LA* (Ref. 20). AP-3.12Q, *Calculations*, is used to perform the calculation and develop the document (Ref. 3).

2. METHOD

The finite element calculation is performed by using the commercially available ANSYS Version (V) 5.4 (Computer Software Configuration Item [CSCI] 30040 V5.4; see Ref. 2) and LS-DYNA V950 (Software Tracking Number [STN] 10300-950-00; see Ref. 21) finite element codes. ANSYS V5.4 is used for preprocessing, i.e. to create finite element representation (FER) used subsequently in LS-DYNA V950 to obtain solution. The results of this calculation are provided in terms of stress intensities in the outer shell (OS) and inner shell (IS).

With regard to the development of this calculation, the control of electronic management of data is evaluated in accordance with AP-SV.1Q, *Control of the Electronic Management of Information* (Ref. 4). The evaluation (Addendum B of Ref. 20) determined that current work processes and procedures are adequate for the control of electronic management of data for this activity.

3. ASSUMPTIONS

In the course of developing this document, the following assumptions are made regarding the structural calculations.

- 3.1 Some of the temperature-dependent material properties (namely: density, Poisson's ratio, and elongation) are not available for the materials used except at room temperature (RT) (20°C). The materials used include: SB-575 N06022 (Alloy 22), SA-240 S30400 (304 stainless steel [SS]), SA-240 S31600 (316NG [nuclear grade] SS), and SA-516 K02700 (A 516 Grade 70 carbon steel [CS]). The RT density, RT Poisson's ratio, and RT elongation are assumed for all materials. The impact of using RT density, RT Poisson's ratio, and RT elongation is anticipated to be small. The rationale for this assumption is twofold: in the first place the said mechanical properties of the materials used (with exception of the elongation for 316NG SS) do not change significantly at the temperatures experienced in the repository emplacement drift; and secondly, the material properties in question do not have dominant impact on the

calculation results. This assumption is used in Section 5.1.

- 3.2 Some of the rate-dependent material properties are not available for materials used at any strain rate. The material properties obtained under the static loading conditions are assumed for all materials. The impact of using material properties obtained under static loading conditions is anticipated to be small. The rationale for this conservative assumption is that the mechanical properties of subject materials do not significantly change at the peak strain rates that occur during the WP drop. This assumption is used in Section 5.1.
- 3.3 The Poisson's ratio of Alloy 22 is not available in literature. The Poisson's ratio of Alloy 625 (SB-443 N06625) is assumed for Alloy 22. The impact of this assumption is anticipated to be negligible. The rationale for this assumption is that the chemical compositions of Alloy 22 and Alloy 625 are similar (see Ref. 6 [SB-575, Table 1] and Ref. 7, respectively). This assumption is used in Section 5.1.
- 3.4 The uniform strain of Alloy 22 is not available in literature. Therefore, it is conservatively assumed that the uniform strain is 90% of the elongation. The rationale for this assumption is the character of stress-strain curve for Alloy 22 (see Ref. 15). This assumption is used in Section 5.1.1.
- 3.5 The uniform strain of 316NG SS is not available in literature. Therefore, it is conservatively assumed that the uniform strain is 90% of the elongation. The rationale for this assumption is the character of stress-strain curve for 316NG SS (see Refs. 8 and 15). This assumption is used in Section 5.1.1.
- 3.6 The uniform strain of 304 SS is not available in literature. Therefore, it is conservatively assumed that the uniform strain is 75% of the elongation. The rationale for this assumption is the character of stress-strain curve for 304 SS (see Ref. 8). This assumption is used in Section 5.1.1.
- 3.7 The uniform strain of A 516 Grade 70 CS is not available in literature. Therefore, it is conservatively assumed that the uniform strain is 50% of the elongation. The rationale for this assumption is the character of stress-strain curve for A 36 CS (see Refs. 8 and 9) that has similar chemical composition with A 516 Grade 70 CS (see Ref. 6, SA-516/SA-516M and SA-36/SA-36M). This assumption is used in Section 5.1.1.
- 3.8 The friction coefficients for contacts involving Alloy 22 are not available in literature. It is, therefore, assumed that the dynamic (sliding) friction coefficient for all contacts is 0.4. The rationale for this assumption is that this friction coefficient represents the lower bound for most dry contacts involving steel and nickel (see Refs. 10 and 11); nickel being the dominant component in Alloy 22 (Ref. 6, SB-575). This assumption is used in Section 5.4.

- 3.9 The variation of functional friction coefficient between the static and dynamic value as a function of relative velocity of the surfaces in contact is not available in literature for the materials used in this calculation (see Section 5.4). Therefore, the effect of relative velocity of the surfaces in contact is neglected in these calculations by assuming that the functional friction coefficient and static friction coefficient are both equal to the dynamic friction coefficient. The impact of this assumption on results presented in this document is anticipated to be negligible. The rationale for this conservative assumption is that it provides the bounding set of results by minimizing the friction coefficient within the given FEA (finite element analysis) framework. This assumption is used in Section 5.4.
- 3.10 The Poisson's ratio of A 516 Grade 70 CS is not available in literature. The Poisson's ratio of cast CS is assumed for A 516 Grade 70 CS. The impact of this assumption is anticipated to be negligible. The rationale for this assumption is that the elastic constants of CSs are only slightly affected by changes in composition and structure (Ref. 17). This assumption is used in Section 5.1.
- 3.11 This calculation is performed by assuming the following design parameters for 21-PWR fuel assembly: mass = 773.4 kg, width = 216.9 mm, and length = 4407 mm. The rationale for this assumption is that these parameters correspond to the heaviest 21-PWR fuel assembly available in literature (Ref. 18, Table 7-1) and, therefore, provide the bounding set of results. This assumption is used in Section 5.3.
- 3.12 The change of minimum elongation with increase of temperature for the materials used in this calculation is not available in literature. Therefore, the magnitude of this change at $T = 316\text{ }^{\circ}\text{C}$ for Alloy 22 and 316NG SS is assumed to be +10% and -30%, respectively, based on the relative change of typical elongation for said materials available in vendor catalogues (see Refs. 14 and 19; note that 316NG SS has the same material properties as 316 SS [see Ref. 12]). The rationale for this conservative assumption is that the relative change of typical elongation should be bounding for the relative change of minimum elongation. This assumption is applied just to one calculation for the sake of comparison. This assumption is used in Section 5.1.3.

4. USE OF COMPUTER SOFTWARE AND MODELS

4.1 SOFTWARE

One of the FEA computer codes used for this calculation is ANSYS V5.4, which is obtained from Software Configuration Management in accordance with appropriate procedures, and is identified by CSCI 30040 V5.4 (see Ref. 2). ANSYS V5.4 is a commercially available FEA code and is appropriate for structural calculations of WPs as performed in this calculation. The calculations using ANSYS V5.4 software were executed on the Hewlett-Packard (HP) workstation identified with CRWMS M&O (Civilian Radioactive Waste Management System Management and Operating Contractor) tag number 117162. ANSYS evaluation performed for this calculation is fully within the range of the validation performed for ANSYS V5.4 code. Access to the code is granted by the Software Configuration Secretariat in accordance with the appropriate procedures.

The input files (identified by .inp file extensions) and output files (identified by .out file extensions) for ANSYS V5.4 are provided in Attachment III.

The second FEA computer code, used for this calculation, is the Livermore Software Technology Corporation (LSTC) LS-DYNA V950, which is unqualified software (see Ref. 21). The interim use of LS-DYNA V950 (SAN: LV-2000-103, STN: 10300-950-00) in support of the site recommendation is delineated in Section 5.11 of AP-SI.1Q, *Software Management*, (Ref. 5). LS-DYNA V950 is obtained from the Software Configuration Secretariat. LS-DYNA V950 is appropriate for its intended use. LS-DYNA V950 validation will be performed in accordance with AP-SI.1Q, *Software Management*, Section 5.11. The calculations were executed on HP 9000 series workstations identified with CRWMS M&O tag numbers 117161 and 117162.

The input files (identified by .k and .inc file extensions) and output files (d3hsp) for LS-DYNA V950 are provided in Attachment III.

4.2 SOFTWARE ROUTINES

None used.

4.3 MODELS

None used.

5. CALCULATION

5.1 MATERIAL PROPERTIES

Material properties used in these calculations are listed in this section. Some of the temperature-dependent and rate-dependent material properties are not available for Alloy 22, 304 SS, 316NG SS, 316L SS, and A 516 Grade 70 CS. Therefore, RT density, RT Poisson's ratio, and RT elongation are used for all materials (see Assumption 3.1). Moreover, all rate-dependent material properties used in this calculation are obtained under the static loading conditions (see Assumption 3.2).

SB-575 N06022 (Alloy 22) (OS, OS lids, upper and lower trunnion collar sleeves):

- Density = 8690 kg/m^3 (0.314 lb/in^3) (at RT) (Ref. 6, SB-575, Section 7.1)
- Yield strength = 310 MPa (45.0 ksi) (at RT) (Ref. 6, Table Y-1)
Yield strength = 236 MPa (34.3 ksi) (at $400 \text{ }^\circ\text{F} = 204 \text{ }^\circ\text{C}$) (Ref. 6, Table Y-1)
Yield strength = 211 MPa (30.6 ksi) (at $600 \text{ }^\circ\text{F} = 316 \text{ }^\circ\text{C}$) (Ref. 6, Table Y-1)
- Tensile strength = 689 MPa (100 ksi) (at RT) (Ref. 6, Table U)
Tensile strength = 657 MPa (95.3 ksi) (at $400 \text{ }^\circ\text{F} = 204 \text{ }^\circ\text{C}$) (Ref. 6, Table U)
Tensile strength = 628 MPa (91.1 ksi) (at $600 \text{ }^\circ\text{F} = 316 \text{ }^\circ\text{C}$) (Ref. 6, Table U)
- Elongation = 0.45 (at RT) (Ref. 6, SB-575, Table 3)
- Poisson's ratio = 0.278 (at RT) (Ref. 7, p. 143; see Assumption 3.3)
- Modulus of elasticity = 206 GPa (at RT) (Ref. 14, p. 14)
Modulus of elasticity = 196 GPa (at $400 \text{ }^\circ\text{F} = 204 \text{ }^\circ\text{C}$) (Ref. 14, p. 14)
Modulus of elasticity = 190 GPa (at $600 \text{ }^\circ\text{F} = 316 \text{ }^\circ\text{C}$) (Ref. 14, p. 14)

SA-240 S31600 (316NG SS, which is 316 SS with tightened control on carbon and nitrogen content and has the same material properties as 316 SS [see Ref. 12]) (IS, IS lids, IS lid lifting feature, and shell interface ring):

- Density = 7980 kg/m^3 (at RT) (Ref. 13, Table X1, p. 7)
- Yield strength = 207 MPa (30.0 ksi) (at RT) (Ref. 6, Table Y-1)
Yield strength = 148 MPa (21.4 ksi) (at $400 \text{ }^\circ\text{F} = 204 \text{ }^\circ\text{C}$) (Ref. 6, Table Y-1)
Yield strength = 130 MPa (18.9 ksi) (at $600 \text{ }^\circ\text{F} = 316 \text{ }^\circ\text{C}$) (Ref. 6, Table Y-1)

- Tensile strength = 517 MPa (75.0 ksi) (at RT) (Ref. 6, Table U)
Tensile strength = 496 MPa (71.9 ksi) (at 400 °F = 204 °C) (Ref. 6, Table U)
Tensile strength = 495 MPa (71.8 ksi) (at 600 °F = 316 °C) (Ref. 6, Table U)
- Elongation = 0.40 (at RT) (Ref. 6, SA-240, Table 2)
- Poisson's ratio = 0.298 (at RT) (Ref. 7, Figure 15, p. 755)
- Modulus of elasticity = 195 GPa (28.3 · 10⁶ psi) (at RT) (Ref. 6, Table TM-1)
Modulus of elasticity = 183 GPa (26.5 · 10⁶ psi) (at 400 °F = 204 °C) (Ref. 6, Table TM-1)
Modulus of elasticity = 174 GPa (25.3 · 10⁶ psi) (at 600 °F = 316 °C) (Ref. 6, Table TM-1)

SA-240 S30400 (304 SS) (21-PWR Fuel):

- Yield strength = 207 MPa (30.0 ksi) (at RT) (Ref. 6, Table Y-1)
Yield strength = 143 MPa (20.7 ksi) (at 400 °F = 204 °C) (Ref. 6, Table Y-1)
Yield strength = 127 MPa (18.4 ksi) (at 600 °F = 316 °C) (Ref. 6, Table Y-1)
- Tensile strength = 517 MPa (75.0 ksi) (at RT) (Ref. 6, Table U)
Tensile strength = 441 MPa (64.0 ksi) (at 400 °F = 204 °C) (Ref. 6, Table U)
Tensile strength = 437 MPa (63.4 ksi) (at 600 °F = 316 °C) (Ref. 6, Table U)
- Elongation = 0.40 (at RT) (Ref. 6, SA-240, Table 2)
- Poisson's ratio = 0.290 (at RT) (Ref. 7, Figure 15, p. 755)
- Modulus of elasticity = 195 GPa (28.3 · 10⁶ psi) (at RT) (Ref. 6, Table TM-1)
Modulus of elasticity = 183 GPa (26.5 · 10⁶ psi) (at 400 °F = 204 °C) (Ref. 6, Table TM-1)
Modulus of elasticity = 174 GPa (25.3 · 10⁶ psi) (at 600 °F = 316 °C) (Ref. 6, Table TM-1)

SA-516 K02700 (A 516 Grade 70 CS) (Basket Plates):

- Density = 7850 kg/m³ (0.314 lb/in³) (Ref. 6, SA-20/SA-20M, Section 14.1) (Material supplied to ASTM [American Society for Testing and Materials] A 516/A 516M-90)

specification shall conform to specification ASTM A 20/A 20M-99 [Ref. 6, SA-516/SA-516M, Section 3.1]).

- Yield strength = 262 MPa (38.0 ksi) (at RT) (Ref. 6, Table Y-1)
Yield strength = 224 MPa (32.5 ksi) (at 400 °F = 204 °C) (Ref. 6, Table Y-1)
Yield strength = 201 MPa (29.1 ksi) (at 600 °F = 316 °C) (Ref. 6, Table Y-1)
- Tensile strength = 483 MPa (70.0 ksi) (at RT) (Ref. 6, Table U)
Tensile strength = 483 MPa (70.0 ksi) (at 400 °F = 204 °C) (Ref. 6, Table U)
Tensile strength = 483 MPa (70.0 ksi) (at 600 °F = 316 °C) (Ref. 6, Table U)
- Elongation = 0.21 (at RT) (Ref. 6, SA-516/SA-516M, Table 2)
- Poisson's ratio = 0.300 (at RT) (Ref. 17, p. 374) (see Assumption 3.10)
- Modulus of elasticity = 203 GPa (29.5 · 10⁶ psi) (at RT) (Ref. 6, Table TM-1)
Modulus of elasticity = 191 GPa (27.7 · 10⁶ psi) (at 400 °F = 204 °C) (Ref. 6, Table TM-1)
Modulus of elasticity = 184 GPa (26.7 · 10⁶ psi) (at 600 °F = 316 °C) (Ref. 6, Table TM-1)

5.1.1 Calculations for True Measures of Ductility

The material properties in Section 5.1 refer to engineering stress and strain definitions: $s = P/A_0$ and $e = L/L_0 - 1$ (see Ref. 1). Where P stands for the force applied during a static tensile test, L is the length of the deformed specimen, and L_0 and A_0 are the original length and cross-sectional area of the specimen, respectively. The engineering stress-strain curve does not give a true indication of the deformation characteristics of a material during plastic deformation since it is based entirely on the original dimensions of the specimen. In addition, ductile metal that is pulled in tension becomes unstable and necks down during the course of the test. Hence, LS-DYNA V950 FEA code requires input in terms of true stress and strain definitions: $\sigma = P/A$ and $\epsilon = \ln(L/L_0)$ (see Ref. 1).

The relationships between the true stress and strain definitions and the engineering stress and strain definitions, $\sigma = s \cdot (1 + e)$ and $\epsilon = \ln(1 + e)$, can be readily derived based on constancy of volume ($A_0 \cdot L_0 = A \cdot L$) and strain homogeneity during plastic deformation (see Ref. 1). These expressions are applicable only in the hardening region of the stress-strain curve that is limited by the onset of necking.

The following parameters are used in the subsequent calculations:

$$s_y \approx \sigma_y = \text{yield strength}$$

$$s_u = \text{engineering tensile strength}$$

$$\sigma_u = \text{true tensile strength}$$

$$e_y \approx \varepsilon_y = \text{strain corresponding to yield strength}$$

$$e_u = \text{engineering uniform strain (engineering strain corresponding to tensile strength)}$$

$$\varepsilon_u = \text{true uniform strain (true strain corresponding to tensile strength)}$$

In absence of data on the uniform strain in available literature, it needs to be estimated based on the character of stress-strain curves and elongation (strain corresponding to rupture of the tensile specimen).

The stress-strain curves for Alloy 22 and 316NG SS do not manifest three-stage deformation character (see Refs. 8 and 15). Therefore, the elongation reduced by 10%, to take into account the specimen-failure part of the stress-strain curve (see Assumptions 3.4 and 3.5), can be used in place of uniform strain for these two materials.

In the case of Alloy 22 ($e_u = 0.9 \cdot \text{elongation} = 0.41$) the true uniform strain is

$$\varepsilon_u = \ln(1 + e_u) = \ln(1 + 0.41) = 0.34$$

The true tensile strength depends on temperature, thus:

$$\sigma_u = s_u \cdot (1 + e_u) = 689 \cdot (1 + 0.41) = 971 \text{ MPa (at RT)}$$

$$\sigma_u = s_u \cdot (1 + e_u) = 657 \cdot (1 + 0.41) = 926 \text{ MPa (at } 400 \text{ }^\circ\text{F} = 204 \text{ }^\circ\text{C)}$$

$$\sigma_u = s_u \cdot (1 + e_u) = 628 \cdot (1 + 0.41) = 885 \text{ MPa (at } 600 \text{ }^\circ\text{F} = 316 \text{ }^\circ\text{C)}$$

For 316NG SS, $e_u = 0.9 \cdot \text{elongation} = 0.36$, therefore the true uniform strain is:

$$\varepsilon_u = \ln(1 + e_u) = \ln(1 + 0.36) = 0.31$$

The true tensile strength on three different temperatures is:

$$\sigma_u = s_u \cdot (1 + e_u) = 517 \cdot (1 + 0.36) = 703 \text{ MPa (at RT)}$$

$$\sigma_u = s_u \cdot (1 + e_u) = 496 \cdot (1 + 0.36) = 675 \text{ MPa (at } 400 \text{ }^\circ\text{F} = 204 \text{ }^\circ\text{C)}$$

$$\sigma_u = s_u \cdot (1 + e_u) = 495 \cdot (1 + 0.36) = 673 \text{ MPa (at } 600 \text{ }^\circ\text{F} = 316 \text{ }^\circ\text{C)}$$

Contrary to the two previous cases, the stress-strain curves for 304 SS exhibits pronounced three-stage (elastic-hardening-softening) deformation character. The uniform strain is, therefore, estimated to be 75% of elongation based on the available stress-strain curves (see Assumption 3.6). Hence,

$e_u = 0.75 \cdot \text{elongation} = 0.75 \cdot 0.40 = 0.30$. The true uniform strain is therefore

$$\varepsilon_u = \ln(1 + e_u) = \ln(1 + 0.30) = 0.26$$

The true tensile strength is

$$\sigma_u = s_u \cdot (1 + e_u) = 517 \cdot (1 + 0.30) = 672 \text{ MPa (at RT)}$$

$$\sigma_u = s_u \cdot (1 + e_u) = 441 \cdot (1 + 0.30) = 573 \text{ MPa (at } 400 \text{ }^\circ\text{F} = 204 \text{ }^\circ\text{C)}$$

$$\sigma_u = s_u \cdot (1 + e_u) = 437 \cdot (1 + 0.30) = 568 \text{ MPa (at } 600 \text{ }^\circ\text{F} = 316 \text{ }^\circ\text{C)}$$

Finally, the stress-strain curves for A 516 Grade 70 CS exhibits stress-strain curve character typical for CS. The uniform strain is estimated to be 50% of elongation based on the available stress-strain curves for A 36 CS (see Assumption 3.7); hence, $e_u = 0.50 \cdot \text{elongation} = 0.50 \cdot 0.21 = 0.11$. The true uniform strain is therefore

$$\varepsilon_u = \ln(1 + e_u) = \ln(1 + 0.11) = 0.10$$

Since the engineering tensile strength does vary with temperature for the temperature range of interest, the true tensile strength is

$$\sigma_u = s_u \cdot (1 + e_u) = 483 \cdot (1 + 0.105) = 534 \text{ MPa (at RT, } 400 \text{ }^\circ\text{F} = 204 \text{ }^\circ\text{C, and } 600 \text{ }^\circ\text{F} = 316 \text{ }^\circ\text{C)}$$

5.1.2 Calculations for Tangent Moduli

As previously discussed the results of this simulation are required to include elastic and plastic deformations for Alloy 22, 304 SS, 316NG SS, and A 516 Grade 70 CS. When these materials are driven into the plastic range, the slope of stress-strain curve continuously changes. A ductile failure is preceded by a protracted regime of hardening (and possibly softening) and substantial accumulation of inelastic strains. Thus, a simplification for stress-strain curve is needed to incorporate plasticity into FEA. A standard approximation commonly used in engineering is to use a straight line that connects the yield point and the tensile-strength point of the material. The parameters used in the subsequent calculations in addition to those defined in Section 5.1.1 are modulus of elasticity (E) and tangent (hardening) modulus (E_t).

The tangent modulus represents the slope of the stress-strain curve in the hardening region, and it can be, therefore, readily calculated by using the following expression:

$$E_1 = (\sigma_u - \sigma_y) / (\epsilon_u - \epsilon_y) = (\sigma_u - \sigma_y) / (\epsilon_u - \sigma_y / E)$$

The tangent moduli that are calculated by using the preceding expression and material properties given in Sections 5.1 and 5.1.1 are presented in Table 1.

Table 1. Tangent moduli at three different temperatures

	Tangent Modulus (GPa)		
	$T = RT$	$T = 204 \text{ }^\circ C$	$T = 316 \text{ }^\circ C$
Alloy 22	1.95	2.04	1.99
316NG SS	1.61	1.70	1.76
304 SS	1.80	1.66	1.70
A 516 CS	2.76	3.14	3.37

5.1.3 Effect of Change of Elongation at $T = 316 \text{ }^\circ C$ on Material Properties

The change of minimum elongation with increase of temperature for the materials used in this calculation is not available in literature. Therefore, for Alloy 22 and 316NG SS the magnitude of this change at $T = 316 \text{ }^\circ C$ is estimated based on the relative change of typical elongation for said materials (see Assumption 3.12). In the case of Alloy 22 indicated increase of typical elongation corresponding to increase of temperature from RT to $T = 316 \text{ }^\circ C$ is 10%. On the other hand, suggested elongation decrease for 316NG SS within the same temperature range is 30% (Assumption 3.12). Consequently, the true measures of ductility and tangent moduli, calculated in Sections 5.1.1 and 5.1.2, have to change to accommodate the variability of elongation due to change of temperature.

In the case of Alloy 22, $e_u = 1.1 \cdot (0.9 \cdot \text{elongation}) = 0.45$, the true uniform strain is

$$\epsilon_u = \ln(1 + e_u) = \ln(1 + 0.45) = 0.37$$

while the true tensile strength is

$$\sigma_u = s_u \cdot (1 + e_u) = 628 \cdot (1 + 0.45) = 911 \text{ MPa}$$

Consequently, the tangent modulus becomes

$$E_1 = (\sigma_u - \sigma_y) / (\epsilon_u - \sigma_y / E) = (911 - 211) / (0.37 - 211 / 190 \cdot 10^3) = 1.90 \text{ GPa}$$

For 316NG SS, $e_u = 0.7 \cdot (0.9 \cdot \text{elongation}) = 0.25$, the true uniform strain is

$$\epsilon_u = \ln(1 + e_u) = \ln(1 + 0.25) = 0.22$$

while the true tensile strength is

$$\sigma_u = s_u \cdot (1 + e_u) = 495 \cdot (1 + 0.25) = 619 \text{ MPa}$$

Finally, the tangent modulus is

$$E_t = (\sigma_u - \sigma_y) / (\epsilon_u - \sigma_y / E) = (619 - 130) / (0.22 - 130 / 174 \cdot 10^3) = 2.23 \text{ GPa}$$

The effects of the change of elongation due to the increase of temperature are taken into account only in one calculation for the sake of comparison with results of the same calculation performed with RT elongation.

5.1.4 Decrease of Velocity of Stress Waves due to Increase of Material Density

The velocity of stress wave propagation is inversely proportional to the square root of the mass density of the material through which the wave propagates (Ref. 16). Hence, an increase of density of material results in a decrease of the velocity of stress wave propagation and consequently in an increase of stress in the contact regions. Thus, caution must be exercised if the modification of density is necessary in dynamic analysis.

In order to meet calculation requirements while reducing the computer-execution time, the density of basket assembly (A 516 Grade 70 CS) is modified during the development of finite element representation (see Section 5.4 for details). Specifically, the density is increased from 7850 kg/m^3 (Section 5.1) to 10700 kg/m^3 (Attachment III, files: main.k, line #85; three significant digits used) resulting in the decrease of the velocity of stress wave propagation in the basket assembly of $\Delta = 1 - \sqrt{7850/10700} = 0.14 = 14\%$.

5.2 CALCULATION FOR IMPACT VELOCITY

To reduce the computer execution time, while preserving all features of the problem relevant to the structural calculation, WP is set in a position just before impact and given an appropriate initial velocity. The initial velocity is defined by drop height, $H = 2 \text{ m}$, and the acceleration due to gravity, $g = 9.81 \text{ m/s}^2$. The two-significant-digits value is, therefore:

$$V = \sqrt{2 \cdot g \cdot H} = \sqrt{2 \cdot 9.81 \cdot 2} = 6.3 \text{ m/s}$$

5.3 MASS AND GEOMETRIC DIMENSIONS OF 21-PWR FUEL ASSEMBLY

This calculation is performed by using the mass and geometric dimensions of the heaviest 21-PWR fuel assembly (see Assumption 3.11):

$$\text{Mass} = 773.4 \text{ kg}$$

$$\text{Diameter} = 0.2169 \text{ m}$$

$$\text{Length} = 4.407 \text{ m}$$

5.3.1 Calculation for Density of 21-PWR Fuel Assembly

The internal structure of WP is simplified in FER by reducing the structure of the 21-PWR fuel assemblies to solid cylinders of square cross section and uniform density. This uniform density is calculated as a ratio of its mass and volume.

$$\text{Volume} = 4.407 \cdot 0.2169^2 = 0.2073 \text{ m}^3$$

$$\text{Density} = 773.4/0.2073 = 3730 \text{ kg/m}^3$$

5.4 FINITE ELEMENT REPRESENTATION

Three-dimensional FER is developed using the dimensions provided in Attachment I and Section 5.1. FER includes all WP components relevant to the structural calculation. The internal structure of the 21-PWR WP, characterized by a plethora of details (basket side guides, stiffeners, corner guides, plates, and tubes; see Attachment I for a detailed description), is complex enough to render FER development a very delicate problem, having in mind available computational capabilities. The aluminum thermal shunts and neutronit basket plates (see Attachment I) are not used as structural members due to the calculation requirement that no structural credit should be given to these basket components. Since only the CS plates are taken into account, the thickness of the basket assembly is reduced. The mass of the removed components is added to that of the remaining basket components made of A 516 Grade 70 CS, by modifying its density. This modification does not affect the calculation results significantly since this increase of density does not result in notable change of velocity of stress wave propagation in the basket structure (see Section 5.1.4). Moreover, the decrease of the velocity of stress wave propagation provides a bounding set of results.

In order to reduce the computer execution time, the finite element calculation is started on the verge of impact between WP and the unyielding surface. The drop height is taken into account by applying the initial velocity (see Section 5.2) to all WP nodes.

Contact elements are used to represent contact between WP (specifically the lower trunnion collar sleeve) and the unyielding surface, and between various WP components. In absence of more appropriate data on friction coefficients for contacts involving Alloy 22, the dynamic friction

coefficient is assumed for all contacts to be 0.4. This friction coefficient represents the lower bound for most dry contacts involving steel and nickel (nickel being the dominant component in Alloy 22) (Assumption 3.8). Moreover, the functional friction coefficient used by LS-DYNA V950 FEA code is defined in terms of static and dynamic friction coefficients, and relative velocity of the surfaces in contact. The effect of the relative velocity of the surfaces in contact is introduced by the way of a fitting parameter - exponential decay coefficient. The variation of friction coefficient between the static and dynamic value as a function of relative velocity of the surfaces in contact is not available in literature for the materials used in this calculation. Therefore, it is not possible to objectively evaluate exponential decay coefficient. Hence, the effect of relative velocity of the surfaces in contact is neglected in these calculations by assuming that the functional friction coefficient and the static friction coefficient are equal to the dynamic friction coefficient. This approach provides the bounding set of results by minimizing the friction coefficient within the given FEA framework (Assumption 3.9).

The non-reflecting boundary is used in FER to avoid artificial stress wave reflections from the boundary of unyielding surface. Consequently, the unyielding surface truly represents a half-space since the contamination of results due to stress wave reflection is prevented.

The mesh of the FER is appropriately generated, and refined in the contact region according to standard engineering practice. Thus, the accuracy and representativeness of the results of this linear calculation are deemed acceptable.

6. RESULTS

This document may be affected by technical product input information that requires confirmation. Any changes to the document that may occur as a result of completing the confirmation activities will be reflected in subsequent revisions. The status of the input information quality may be confirmed by review of the Document Input Reference System database.

The stress-field plots obtained from LS-DYNA V950 (Figs. II-4 and II-6) are reported in terms of maximum shear stress. Since the maximum stress intensities are desired, and the stress intensity time histories are presented throughout the document, the stress field results need to be translated appropriately. The maximum shear stress is defined as one-half the difference between maximum and minimum principal stress. Stress intensity is defined as the difference between maximum and minimum principal stress. Therefore, the results presented in Figures II-4 and II-6 need to be multiplied by two, to obtain the corresponding stress intensities.

The maximum stresses are found by careful examination of each time step recorded by LS-DYNA V950, which outputs the element with the highest magnitude of certain stress component, at each recorded step, for each defined part. The results presented in Table 2 are recorded at OS and IS (including appropriate lids) at the three different temperatures.

Table 2. Maximum Stress Intensity in OS and IS for Three Different Temperatures

Temperature (°C)	Maximum Stress Intensity (MPa)	
	OS	IS
20	404 (Figs. II-4 and II-5)	351 (Figs. II-6 and II-7)
204	319 (Fig. II-8)	331 (Fig. II-9)
316	287 (Fig. II-10)	320 (Fig. II-11)

The same results are presented in Table 3 in non-dimensional form. The $SINT/\sigma_u$ and $SINT/\sigma_y$ represent ratios of the stress intensity and the tensile and yield strengths, respectively, at the temperatures of interest in this calculation.

Table 3. Stress Intensity in Non-dimensional Form in OS and IS for Three Different Temperatures

Temperature (°C)	OS		IS	
	$SINT/\sigma_u$	$SINT/\sigma_y$	$SINT/\sigma_u$	$SINT/\sigma_y$
20	0.416	1.30	0.499	1.70
204	0.344	1.35	0.490	2.24
316	0.324	1.36	0.475	2.46

The change of minimum elongation with increase of temperature for Alloy 22 and 316NG SS at $T = 316\text{ }^{\circ}\text{C}$ is, in absence of data in literature, estimated based on the relative change of typical elongation for said materials (Section 5.1.3). This change in input data reflects on the calculation results. Thus, in the case when the temperature-induced variation of the minimum elongation is taken into account, the maximum stress intensities in OS and IS are 286 MPa (Fig. II-12) and 342 MPa (Fig. II-13), respectively. The same results are presented in Table 4 in non-dimensional form (row "Elongation Changing") for comparison with the results obtained previously by assuming that the change of elongation due to temperature for Alloy 22 and 316NG SS is negligible (row "Elongation Constant").

Table 4. Stress Intensity in Non-dimensional Form for Two Different Approaches Concerning Change of Elongation with Temperature

Elongation	OS		IS	
	$SINT/\sigma_u$	$SINT/\sigma_y$	$SINT/\sigma_u$	$SINT/\sigma_y$
Constant	0.324	1.36	0.475	2.46
Changing	0.314	1.36	0.553	2.63

7. REFERENCES

1. Dieter, G.E. 1976. *Mechanical Metallurgy*. 2nd Edition. Materials Science and Engineering Series. New York, New York: McGraw-Hill Book Company. TIC: 247879.
2. CRWMS M&O 1998. *ANSYS*. V5.4. HP-UX 10.20. 30040 5.4.
3. AP-3.12Q, Rev. 0, ICN 3. *Calculations*. Washington, D.C.: U.S. Department of Energy, Office of Civilian Radioactive Waste Management. ACC: MOL.20001026.0084.
4. AP-SV.1Q, Rev. 0, ICN 2. *Control of the Electronic Management of Information*. Washington, D.C.: U.S. Department of Energy, Office of Civilian Radioactive Waste Management. ACC: MOL. 20000831.0065.
5. AP-SI.1Q, Rev. 2, ICN 4. *Software Management*. Washington, D.C.: U.S. Department of Energy, Office of Civilian Radioactive Waste Management. ACC: MOL.20000223.0508.
6. ASME (American Society of Mechanical Engineers) 1998. *1998 ASME Boiler and Pressure Vessel Code*. New York, New York: American Society of Mechanical Engineers. TIC: 247429.
7. American Society for Metals 1980. *Properties and Selection: Stainless Steels, Tool Materials and Special-Purpose Metals*. Volume 3 of *Metals Handbook*. 9th Edition. Metals Park, Ohio: American Society for Metals. TIC: 209801.
8. Boyer, H.E., ed. 2000. *Atlas of Stress-Strain Curves*. Metals Park, Ohio: ASM International. TIC: 248901.
9. Bowles, J.E. 1980. *Structural Steel Design*. New York, New York: McGraw-Hill. TIC: 249182.
10. Meriam, J.L. and Kraige, L.G. 1987. *Statics*. Volume 1 of *Engineering Mechanics*. 2nd Edition. Pages 441, 443. New York, New York: John Wiley & Sons. TIC: 241293.
11. Avallone, E.A. and Baumeister, T., III, eds. 1987. *Marks' Standard Handbook for Mechanical Engineers*. 9th Edition. New York, New York: McGraw-Hill. TIC: 206891.
12. Pasupathi, V. 1999. "Waste Package Structural Material." Interoffice correspondence from V. Pasupathi (CRWMS M&O) to T.W. Doering, May 7, 1999, LV.WP.VP.05/99-073. ACC: MOL.19990518.0316.

13. ASTM G 1-90 (Reapproved 1999). 1990. *Standard Practice for Preparing, Cleaning, and Evaluating Corrosion Test Specimens*. West Conshohocken, Pennsylvania: American Society for Testing and Materials. TIC: 238771.
14. Haynes International 1997. *Hastelloy C-22 Alloy*. Kokomo, Indiana: Haynes International. TIC: 238121.
15. CRWMS M&O 2000. *Stress-Strain-Curve Character for Alloy 22 and 316 Stainless Steel*. Input Transmittal 00384.T. Las Vegas, Nevada: CRWMS M&O. ACC: MOL.20001013.0053.
16. Meyers, M.A. 1994. *Dynamic Behavior of Materials*. New York, New York: John Wiley & Sons. TIC: 243715.
17. ASM International 1990. *Properties and Selection: Irons, Steels, and High-Performance Alloys*. Volume 1 of *Metals Handbook*. 10th Edition. Materials Park, Ohio: ASM International. TIC: 245666.
18. CRWMS M&O 1997. *Waste Container Cavity Size Determination*. BBAA00000-01717-0200-00026 REV 00. Las Vegas, Nevada: CRWMS M&O. ACC: MOL.19980106.0061.
19. Allegheny Ludlum 1999. "Technical Data Blue Sheet, Stainless Steels, Chromium-Nickel-Molybdenum, Types 316 (S31600), 316L (S31603), 317 (S31700), 317L (S31703)." Pittsburgh, Pennsylvania: Allegheny Ludlum Corporation. Accessed July 31, 2000. TIC: 248631. http://www.alleghenytechnologies.com/ludlum/pages/products/t316_317.pdf
20. CRWMS M&O 2000. *Technical Work Plan for: Waste Package Design Description for LA*. TWP-EBS-MD-000004 REV 00. Las Vegas, Nevada: CRWMS M&O. ACC: MOL.20001107.0304.
21. CRWMS M&O 2000. *Software Code: LSTC LS-DYNA*. V950. HP 9000. 10300-950-00. URN-0368

8. ATTACHMENTS

Attachment I (23 pages): Design sketches (*21-PWR Waste Package Concept for Licence Application* [SK-0219 REV 00], 23 sheets [this attachment uses References 18])

Attachment II (7 pages): Figures obtained from LS-DYNA V950

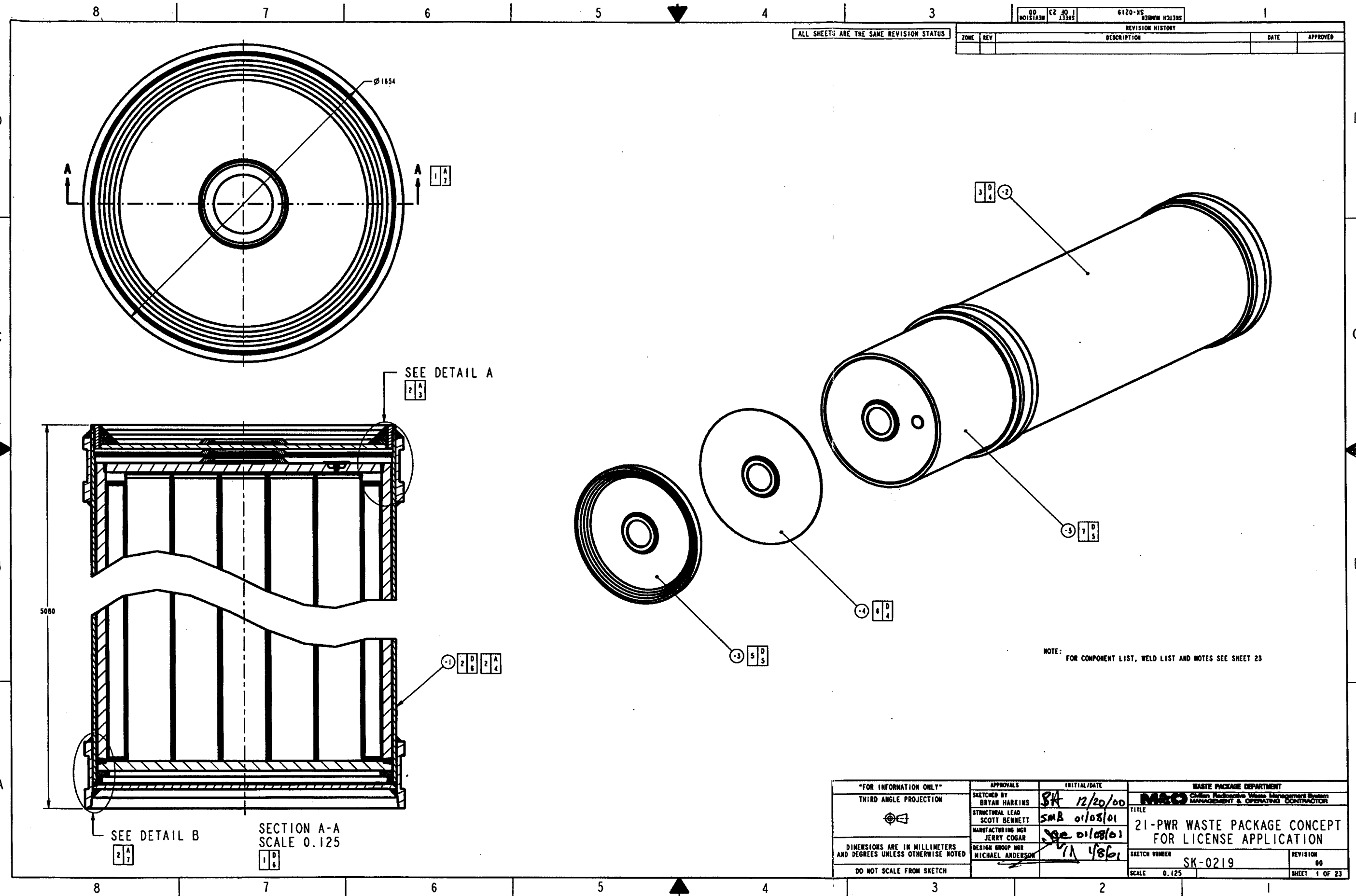
Attachment III (Compact Disc): ANSYS V5.4 and LS-DYNA V950 electronic files

Table 5. Attachment III: File Directories, Names, Dates, Times, and Sizes

Directory	Name	Date	Time	Size
Model	nodes.inc	01/11/01	9:51 AM	6,202 KB
	element.inc	01/11/01	9:51 AM	5,824 KB
	nodeset1.inc	01/11/01	9:51 AM	9 KB
	nodeset2.inc	01/11/01	9:51 AM	3 KB
	nodeset3.inc	01/11/01	9:51 AM	4 KB
	nodeset4.inc	01/11/01	9:51 AM	3 KB
	segment.inc	01/11/01	9:51 AM	45 KB
	pwr9.inp	01/11/01	9:51 AM	39 KB
	pwr9.out	01/11/01	9:51 AM	509 KB
T=20C	d3hsp	01/23/01	9:19 AM	26,410 KB
	main.k	01/23/01	9:19 AM	7 KB
T=204C	d3hsp	01/23/01	9:20 AM	26,394 KB
	main.k	01/23/01	9:20 AM	7 KB
T=316C/original	d3hsp	01/23/01	9:22 AM	26,383 KB
	main.k	01/23/01	9:22 AM	7 KB
T=316C/bounding	d3hsp	01/23/01	9:21 AM	26,383 KB
	main.k	01/23/01	9:21 AM	7 KB

NOTE: The file sizes may vary with operating system.

ALL SHEETS ARE THE SAME REVISION STATUS		REVISION HISTORY		DATE	APPROVED
ZONE	REV	DESCRIPTION			

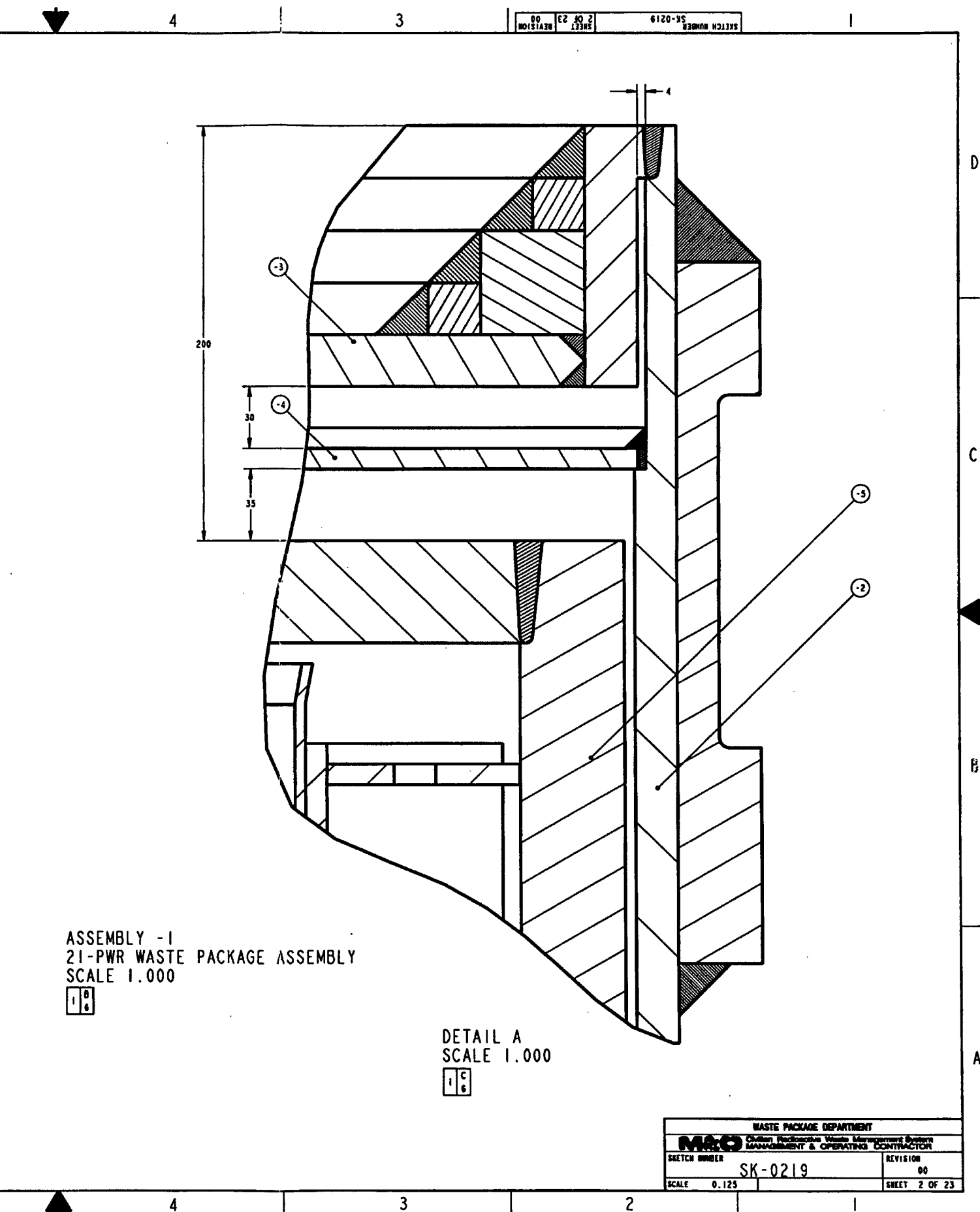
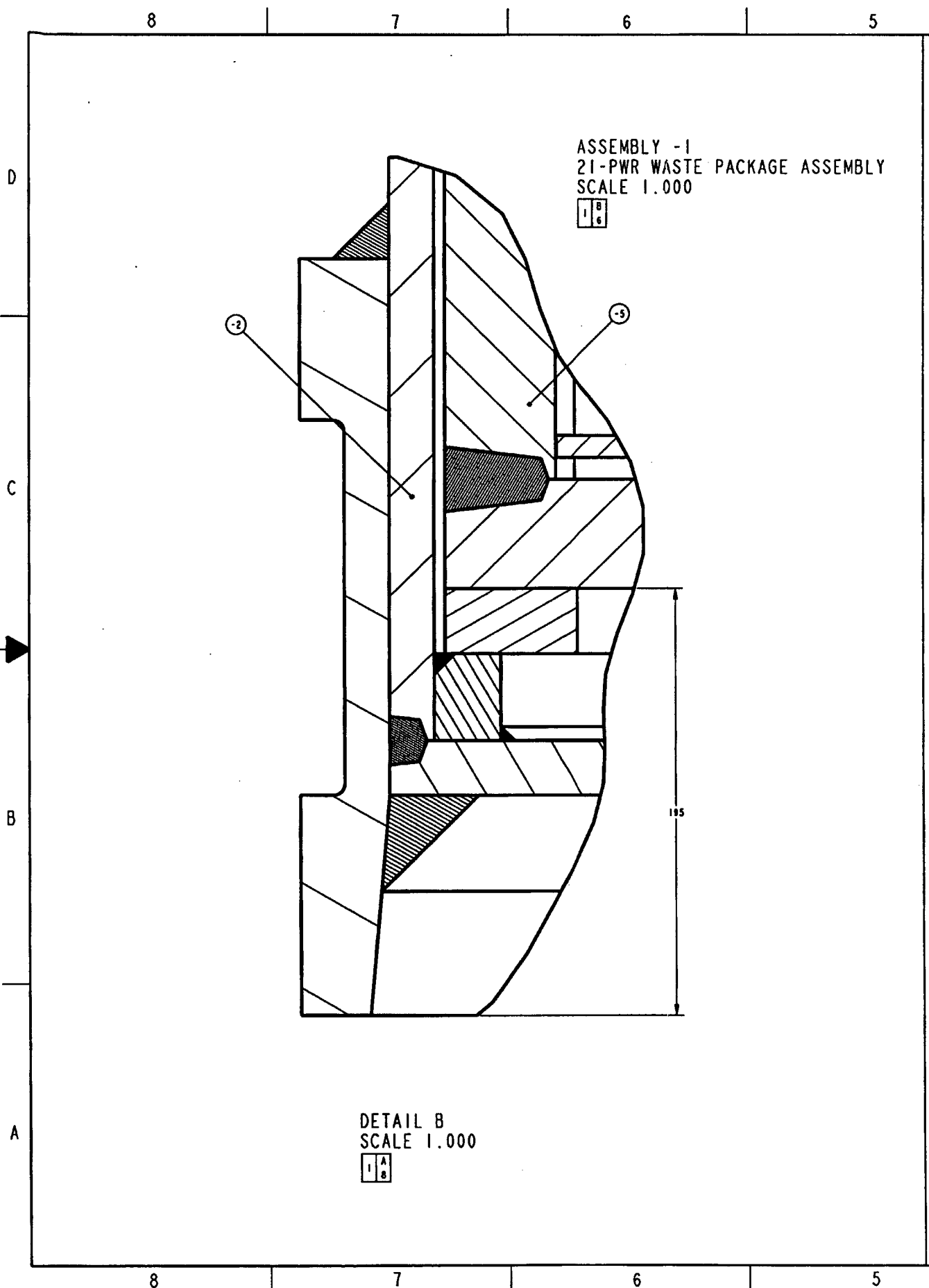


NOTE: FOR COMPONENT LIST, WELD LIST AND NOTES SEE SHEET 23

SEE DETAIL B

SECTION A-A
SCALE 0.125

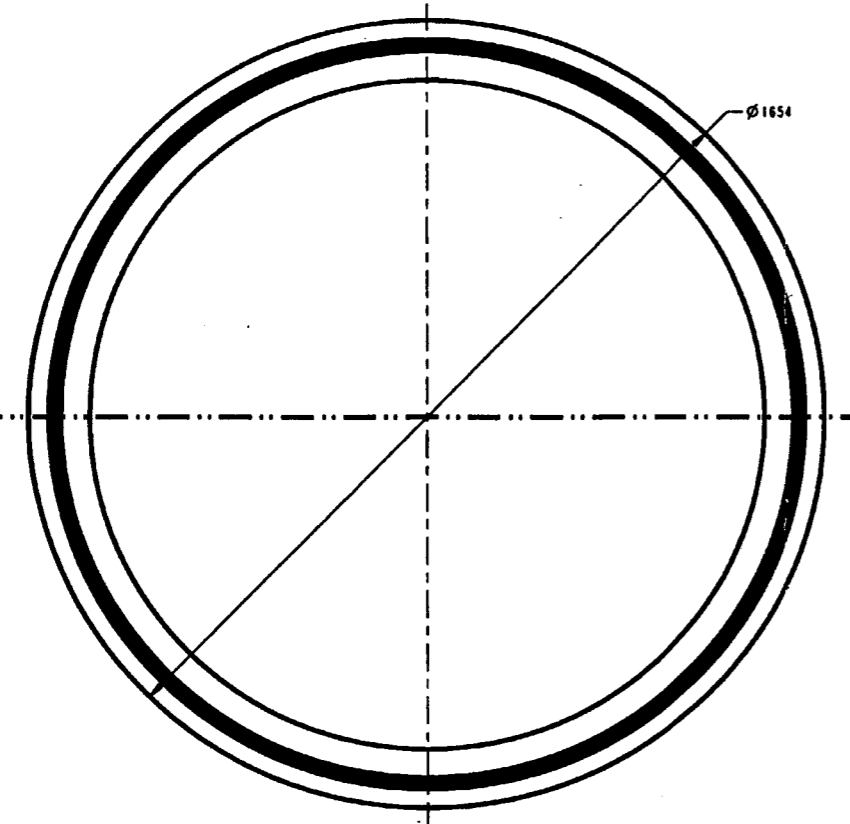
"FOR INFORMATION ONLY" THIRD ANGLE PROJECTION 	APPROVALS	INITIAL/DATE	WASTE PACKAGE DEPARTMENT
	SKETCHED BY BRYAN HARKINS	SK 12/20/00	M&O California Radioactive Waste Management System MANAGEMENT & OPERATING CONTRACTOR
	STRUCTURAL LEAD SCOTT BENNETT	SMB 01/08/01	TITLE
	MANUFACTURING MGR JERRY COGAR	JEC 01/08/01	21-PWR WASTE PACKAGE CONCEPT FOR LICENSE APPLICATION
DIMENSIONS ARE IN MILLIMETERS AND DEGREES UNLESS OTHERWISE NOTED	DESIGN GROUP MGR MICHAEL ANDERSON	MA 4/8/01	SKETCH NUMBER
DO NOT SCALE FROM SKETCH			SK-0219
			REVISION
			00
			SCALE 0.125
			SHEET 1 OF 23



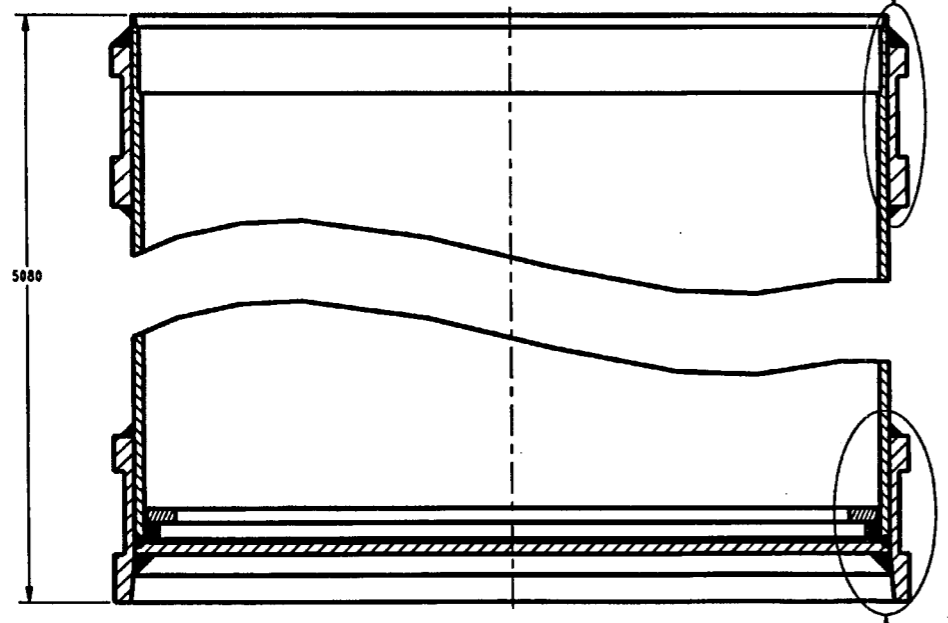
WASTE PACKAGE DEPARTMENT	
M&O Caltrans Radioactive Waste Management System MANAGEMENT & OPERATING CONTRACTOR	
SKETCH NUMBER SK-0219	REVISION 00
SCALE 0.125	SHEET 2 OF 23

ASSEMBLY -2
 OUTER SHELL ASSEMBLY
 SCALE 0.150

1 0 3

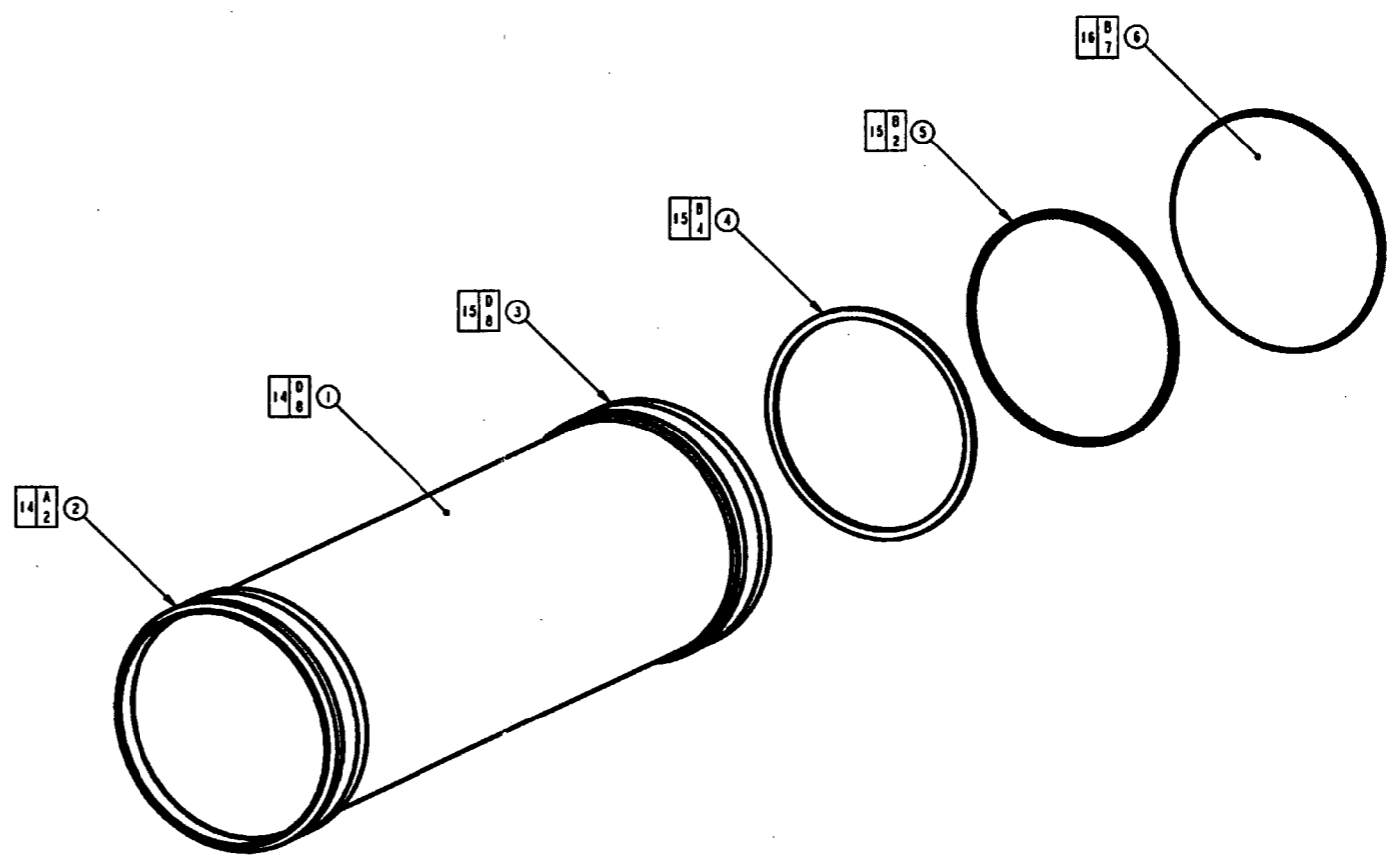


SEE DETAIL C
 4 A 8

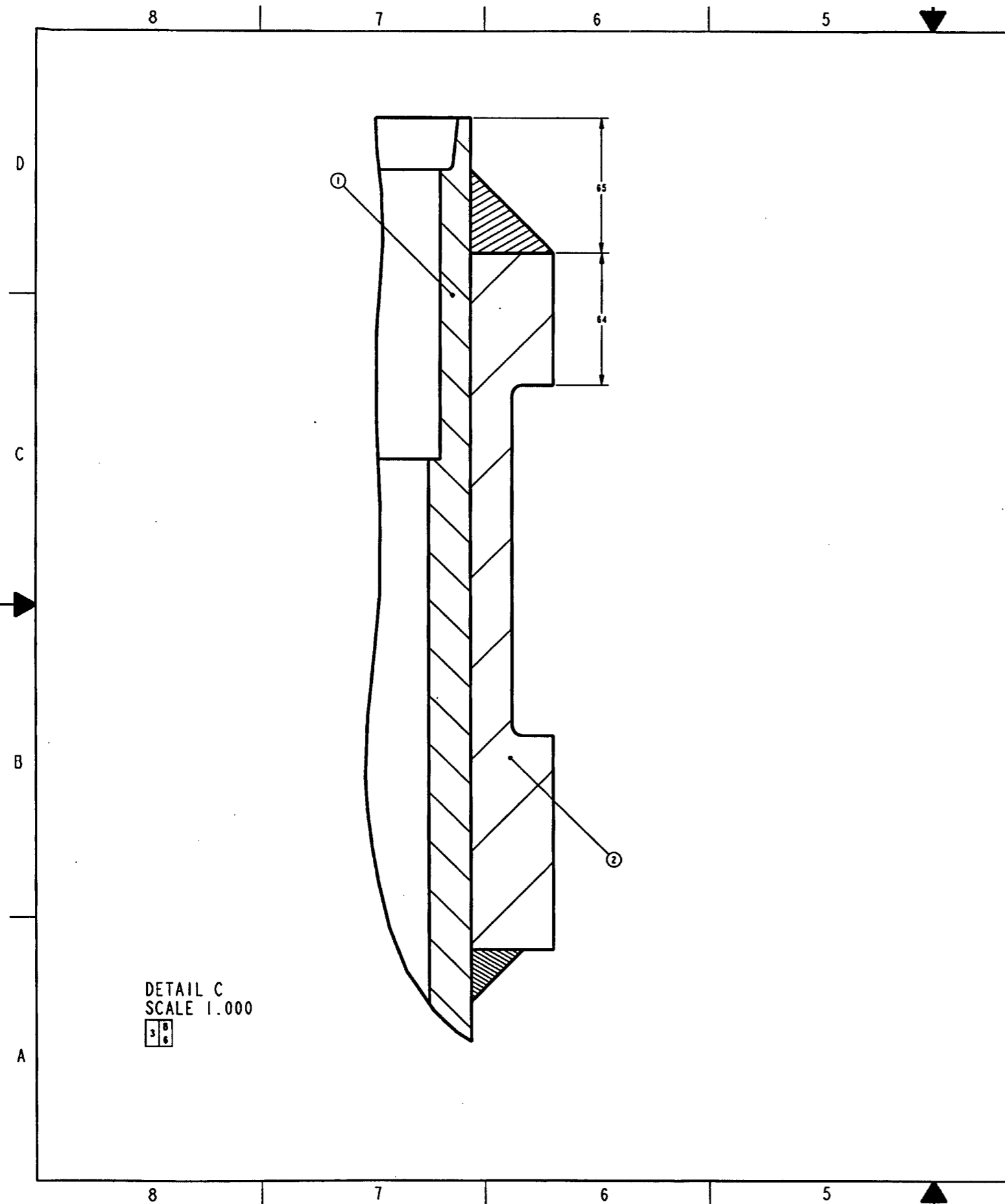


SECTION B-B
 SCALE 0.150
 3 D 5

SEE DETAIL D
 4 A 3

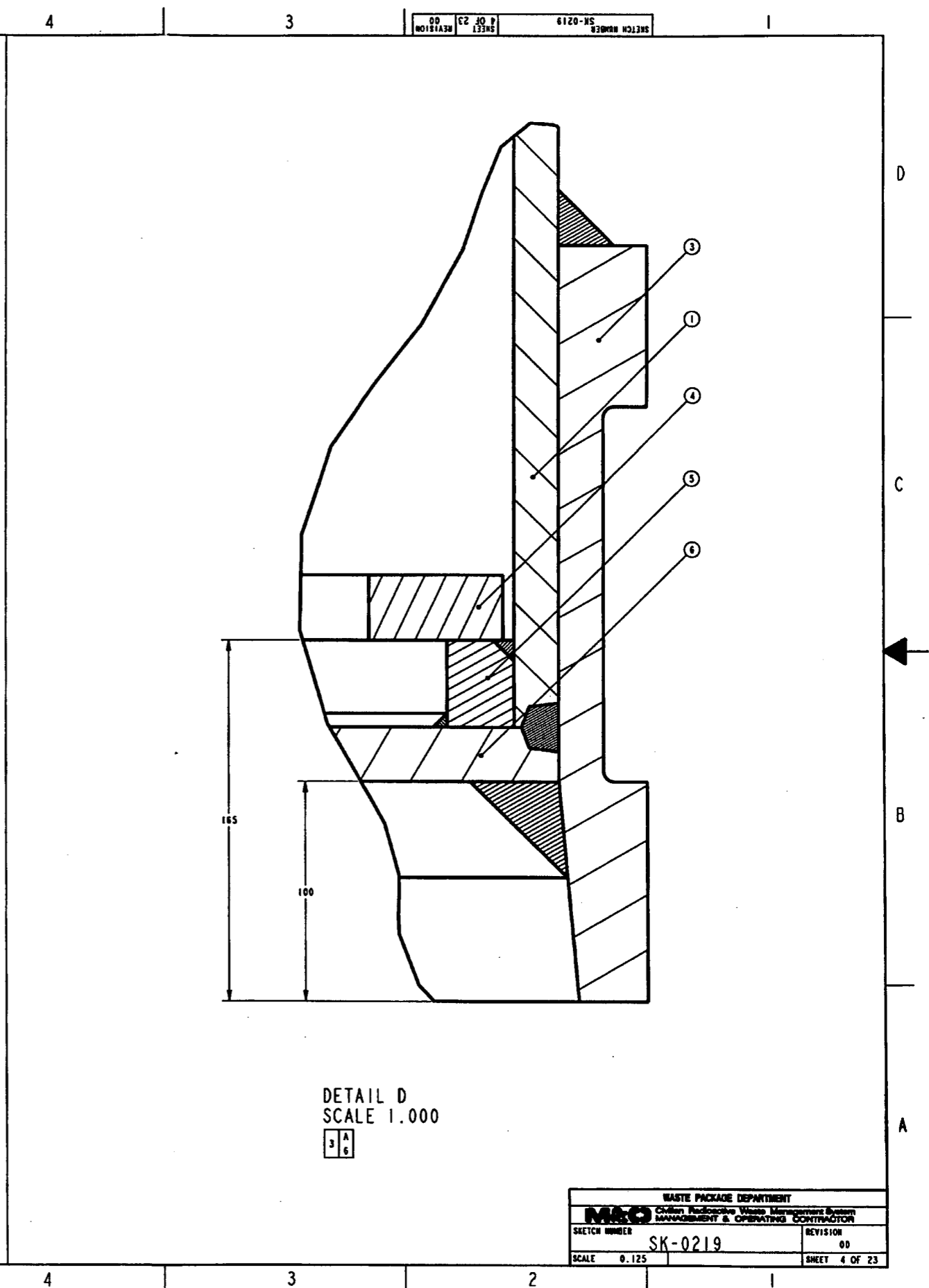


WASTE PACKAGE DEPARTMENT	
M&O Civilian Radioactive Waste Management System MANAGEMENT & OPERATIONS CONTRIBUTION	
SKETCH NUMBER	REVISION
SK-0219	00
SCALE 0.125	SHEET 3 OF 23



DETAIL C
 SCALE 1.000

3	8
6	



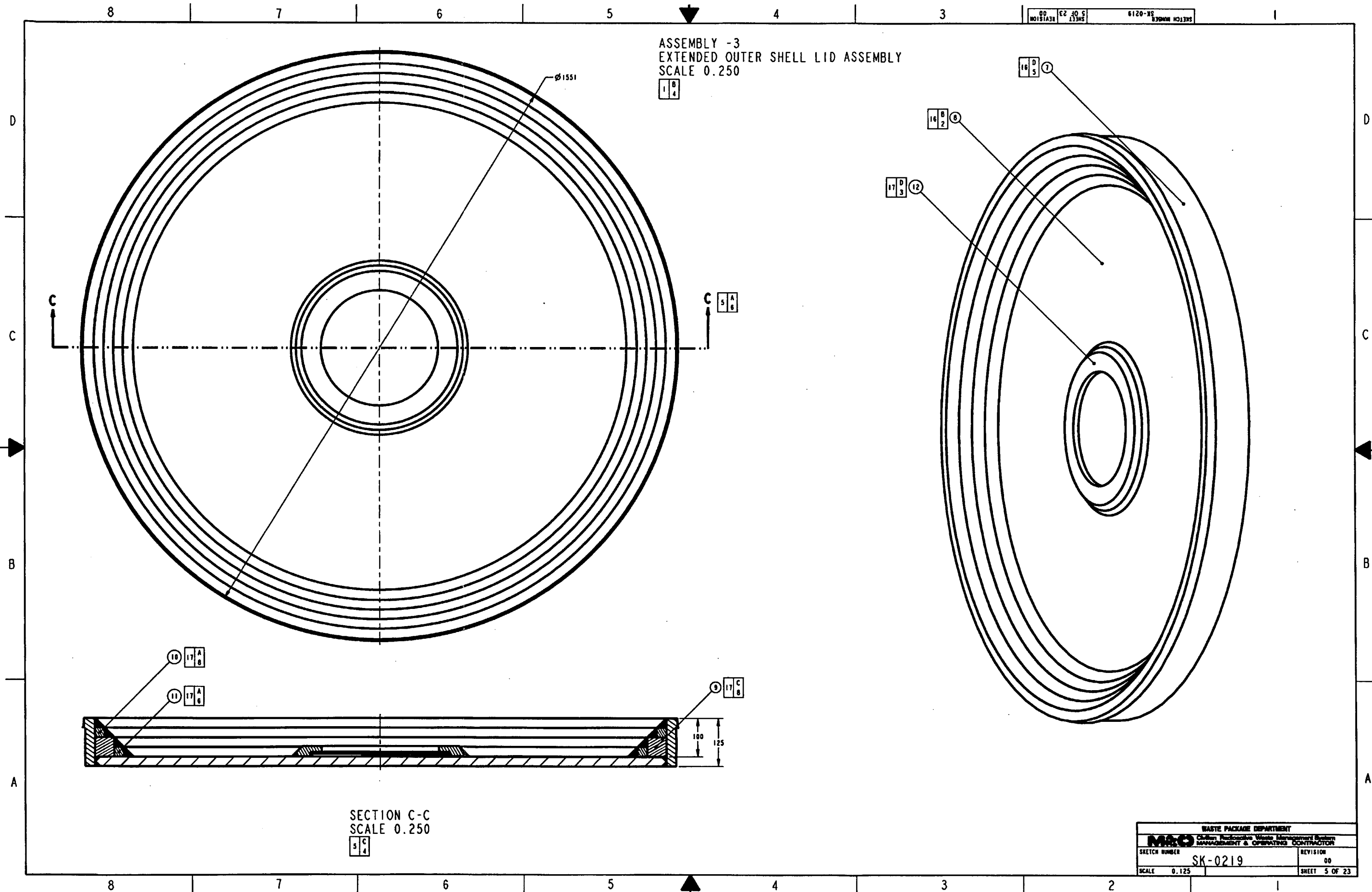
DETAIL D
 SCALE 1.000

3	A
6	

WASTE PACKAGE DEPARTMENT	
Civilian Radioactive Waste Management System MANAGEMENT & OPERATING CONTRACTOR	
SHEET NUMBER	REVISION
SK-0219	00
SCALE 0.125	SHEET 4 OF 23

ASSEMBLY -3
EXTENDED OUTER SHELL LID ASSEMBLY
SCALE 0.250

1 8 4



∅1551

C 5 A 8

16 D 5 7

16 B 2 8

17 D 3 12

10 17 A 8

11 17 A 8

17 C 8

100
125

SECTION C-C
SCALE 0.250

5 C 4

WASTE PACKAGE DEPARTMENT	
M&O Civilian Radioactive Waste Management System MANAGEMENT & OPERATING CONTRACTOR	
SKETCH NUMBER SK-0219	REVISION 00
SCALE 0.125	SHEET 5 OF 23

SKETCH NUMBER SK-0219 SHEET 6 OF 23

ASSEMBLY -4
OUTER SHELL FLAT CLOSURE LID ASSEMBLY
SCALE 0.275

1 B 3

Ø1537

D 1 B 3

17 B 3 12

17 C 5 13

SECTION D-D
SCALE 0.275

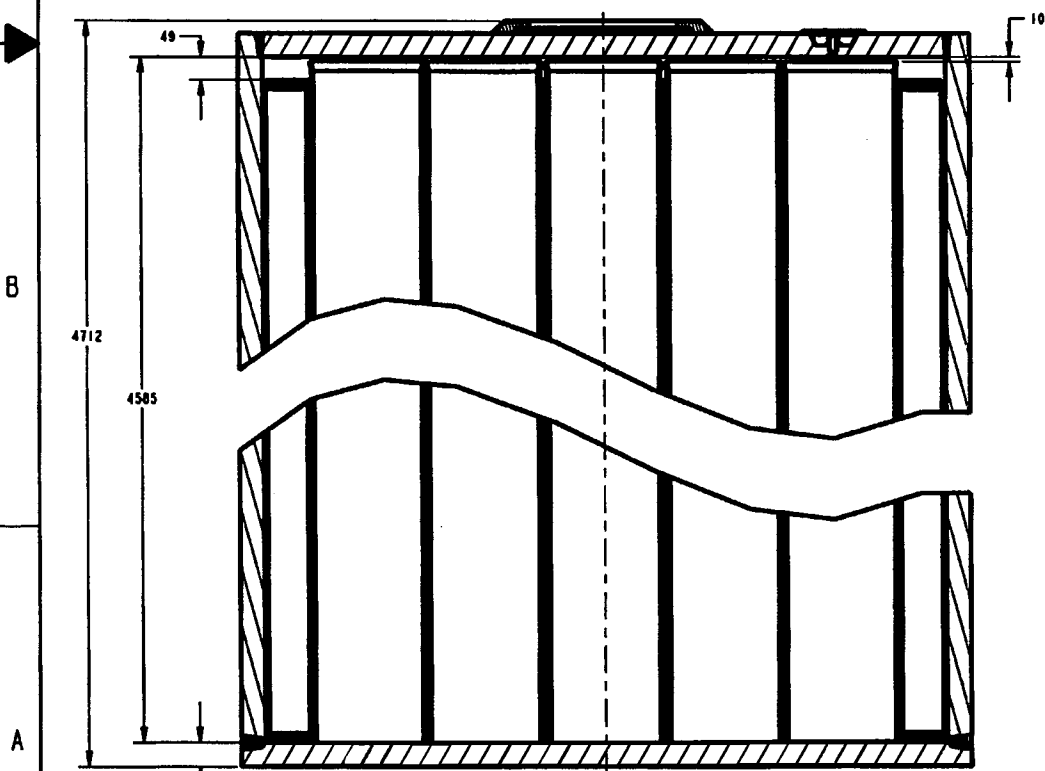
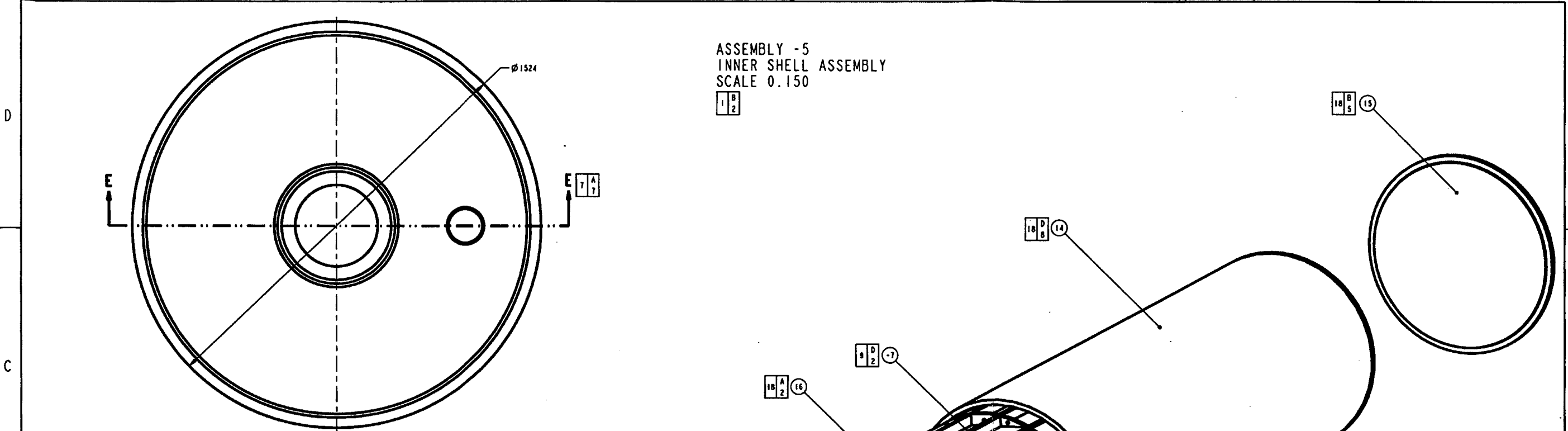
1 C 4

WASTE PACKAGE DEPARTMENT	
M&O Caltrans Radioactive Waste Management System MANAGEMENT & OPERATING CONTRACTOR	
SKETCH NUMBER SK-0219	REVISION 00
SCALE 0.125	SHEET 6 OF 23

ASSEMBLY -5
INNER SHELL ASSEMBLY
SCALE 0.150

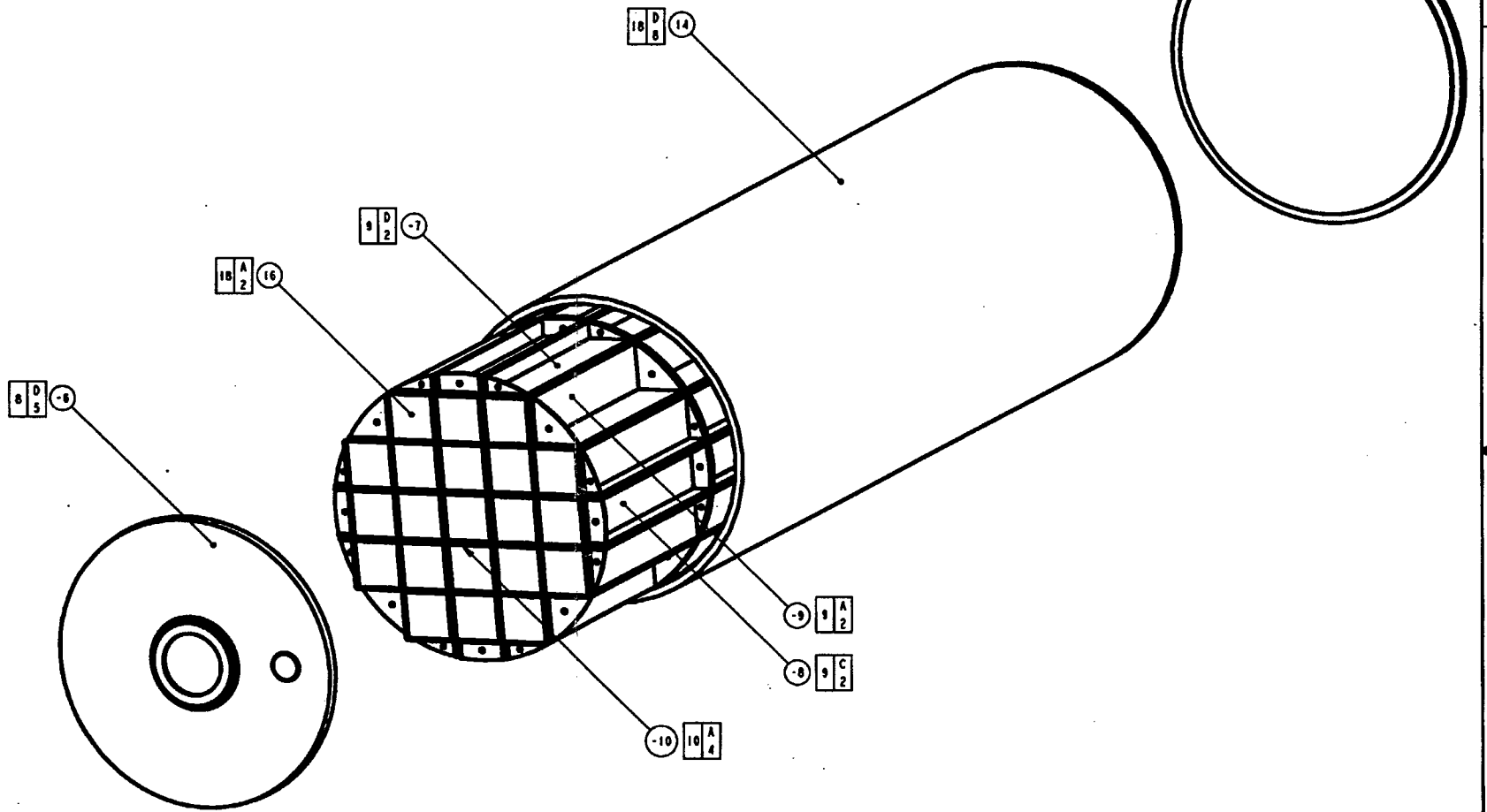
1 B 2

8 7 6 5 4 3



SECTION E-E
SCALE 0.150

7 D 6



WASTE PACKAGE DEPARTMENT	
M&O Civilian Radioactive Waste Management System MANAGEMENT & OPERATING CONTRACTOR	
SKETCH NUMBER SK-0219	REVISION 00
SCALE 0.125	SHEET 7 OF 23

8 7 6 5 4 3 2 1

ASSEMBLY -6
 INNER SHELL TOP LID ASSEMBLY
 SCALE 0.250

7
 C
 5

19
 D
 5


19
 D
 8

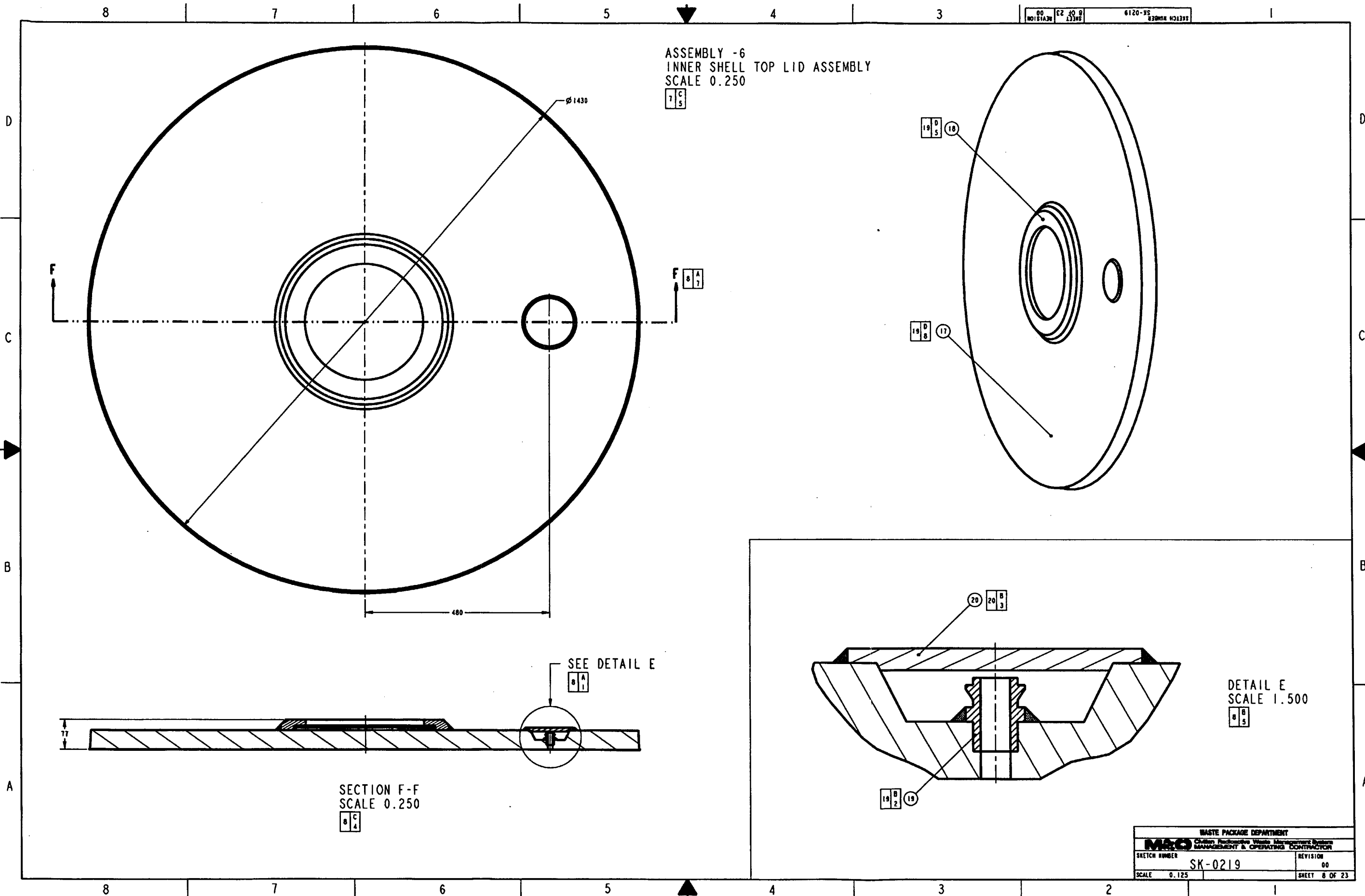
20
 B
 3

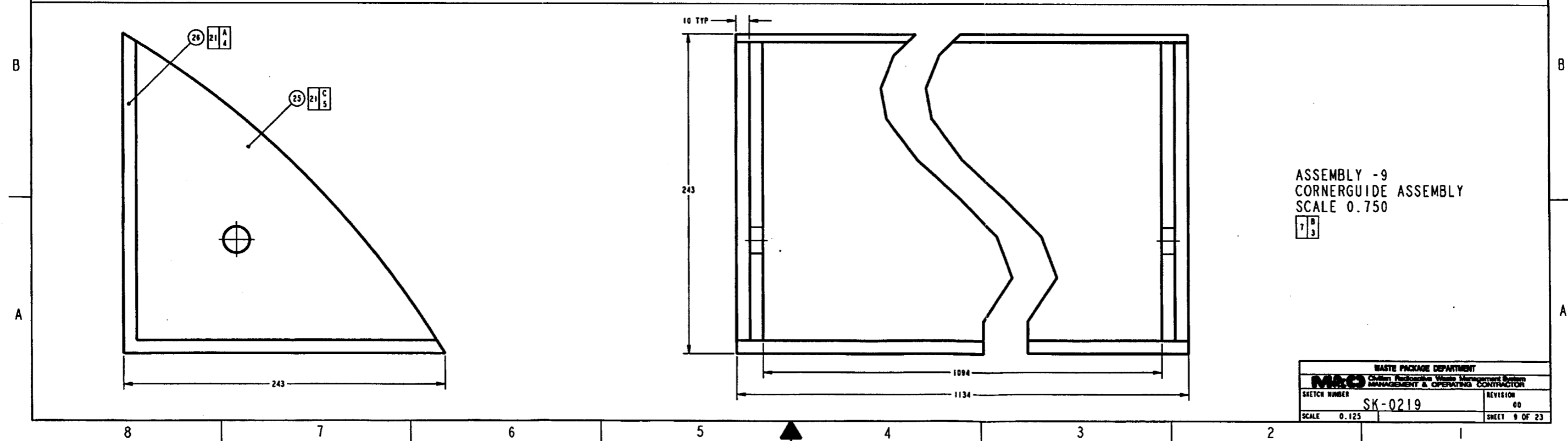
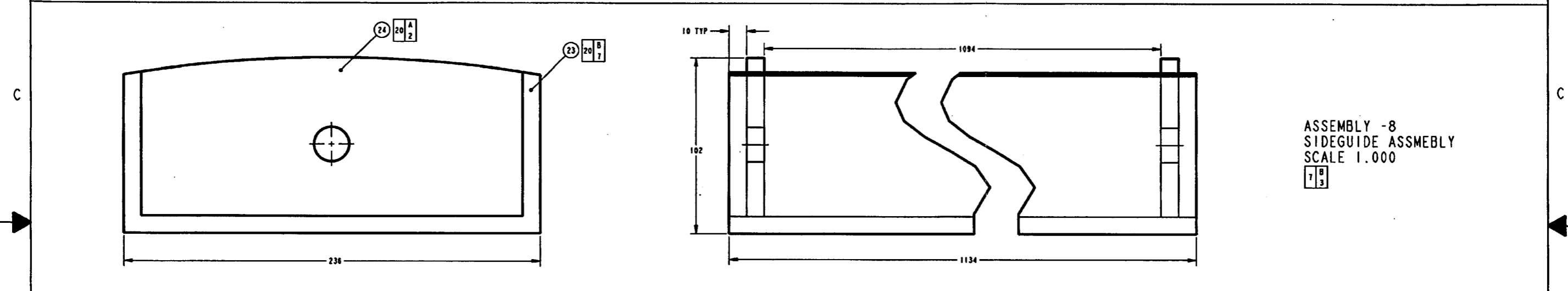
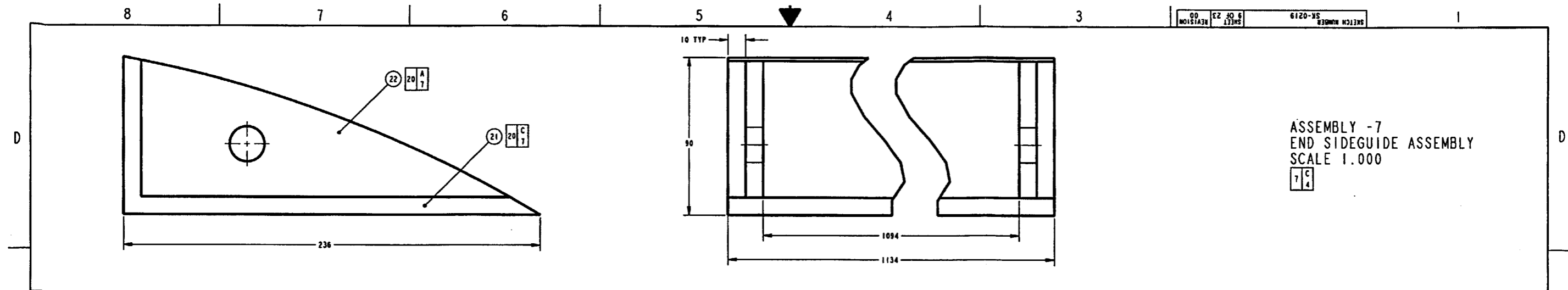
19
 B
 2

DETAIL E
 SCALE 1.500

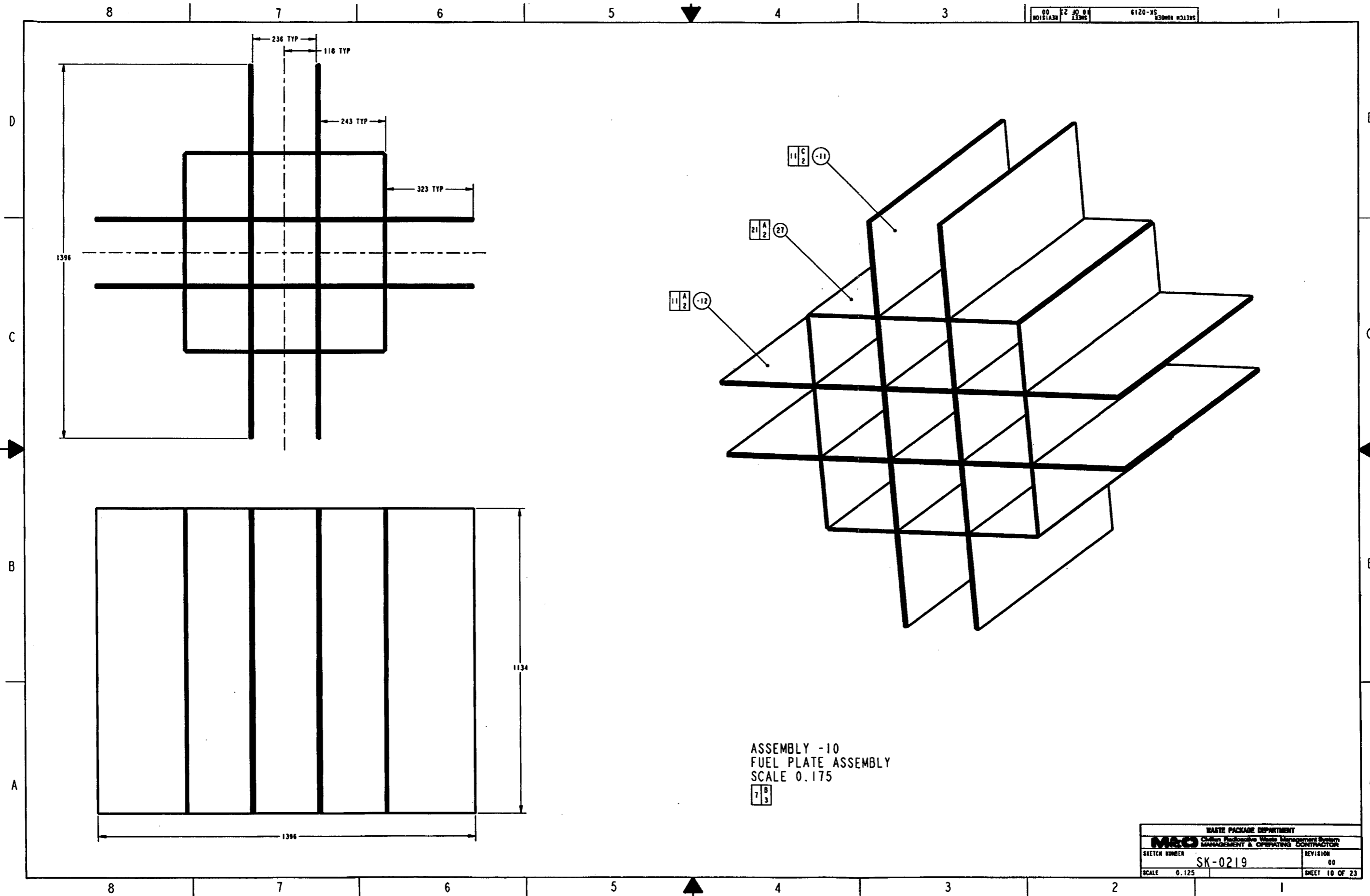
8
 B
 5

WASTE PACKAGE DEPARTMENT	
 Custom Radioactive Waste Management Systems MANAGEMENT & OPERATIONS CONTRACTOR	
SKETCH NUMBER	REVISION
SK-0219	00
SCALE 0.125	SHEET 8 OF 23



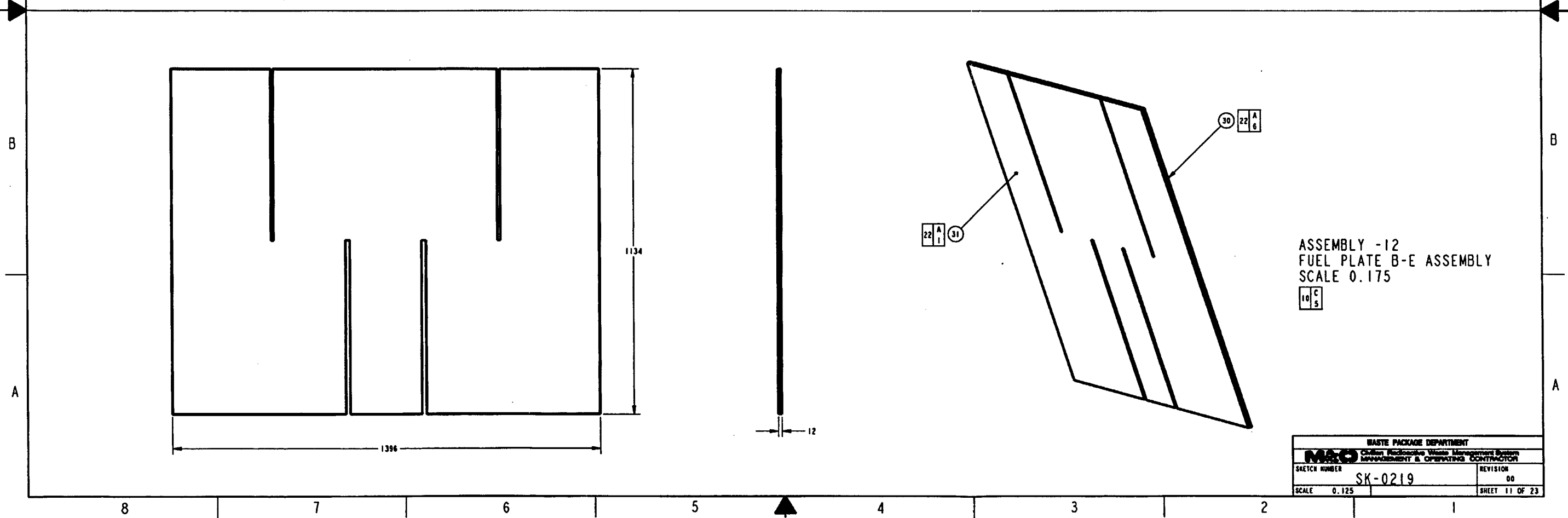
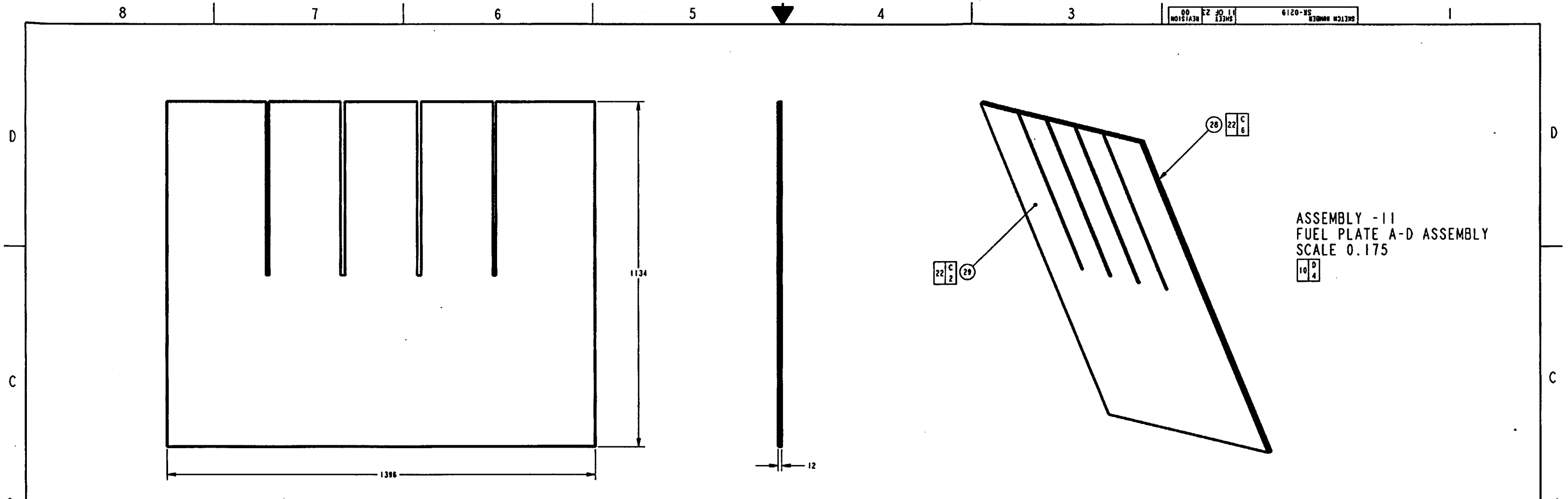


WASTE PACKAGE DEPARTMENT	
M&O Client Facilities Waste Management System MANAGEMENT & OPERATING CONTRACTOR	
SKETCH NUMBER SK-0219	REVISION 00
SCALE 0.125	SHEET 9 OF 23

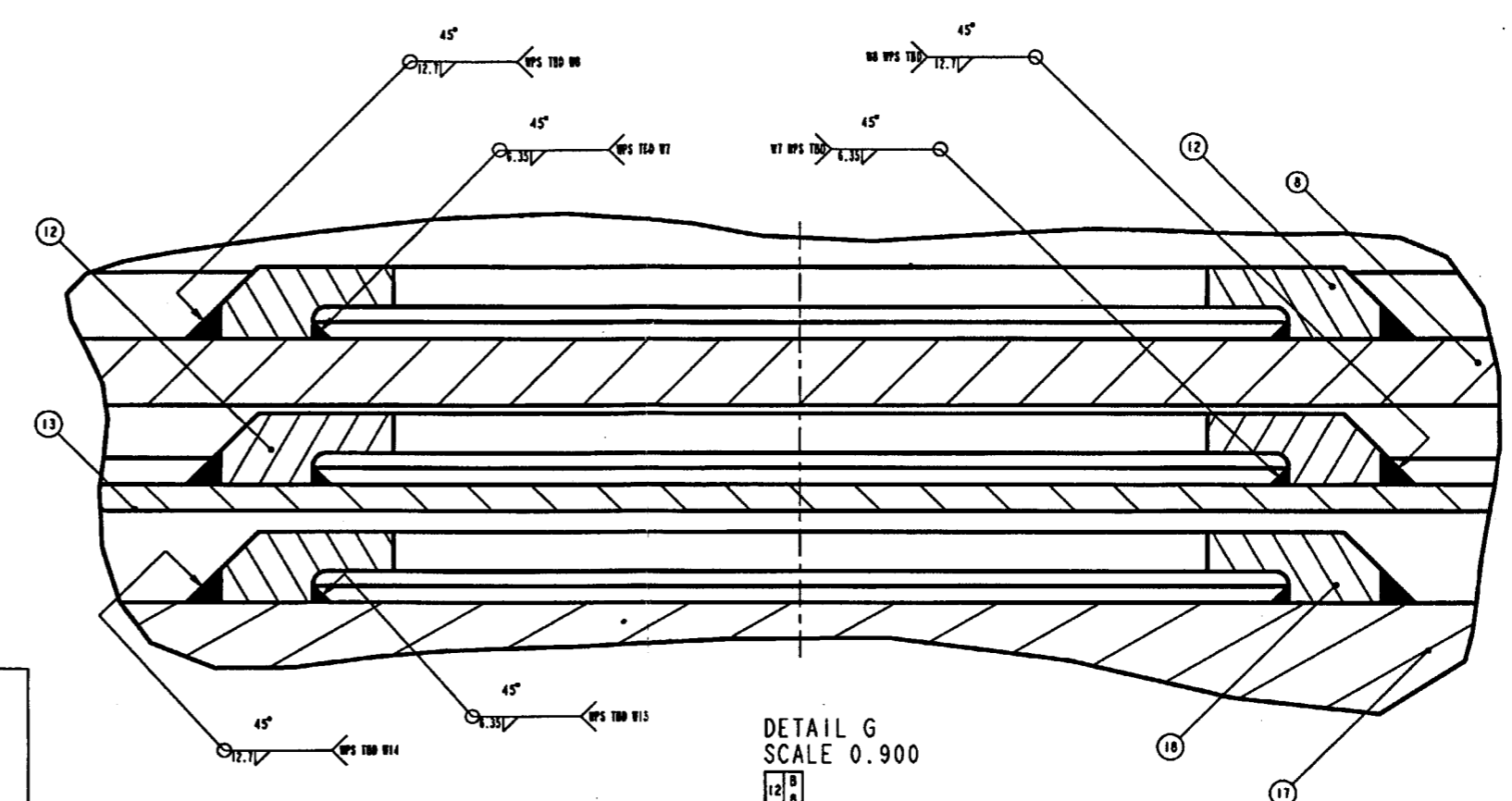
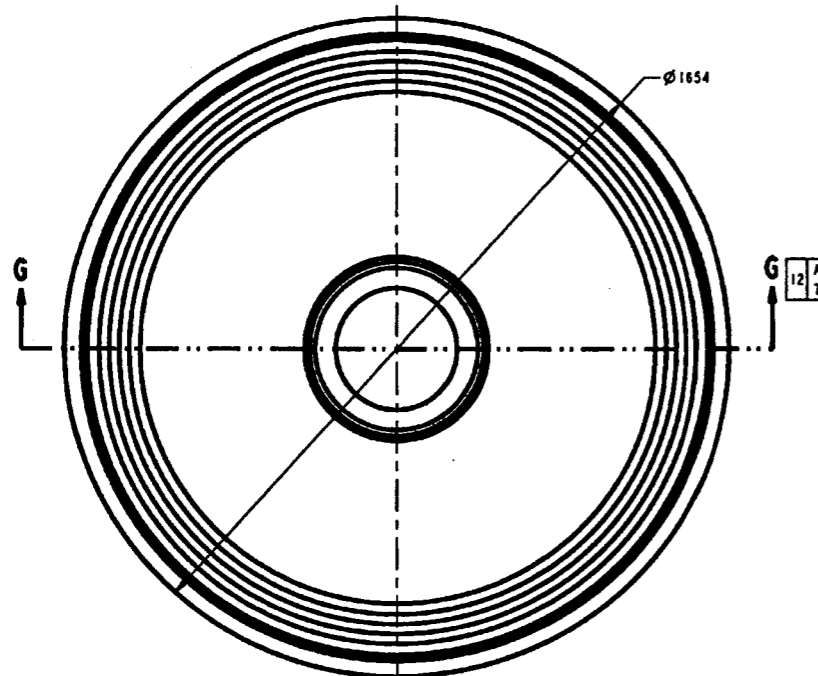


ASSEMBLY -10
 FUEL PLATE ASSEMBLY
 SCALE 0.175

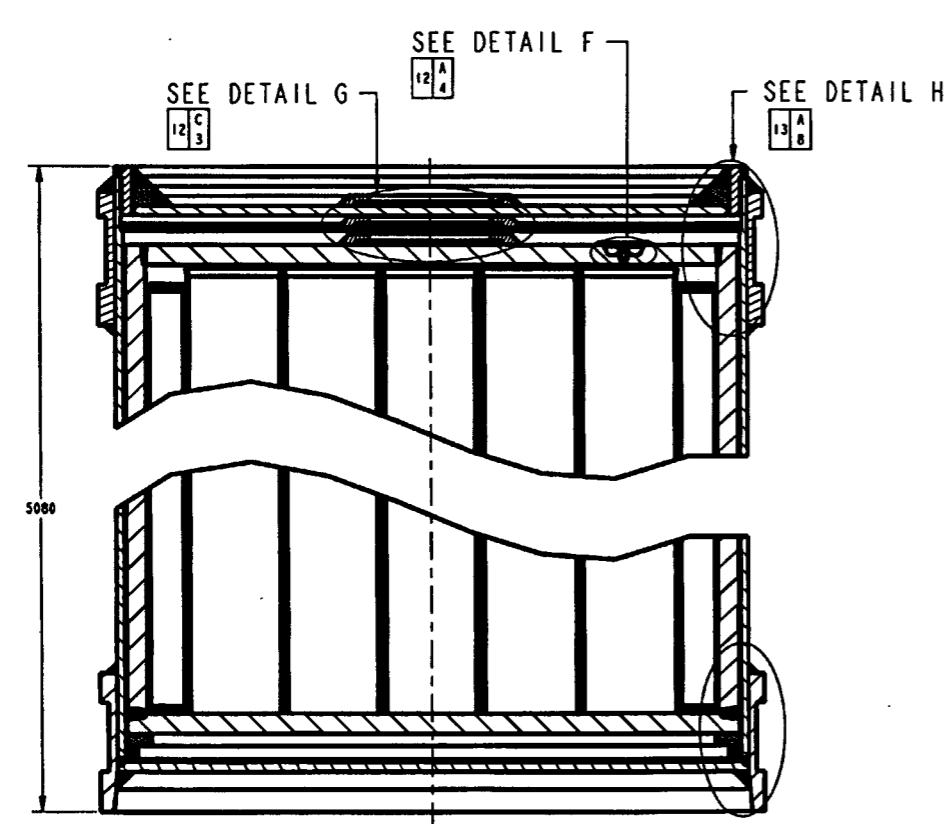
7 B 3



WASTE PACKAGE DEPARTMENT	
M&O Caltrans Radioactive Waste Management System MANAGEMENT & OPERATING CONTRACTOR	
SKETCH NUMBER SK-0219	REVISION 00
SCALE 0.125	SHEET 11 OF 23

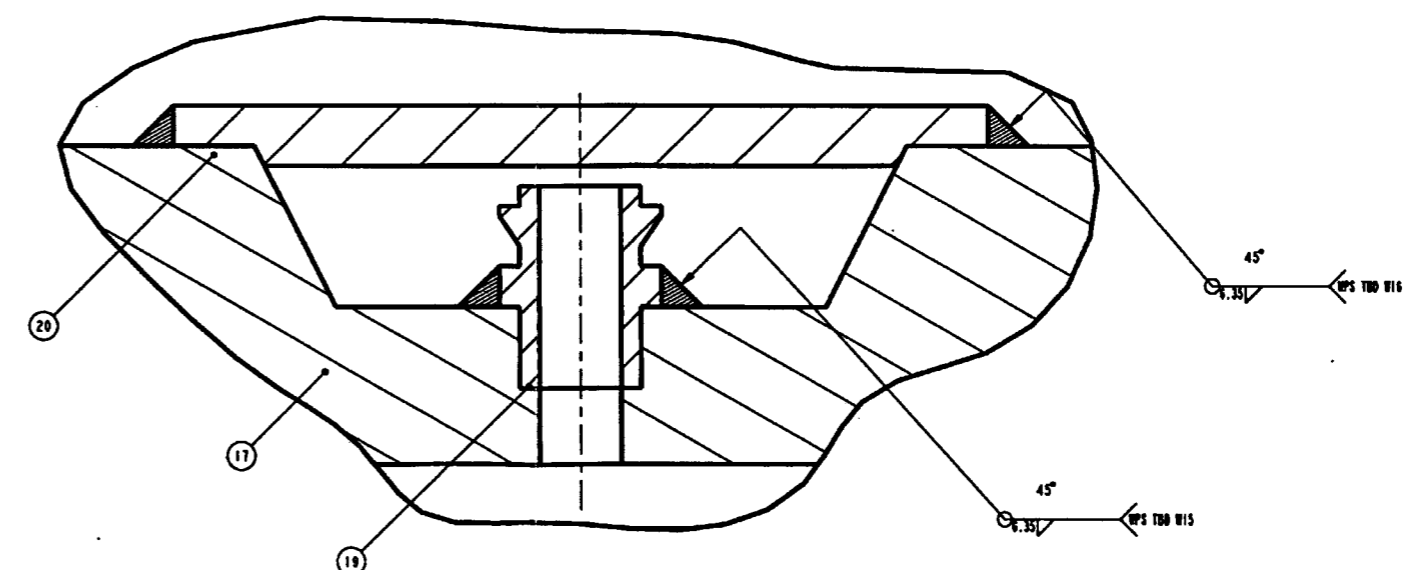


The illegible information does not impact the technical meaning or content of the record. 01/29/01



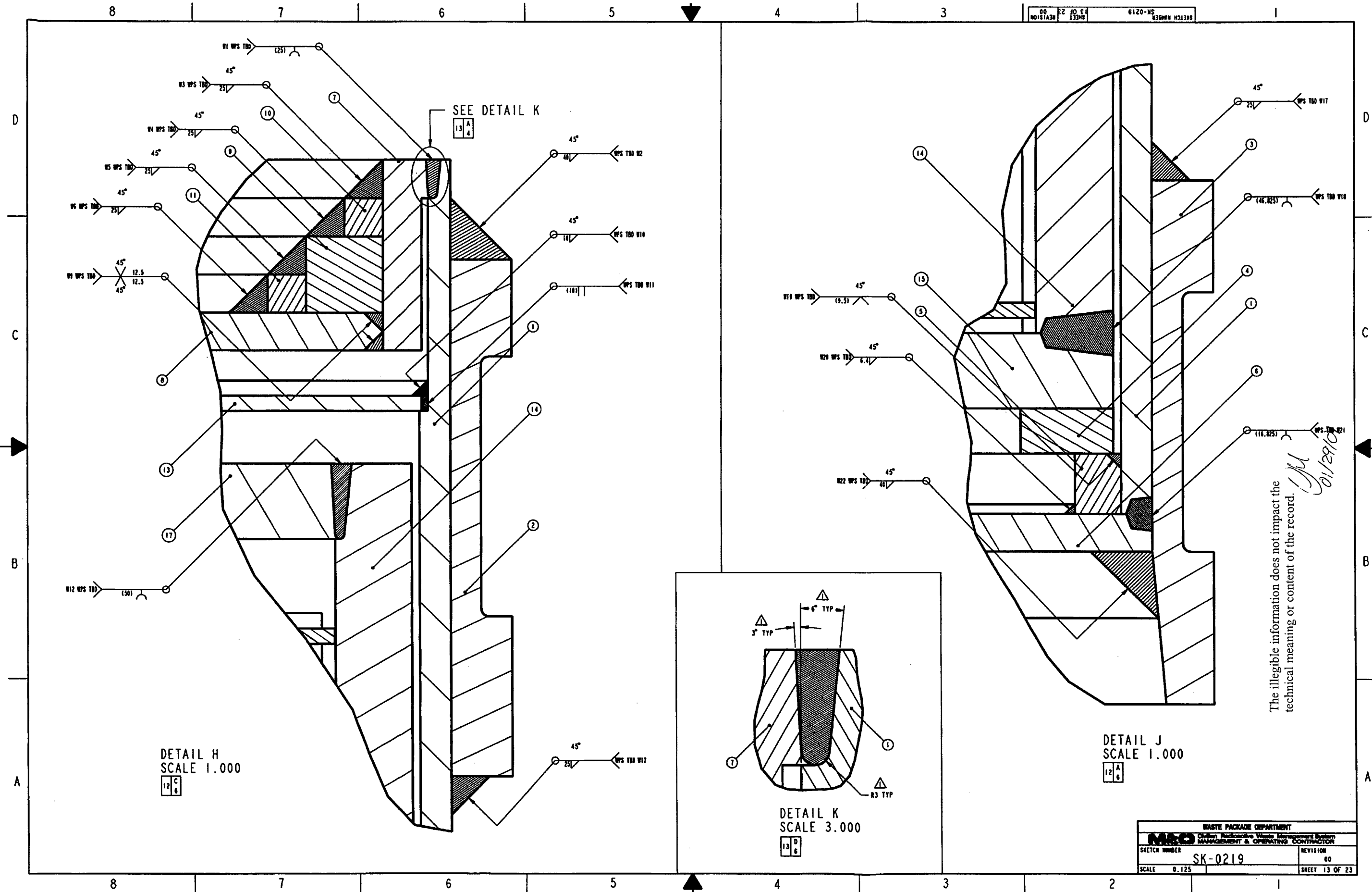
SECTION G-G
 SCALE 0.125

DETAIL J
 13A2



DETAIL F
 SCALE 2.000

WASTE PACKAGE DEPARTMENT	
M&O Custom Radioactive Waste Management System MANAGEMENT & OPERATING CONTRACTOR	
SKETCH NUMBER SK-0219	REVISION 00
SCALE 0.125	SHEET 12 OF 23



DETAIL H
SCALE 1.000
12 C 6

DETAIL K
SCALE 3.000
13 D 6

DETAIL J
SCALE 1.000
12 A 6

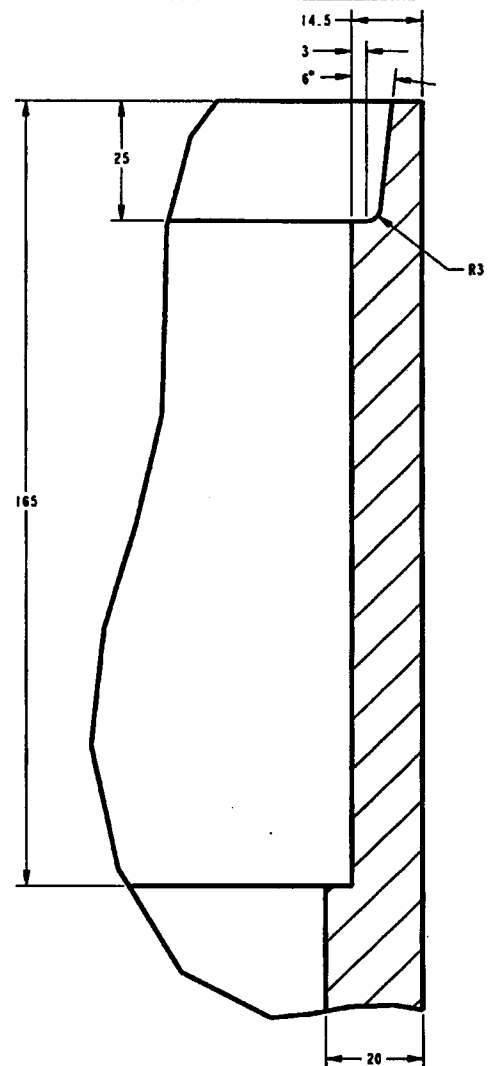
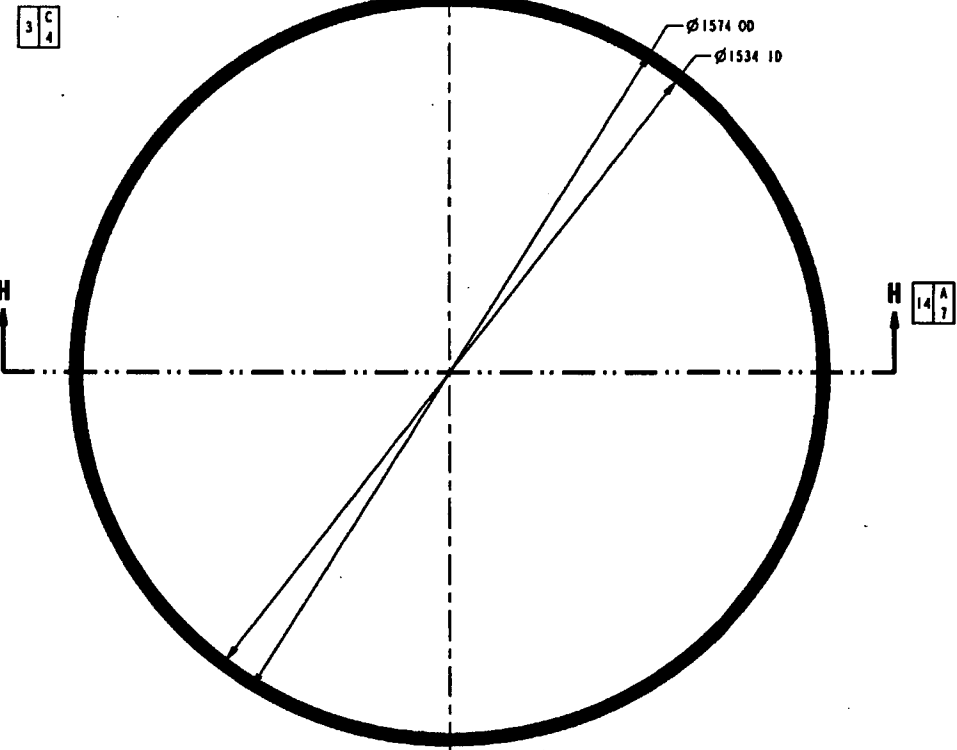
The illegible information does not impact the technical meaning or content of the record.

JM
01/29/10

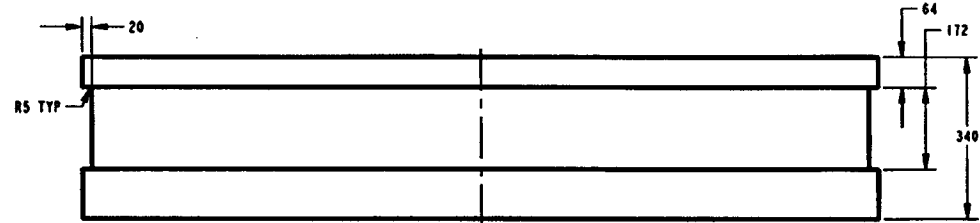
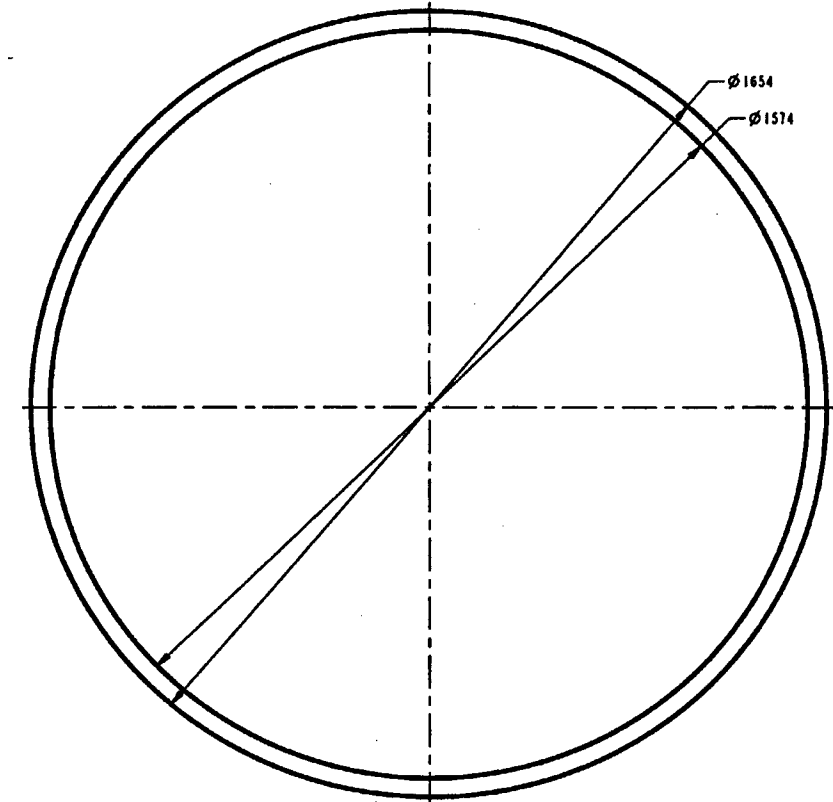
WASTE PACKAGE DEPARTMENT	
M&D CONSULTING ENGINEERS	
CONSULTING ENGINEERS	
SKETCH NUMBER	REVISION
SK-0219	00
SCALE 0.125	SHEET 13 OF 23

SKETCH NUMBER SK-0219
SHEET 14 OF 23
REVISION 00

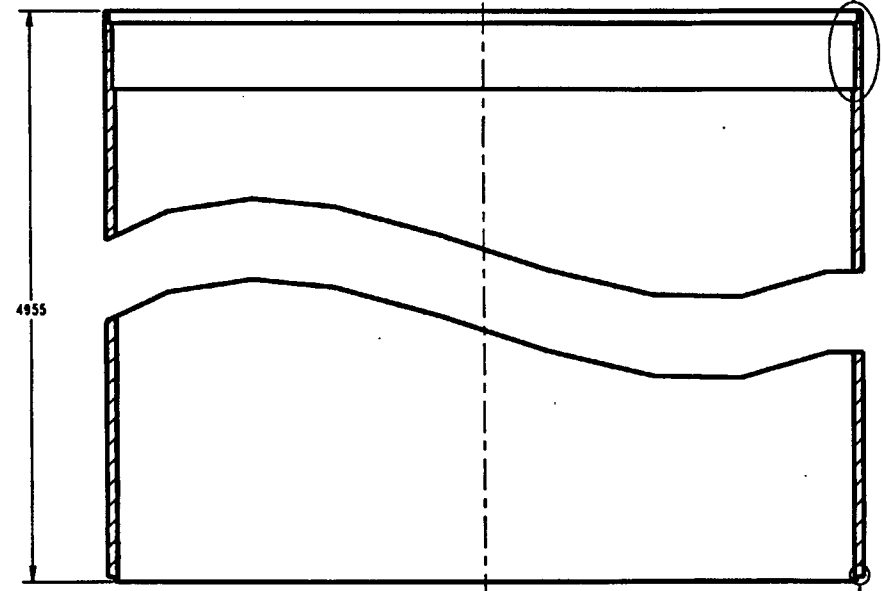
ITEM 1
OUTER SHELL
SCALE 0.150



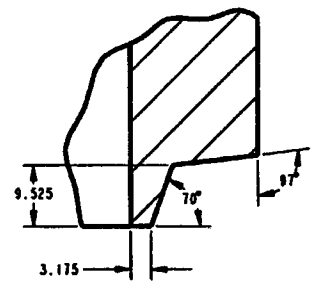
DETAIL L
SCALE 1.500



ITEM 2
UPPER TRUNNION COLLAR SLEEVE
SCALE 0.150



SECTION H-H
SCALE 0.150



DETAIL M
SCALE 2.000

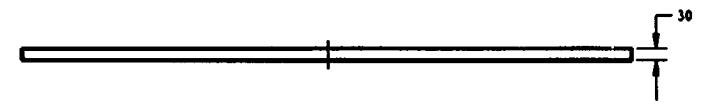
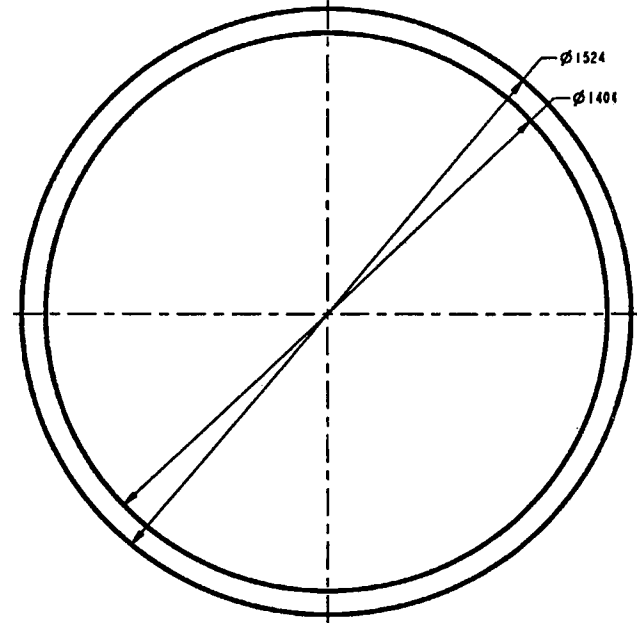
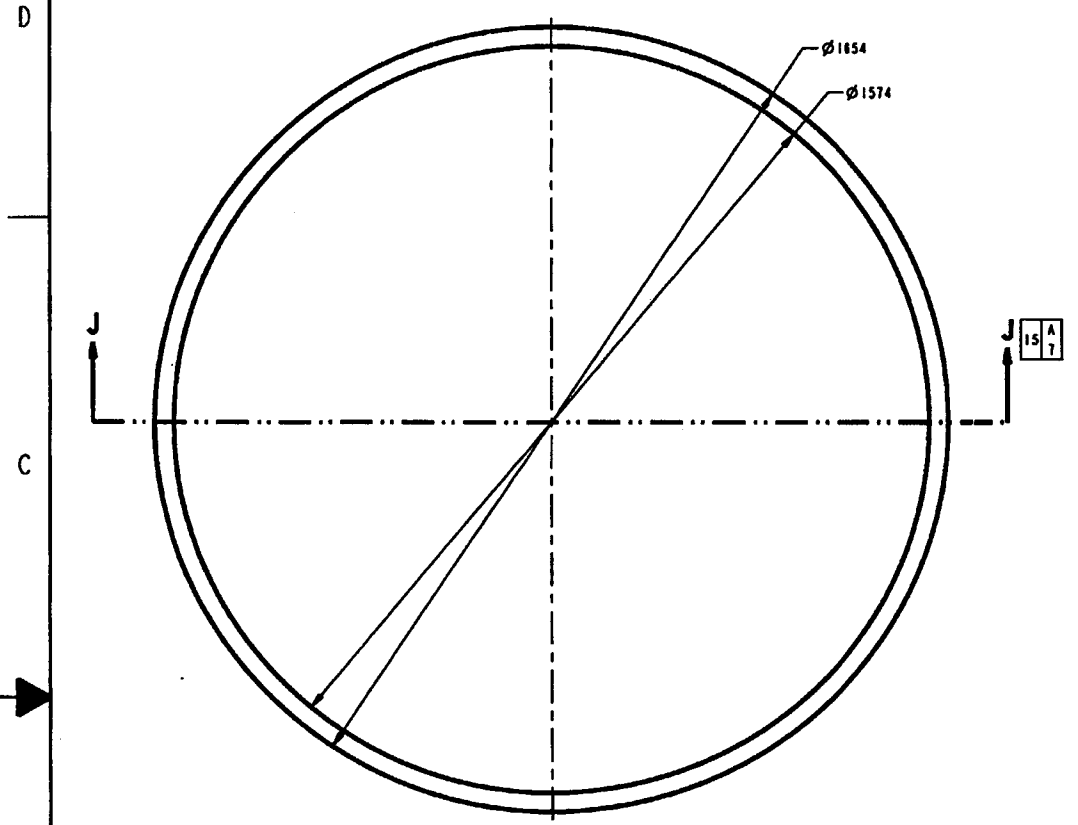
SEE DETAIL L

SEE DETAIL M

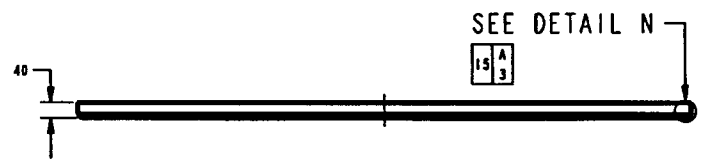
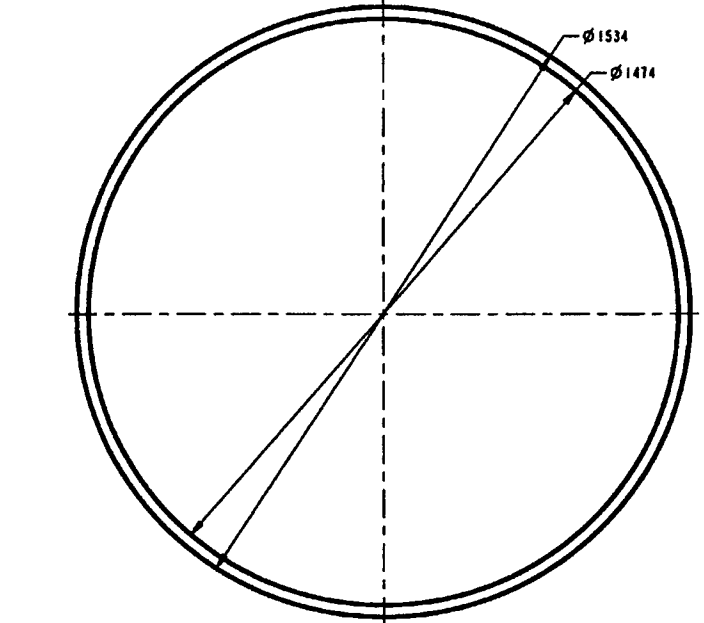
WASTE PACKAGE DEPARTMENT	
Custom Fabrication Waste Management System MANAGEMENT & OPERATING CONTRACTOR	
SKETCH NUMBER	REVISION
SK-0219	00
SCALE 0.125	SHEET 14 OF 23

ITEM 3
 LOWER TRUNNION COLLAR SLEEVE
 SCALE 0.150

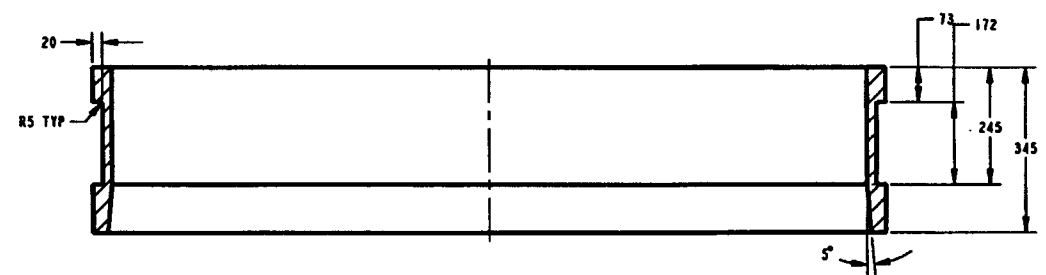
3 C
 4



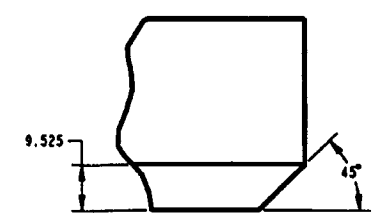
ITEM 4
 SHELL INTERFACE RING
 SCALE 0.125
 3 C
 3



ITEM 5
 INNER SHELL SUPPORT RING
 SCALE 0.125
 3 A
 3

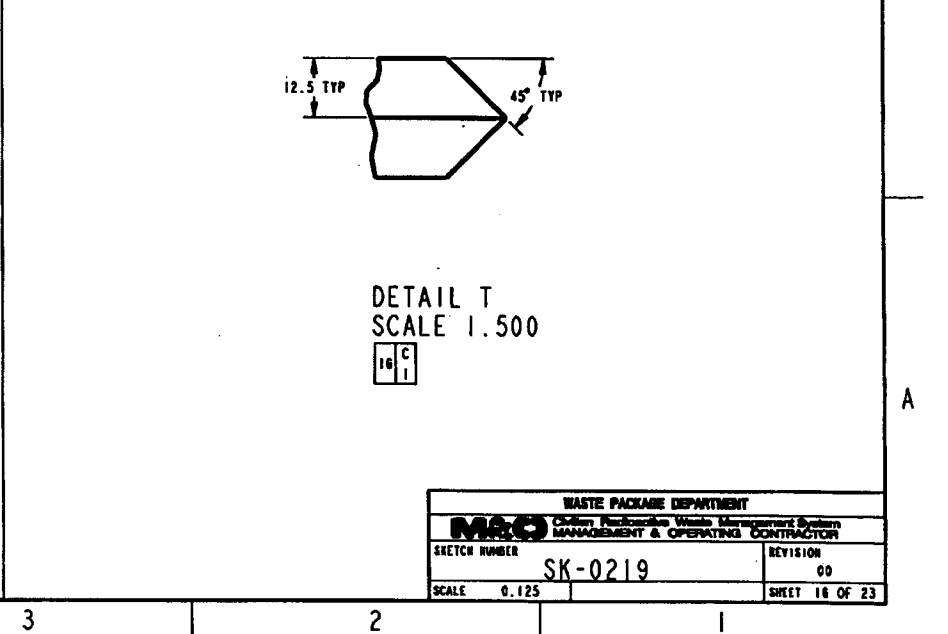
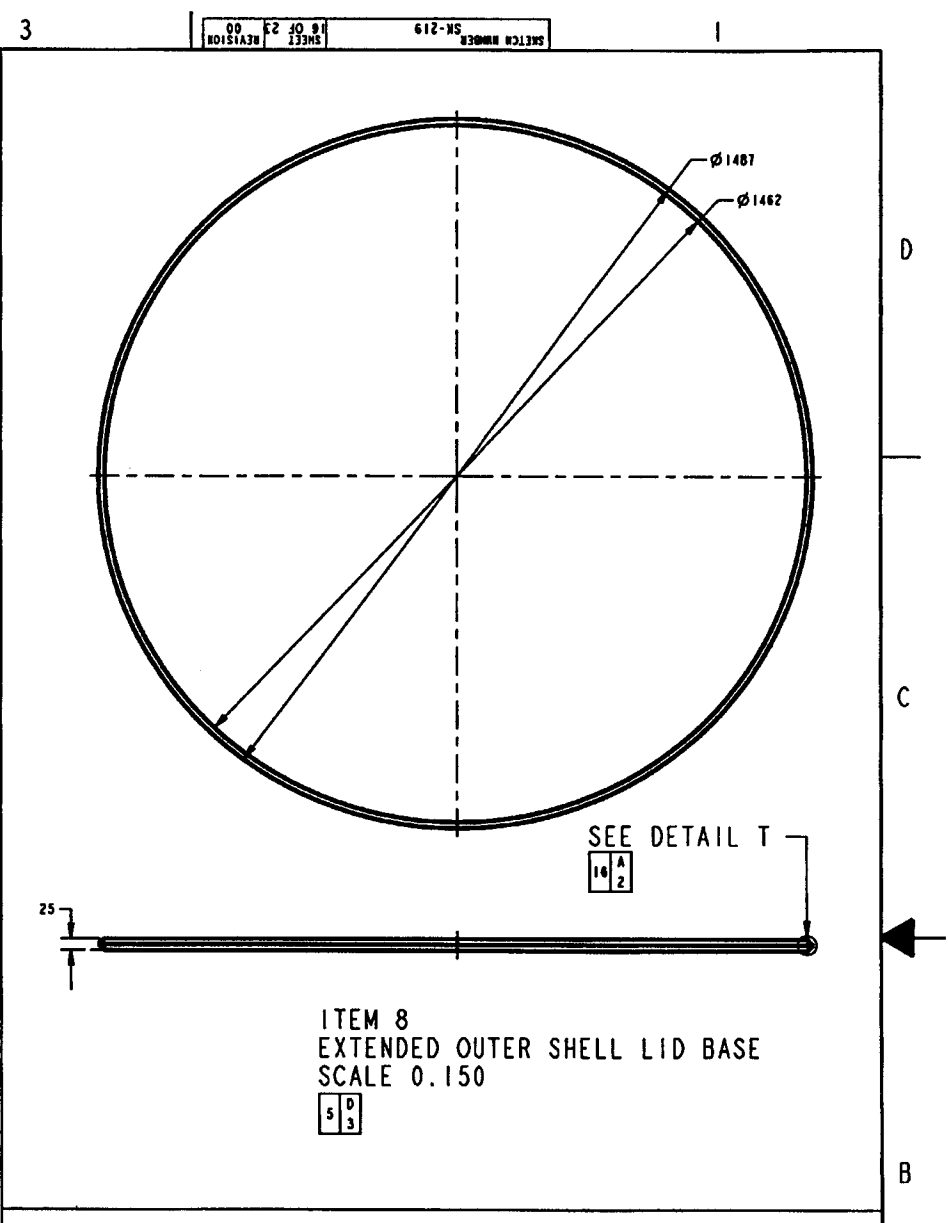
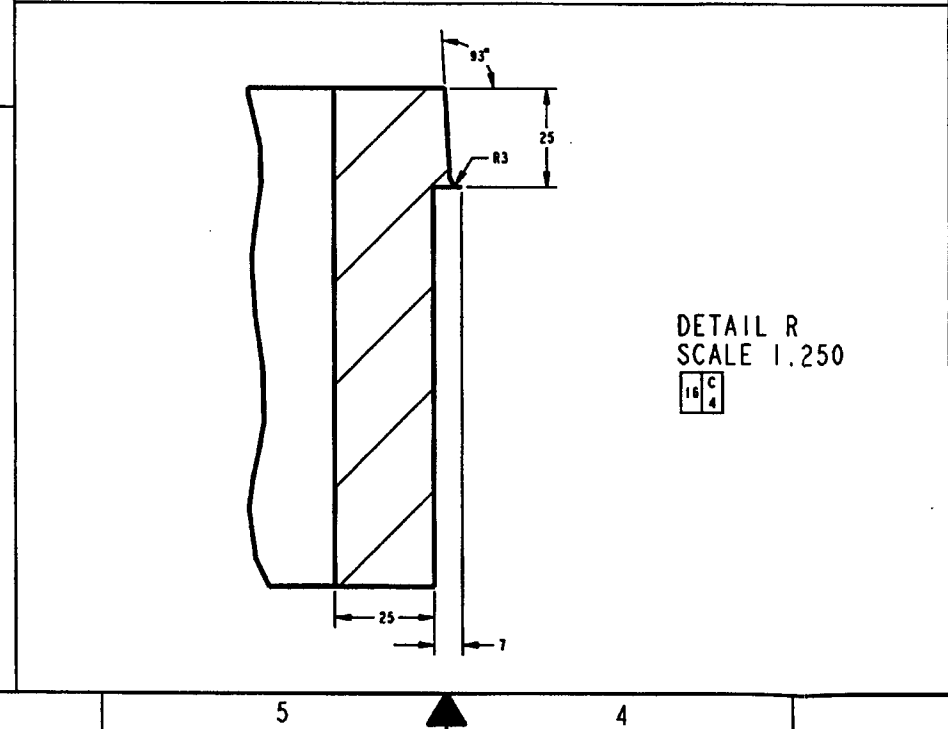
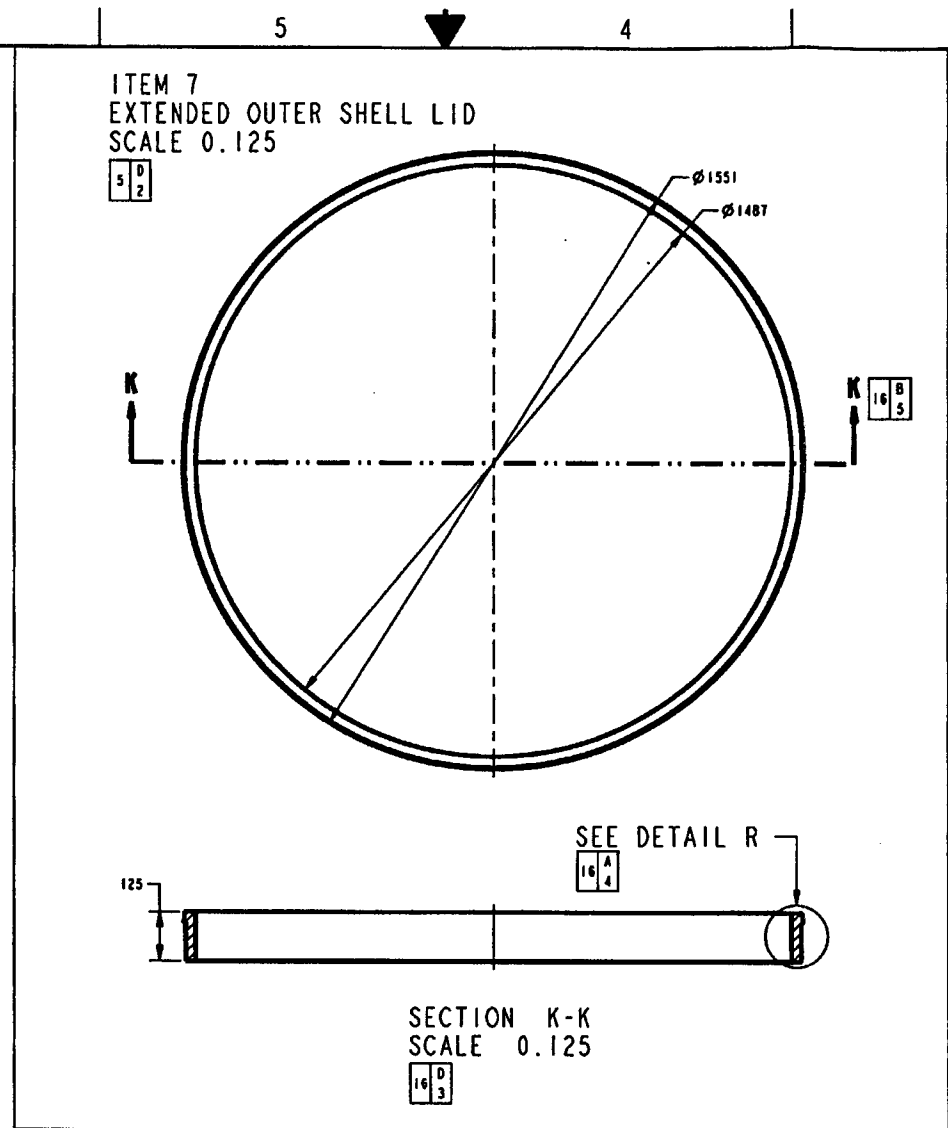
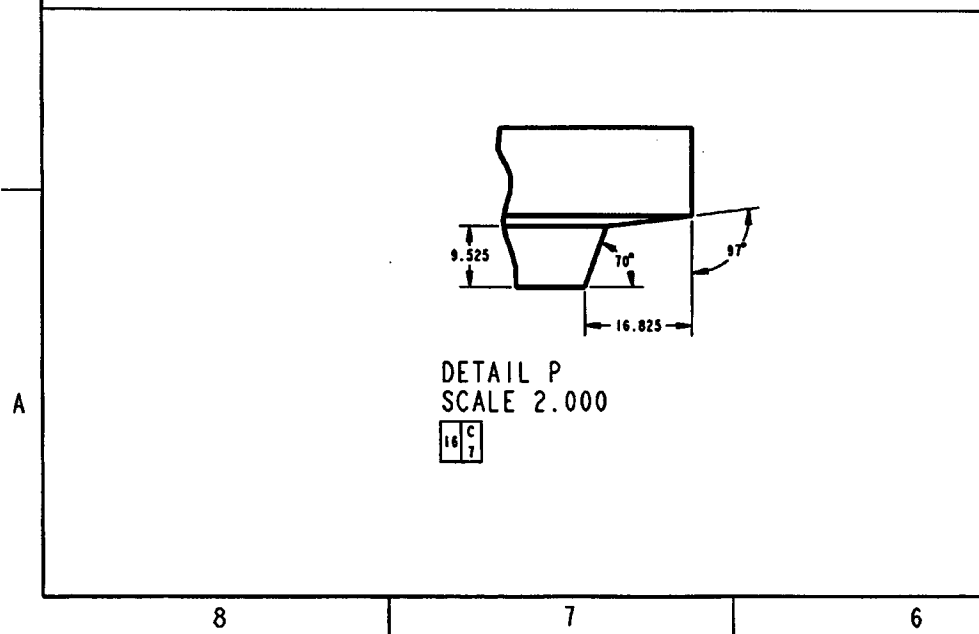
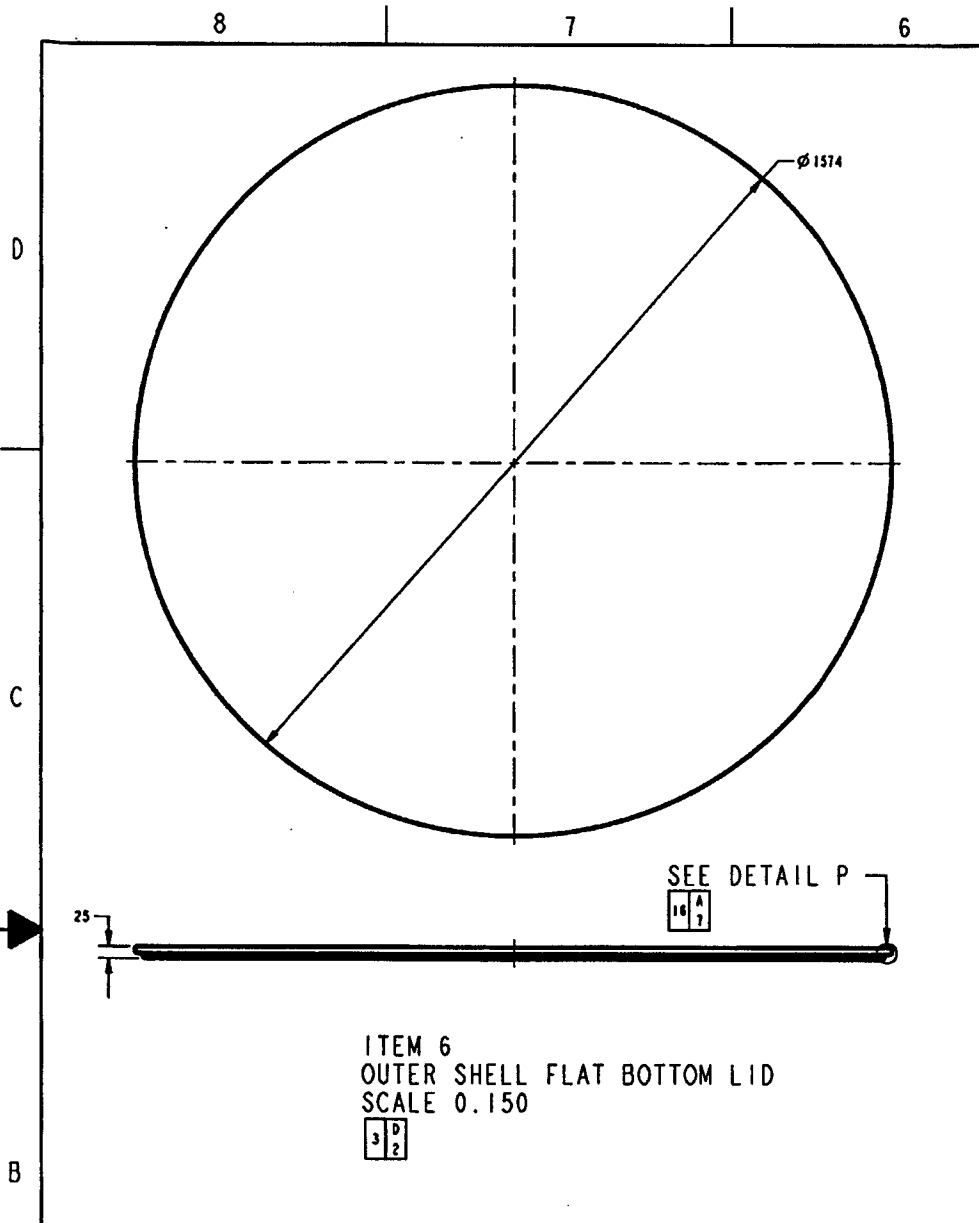


SECTION J-J
 SCALE 0.150
 15 C
 6

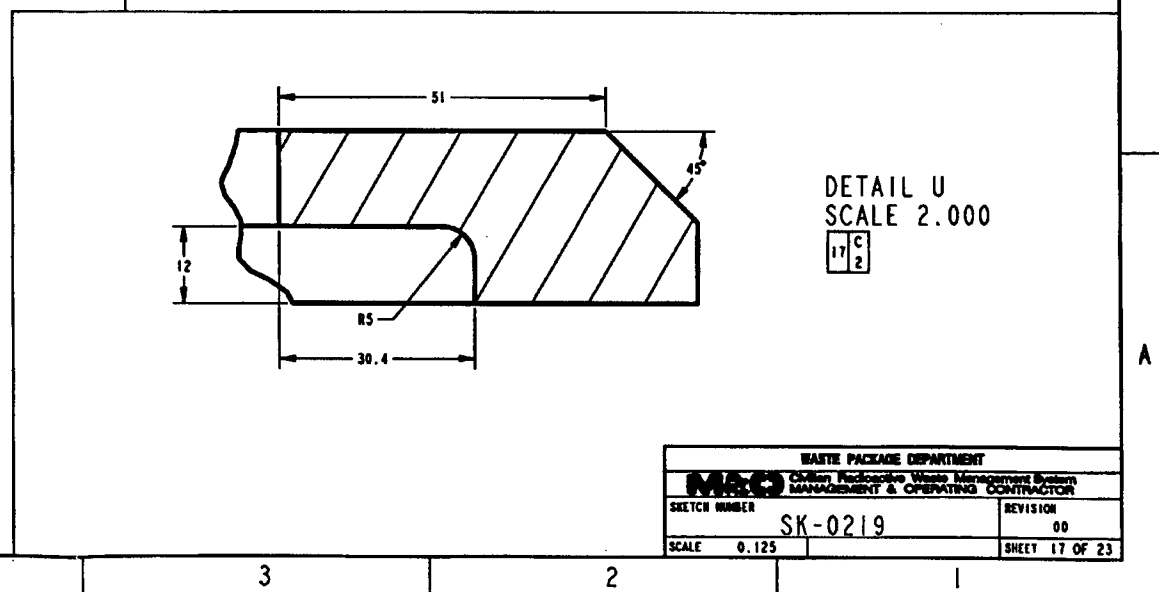
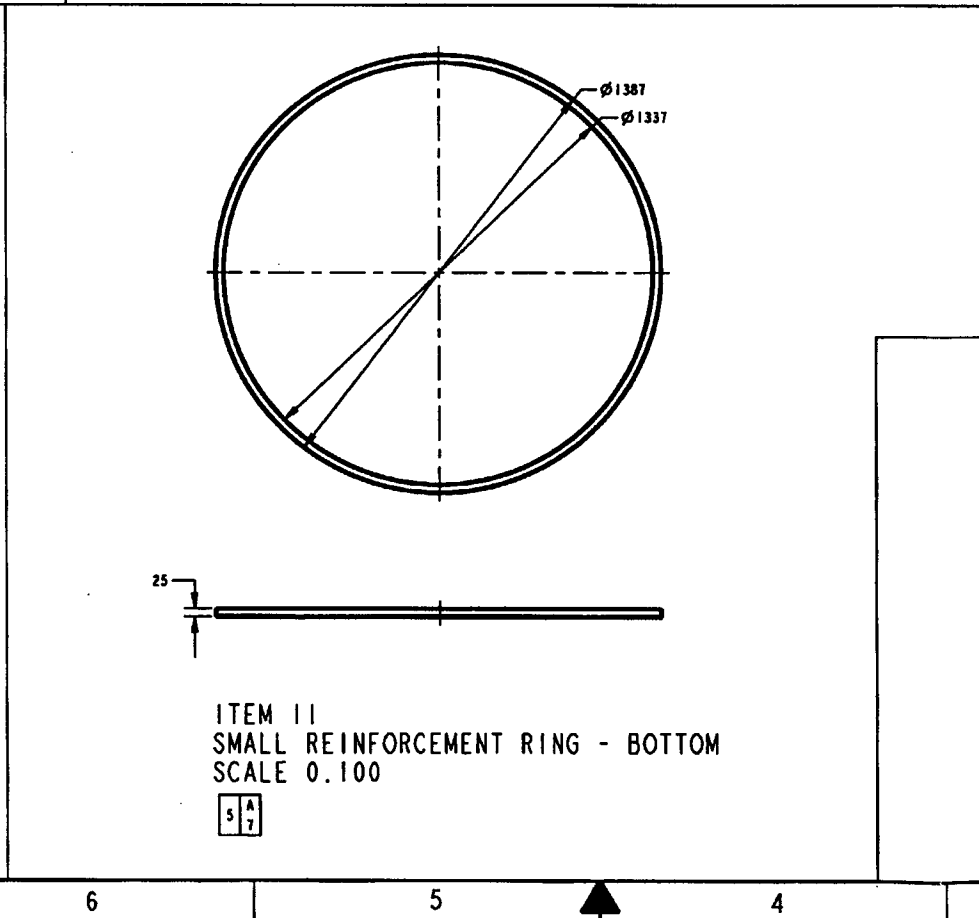
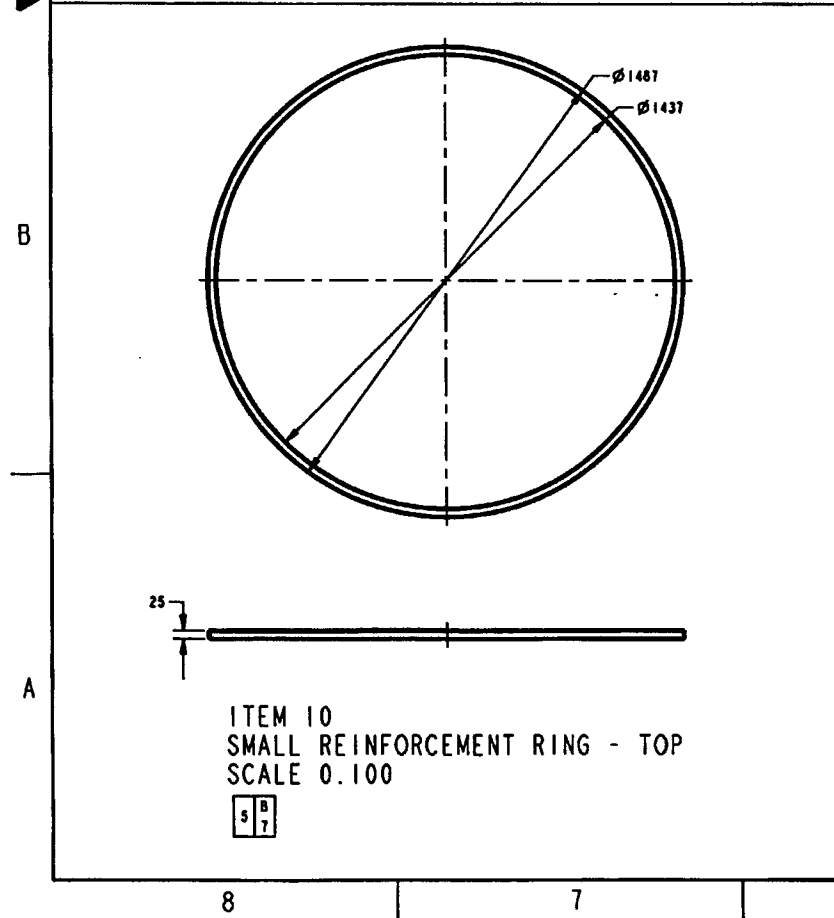
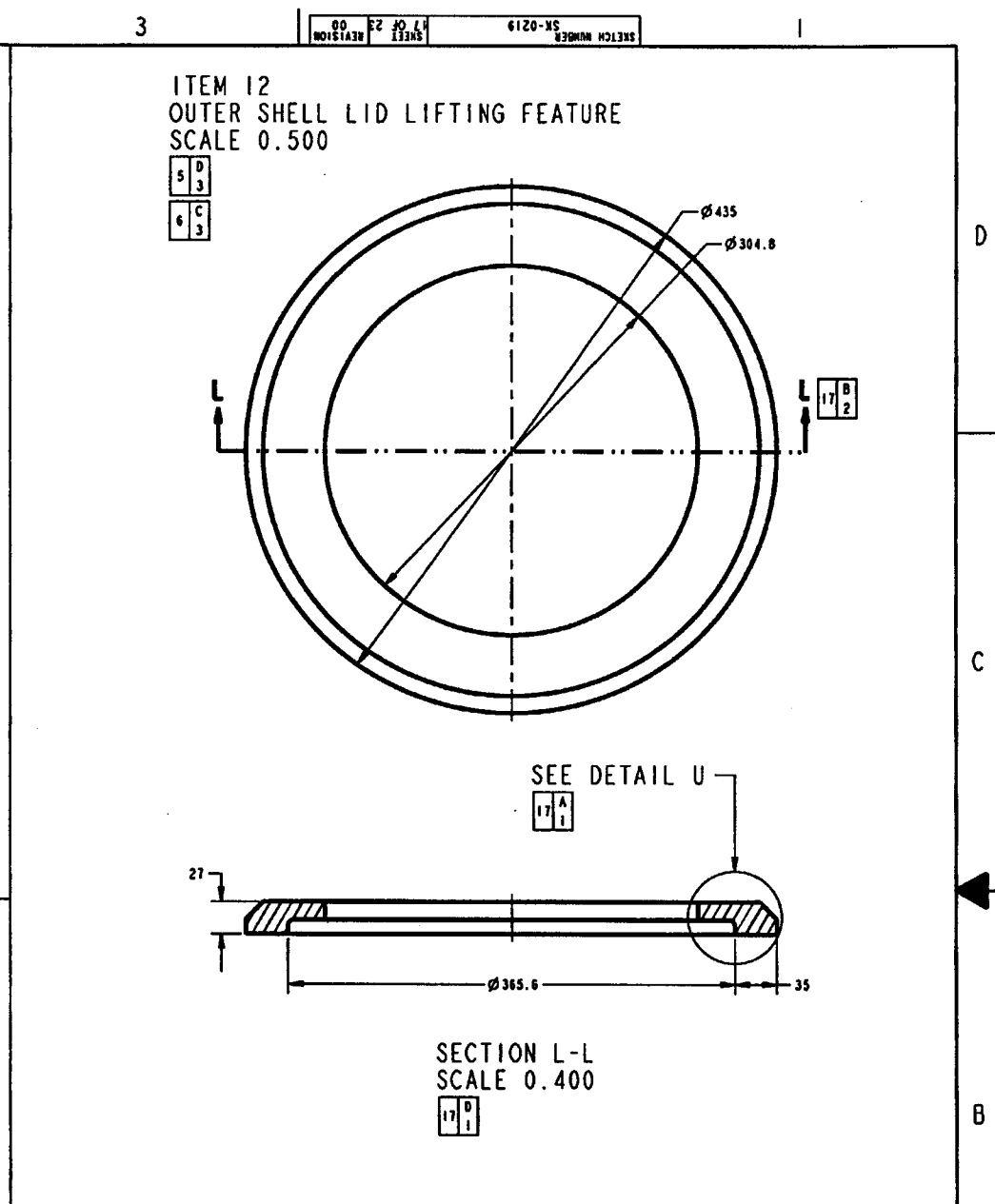
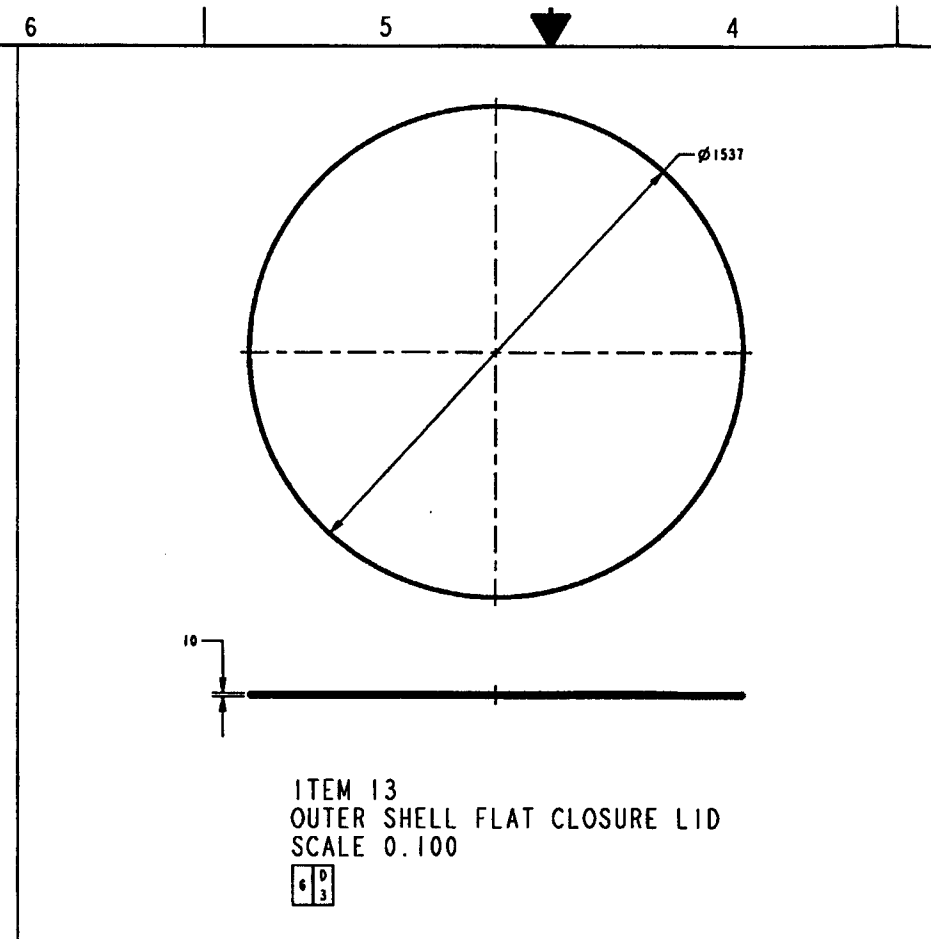
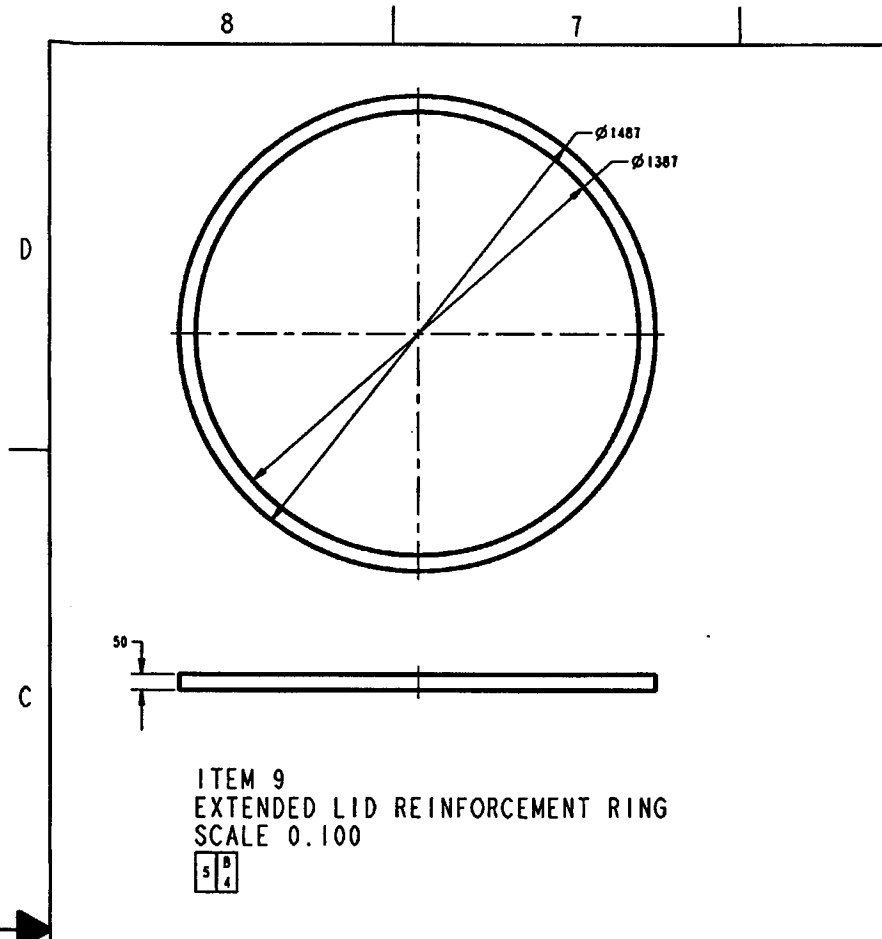


DETAIL N
 SCALE 1.500
 15 C
 1

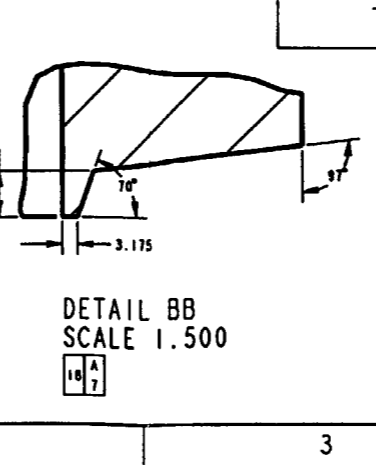
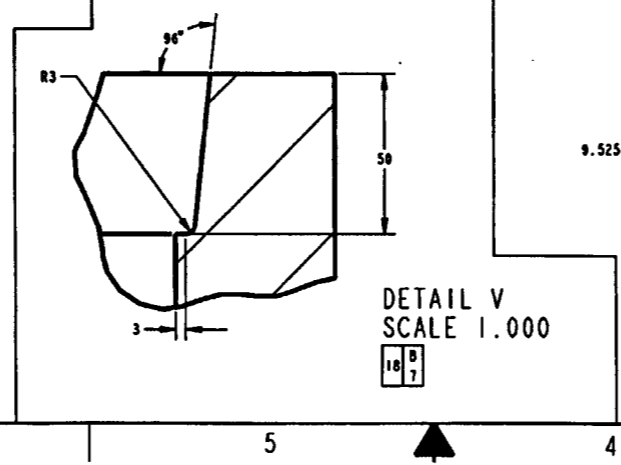
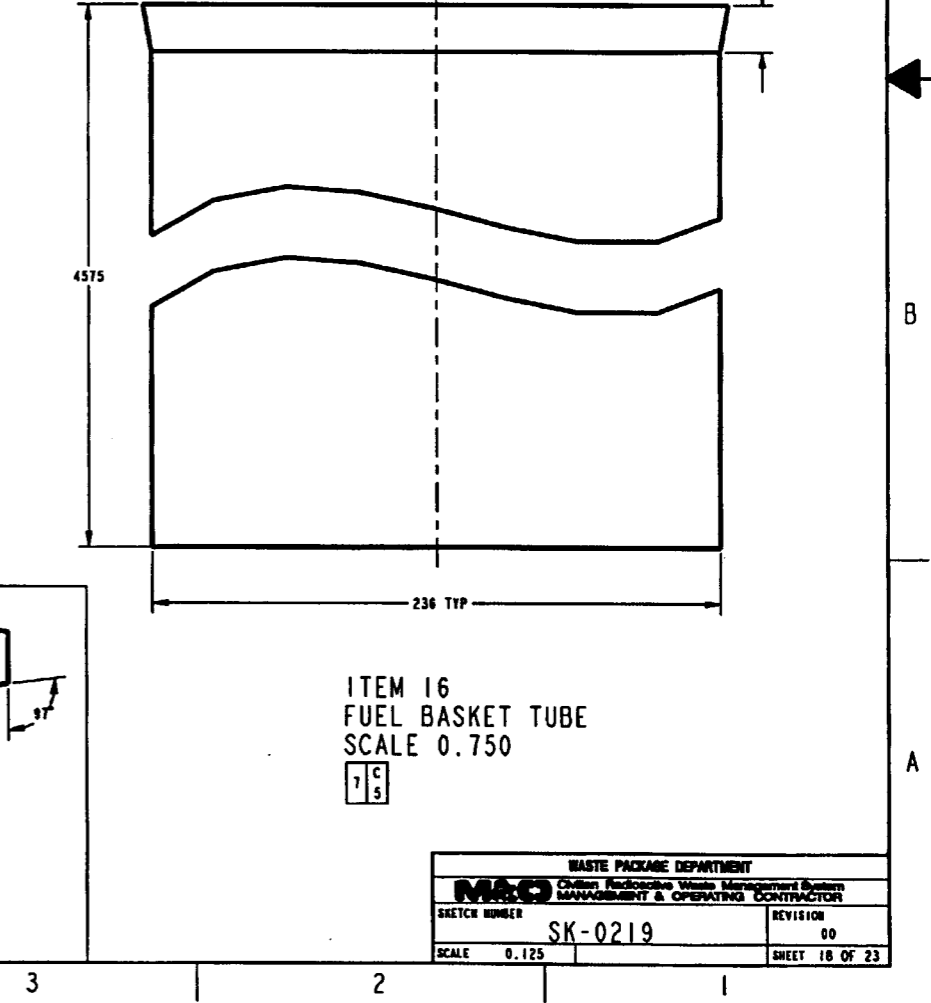
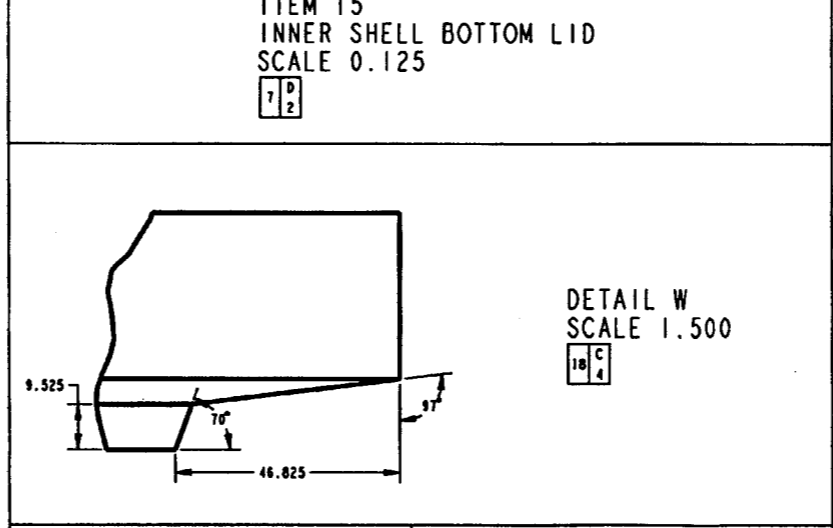
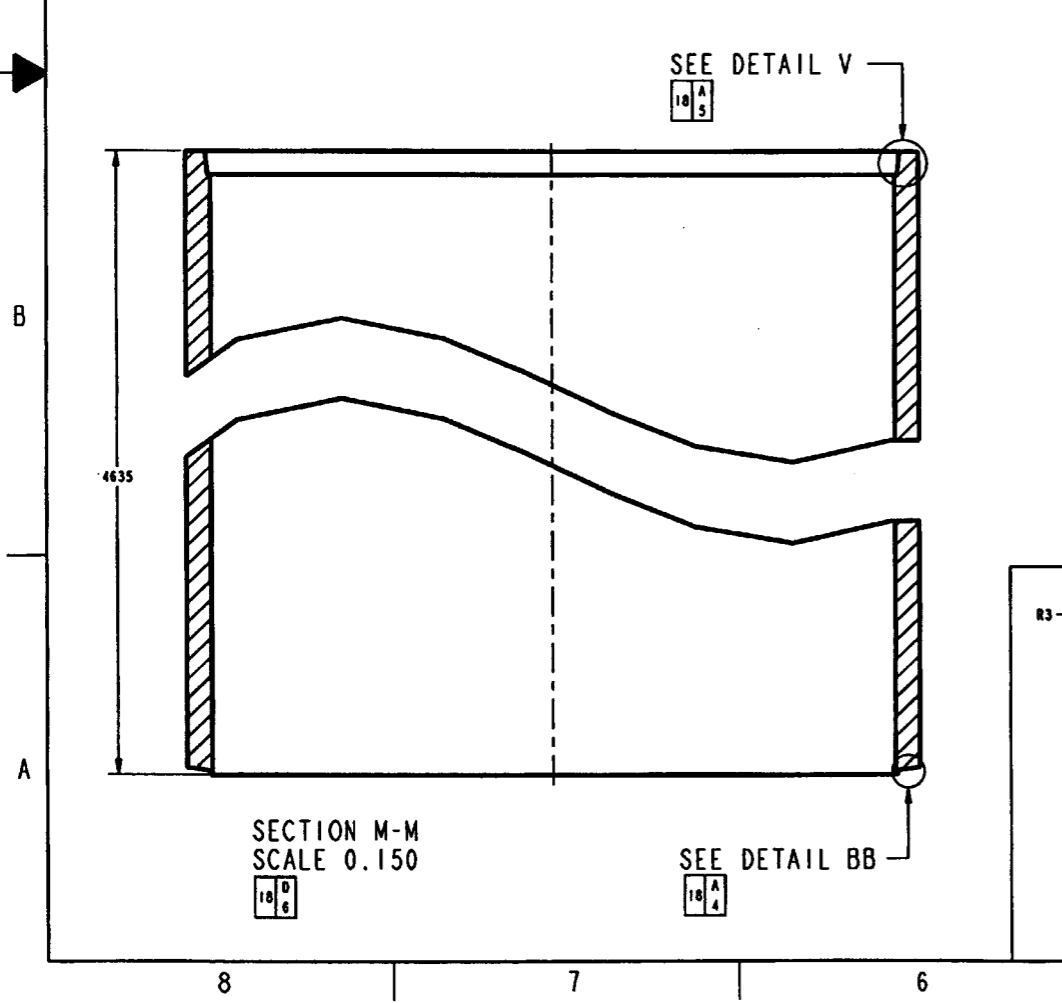
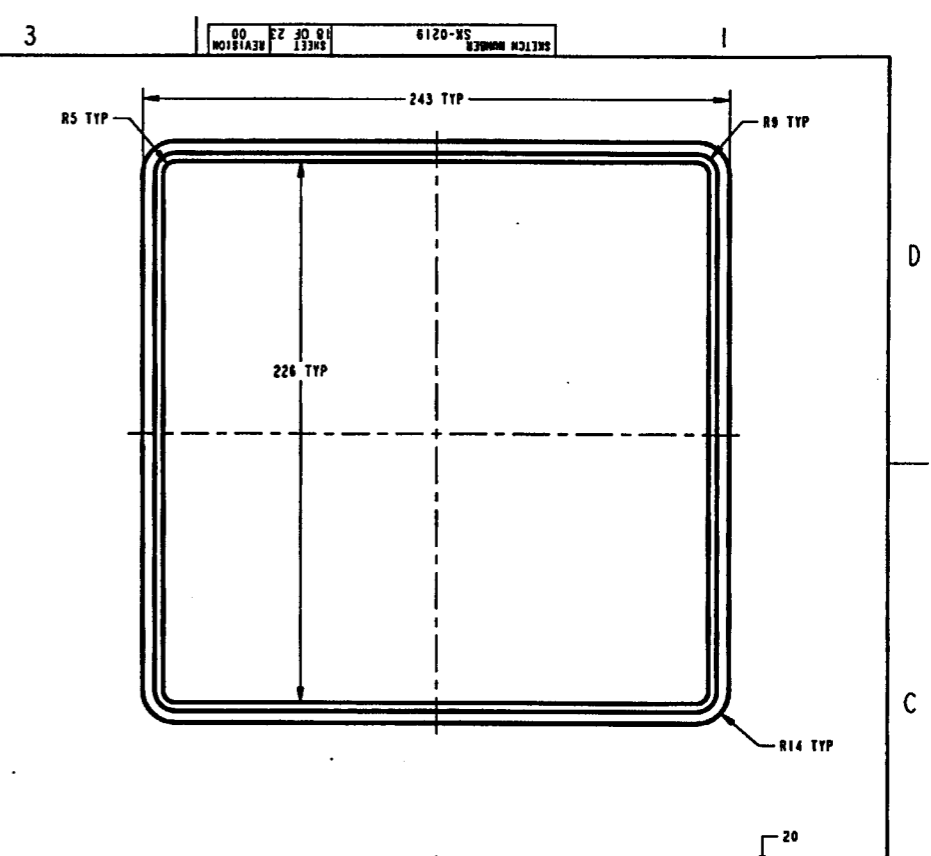
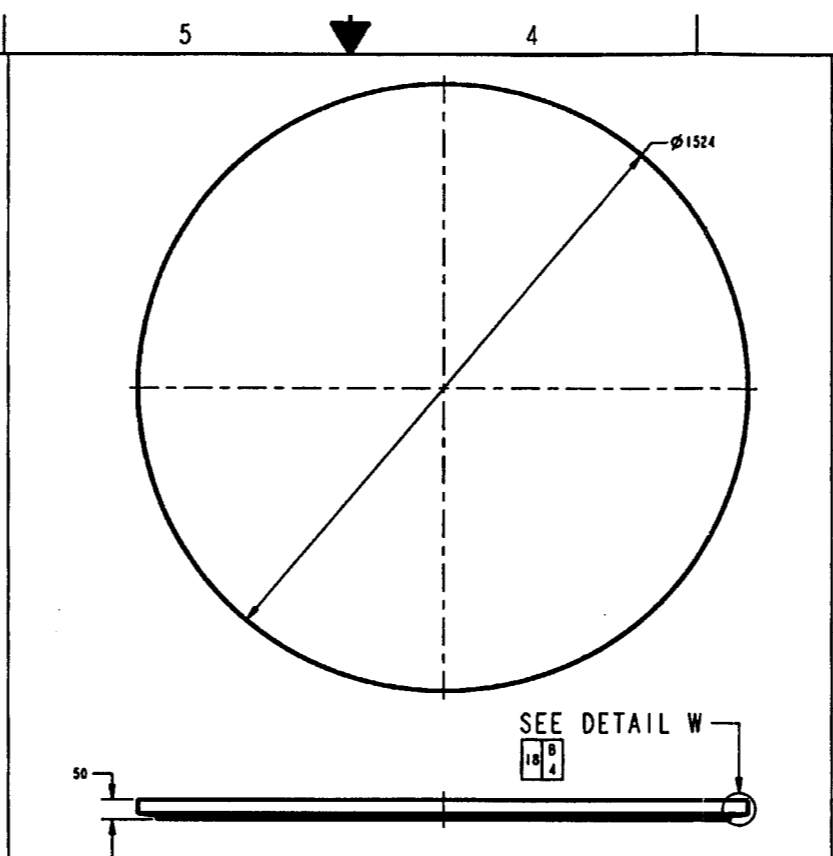
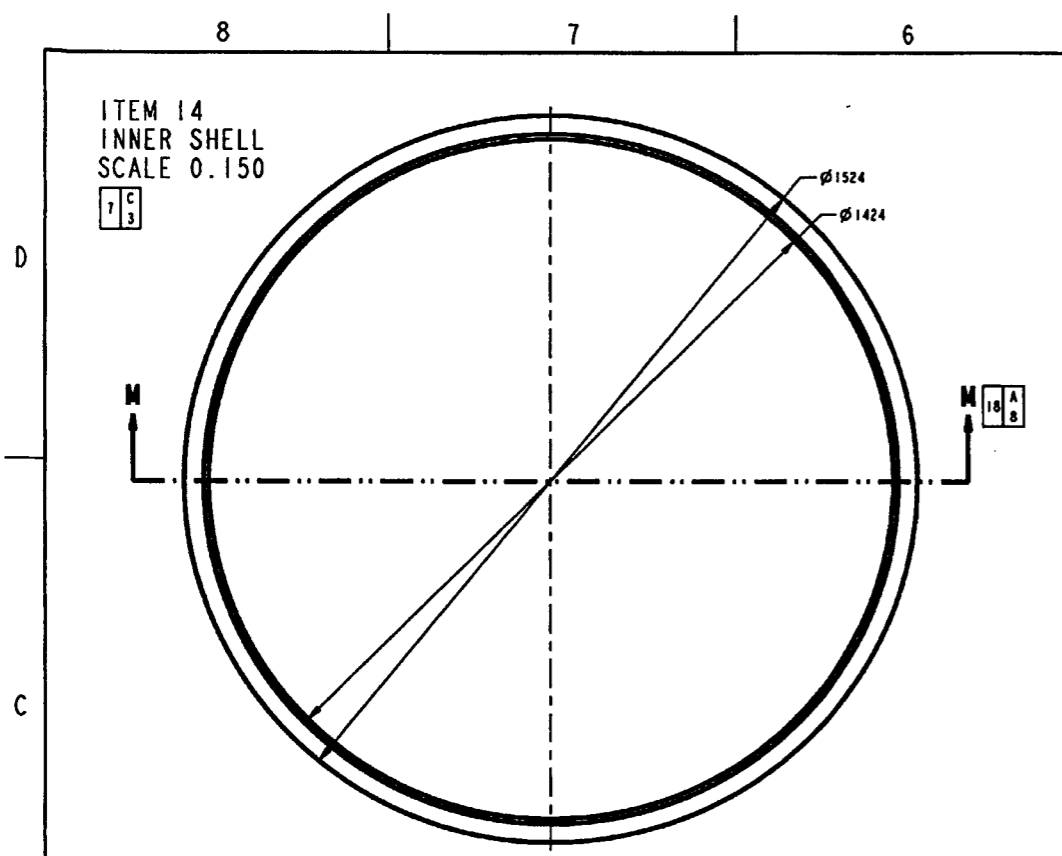
WASTE PACKAGE DEPARTMENT	
Civilian Radioactive Waste Management System MANAGEMENT & OPERATING CONTRACTOR	
SKETCH NUMBER SK-0219	REVISION 00
SCALE 0.125	SHEET 15 OF 23



WASTE PACKAGE DEPARTMENT	
M&O California Radioactive Waste Management System MANAGEMENT & OPERATING CONTRACTOR	
SKETCH NUMBER SK-0219	REVISION 00
SCALE 0.125	SHEET 18 OF 23

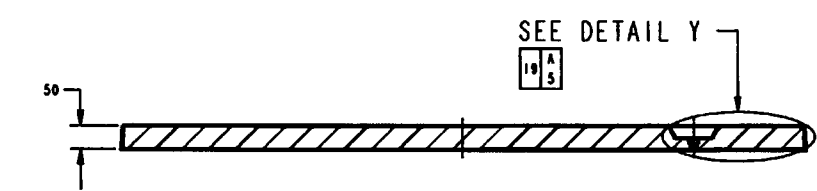
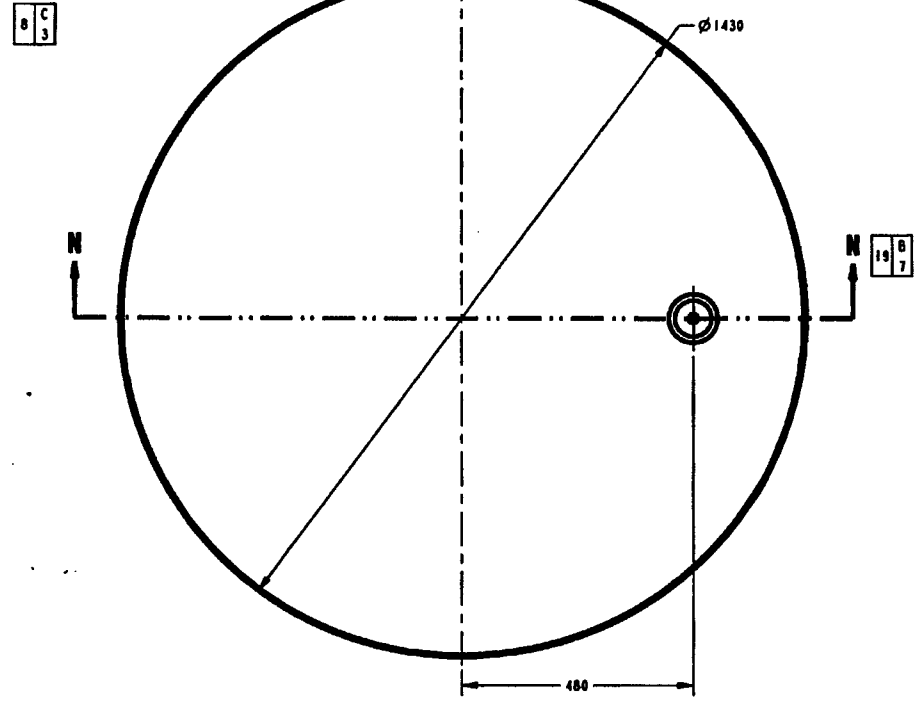


SKETCH NUMBER
SN-0219
REV OF 23
NO 18 A 3



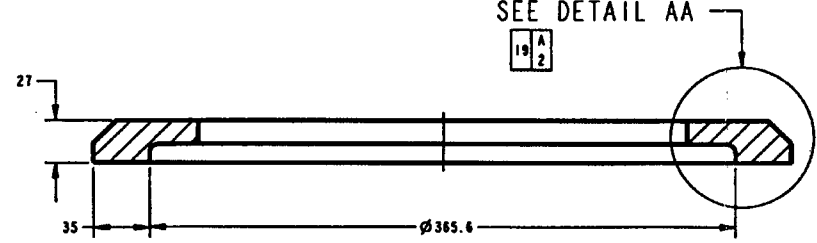
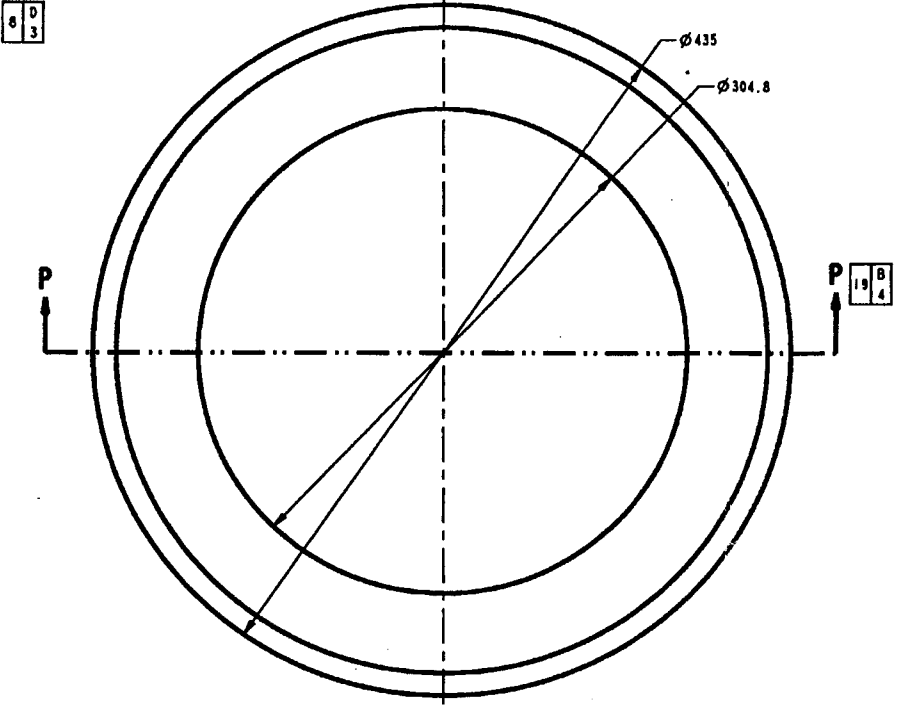
WASTE PACKAGE DEPARTMENT	
M&O Civilian Radioactive Waste Management System MANAGEMENT & OPERATING CONTRACTOR	
SKETCH NUMBER SK-0219	REVISION 00
SCALE 0.125	SHEET 18 OF 23

ITEM 17
 INNER SHELL TOP LID
 SCALE 0.150

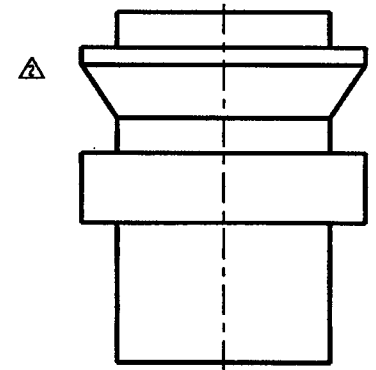
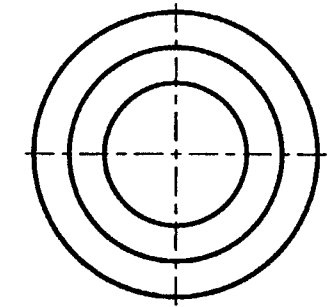


SECTION N-N
 SCALE 0.150

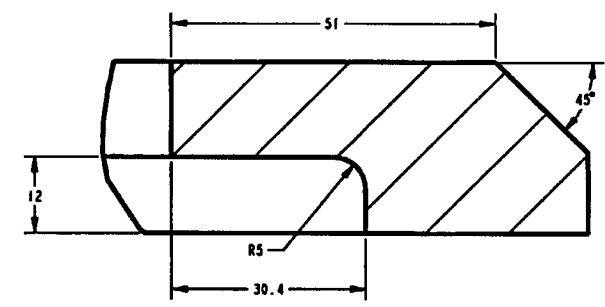
ITEM 18
 INNER LID LIFTING FEATURE
 SCALE 0.500



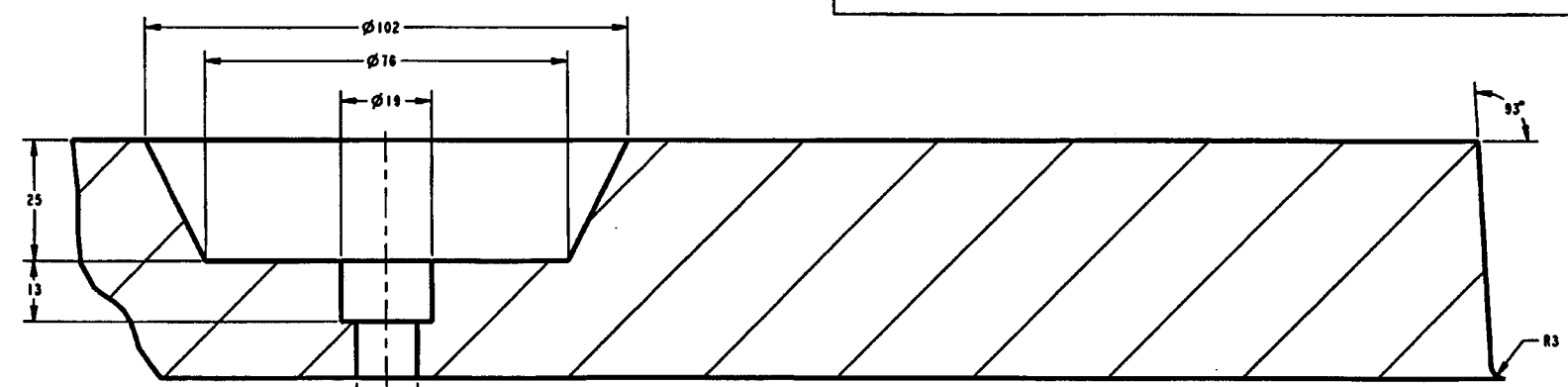
SECTION P-P
 SCALE 0.500



ITEM 19
 EVACUATION-BACKFILL QUICK RELEASE VALVE
 SCALE 3.500

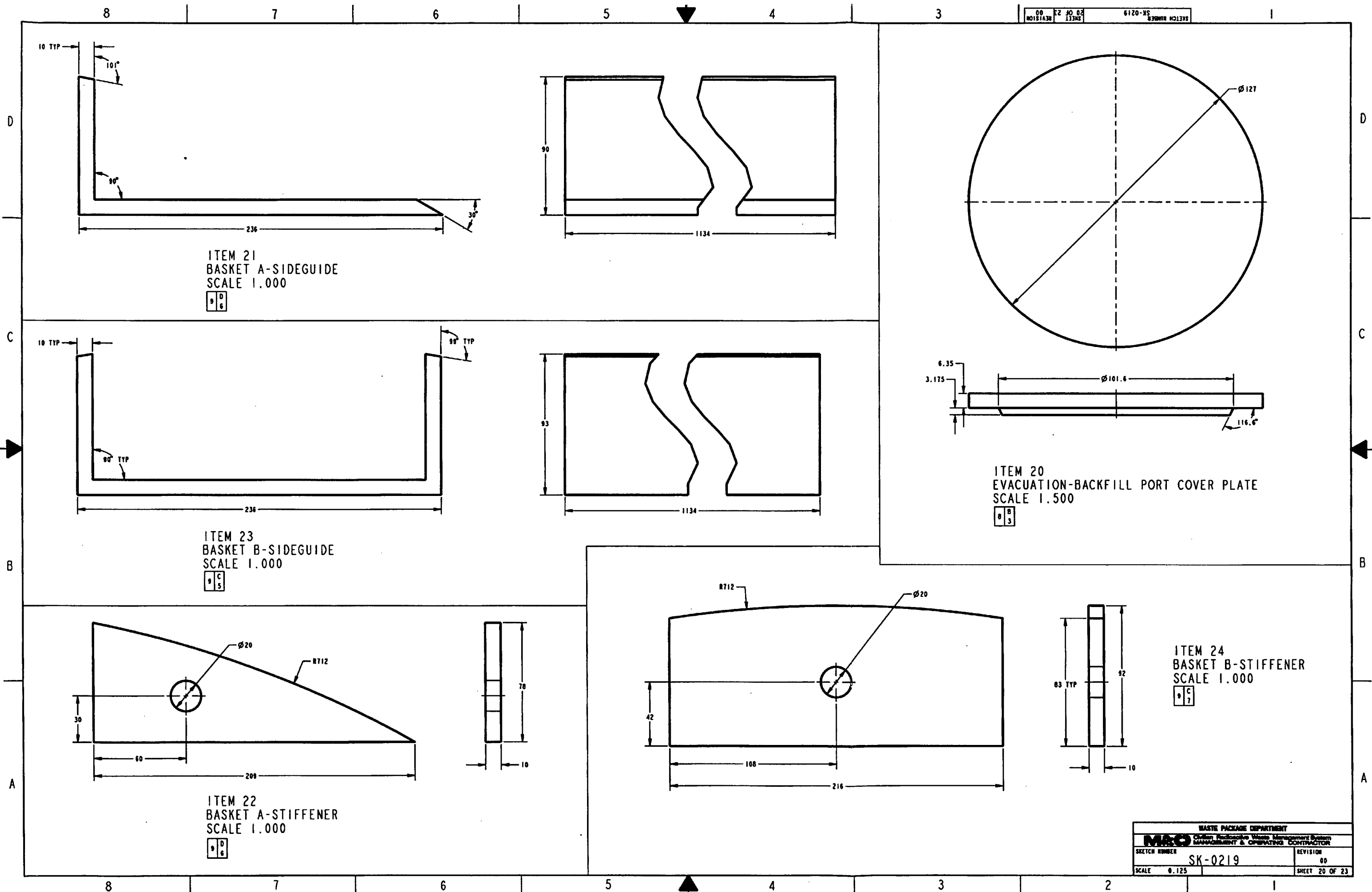


DETAIL AA
 SCALE 2.000



DETAIL Y
 SCALE 1.500

WASTE PACKAGE DEPARTMENT	
Civilian Radioactive Waste Management System	
MANAGEMENT & OPERATING CONTRACTOR	
SKETCH NUMBER	REVISION
SK-0219	00
SCALE 0.125	SHEET 19 OF 23



ITEM 21
 BASKET A-SIDEGUIDE
 SCALE 1.000
 9 0 6

ITEM 23
 BASKET B-SIDEGUIDE
 SCALE 1.000
 9 C 5

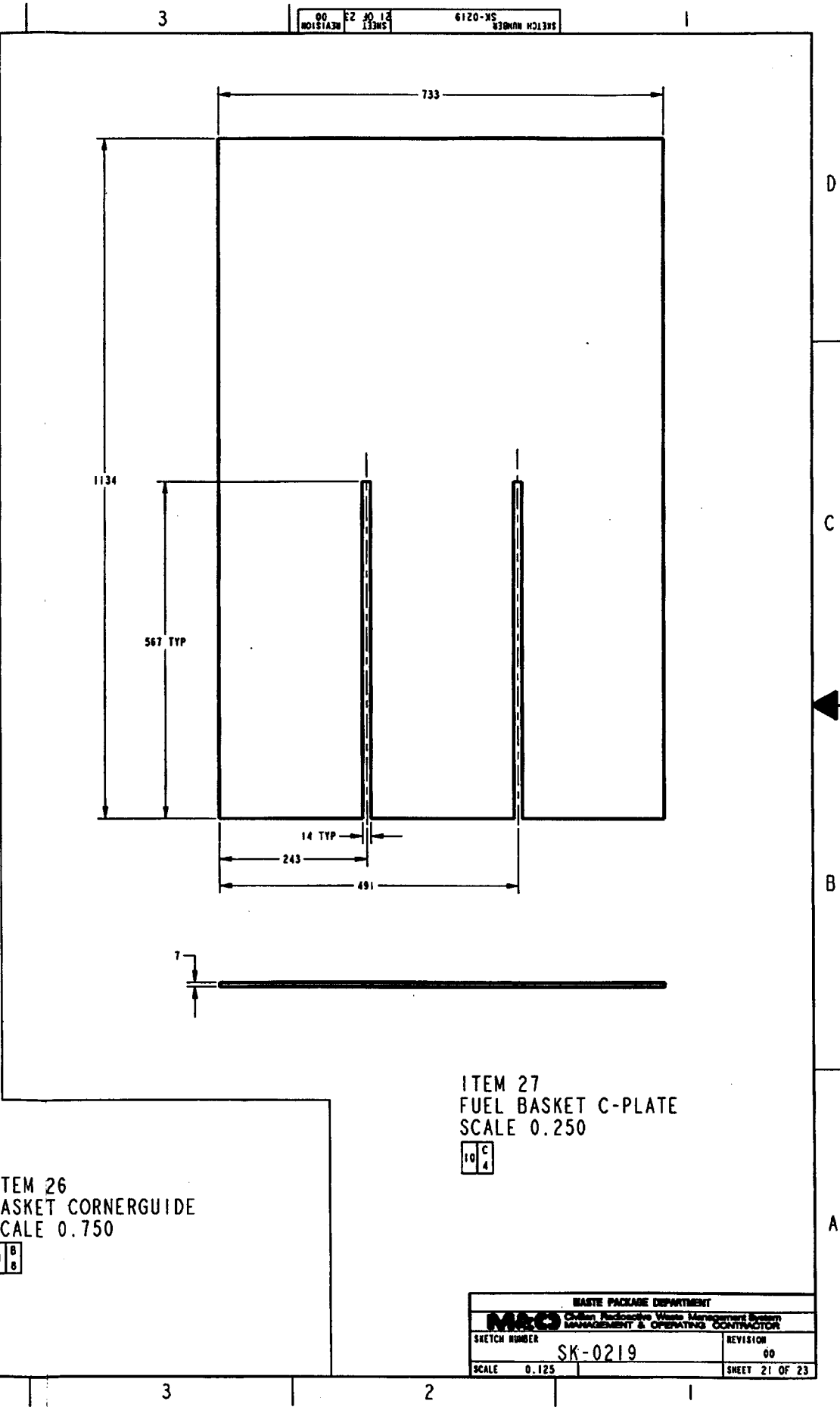
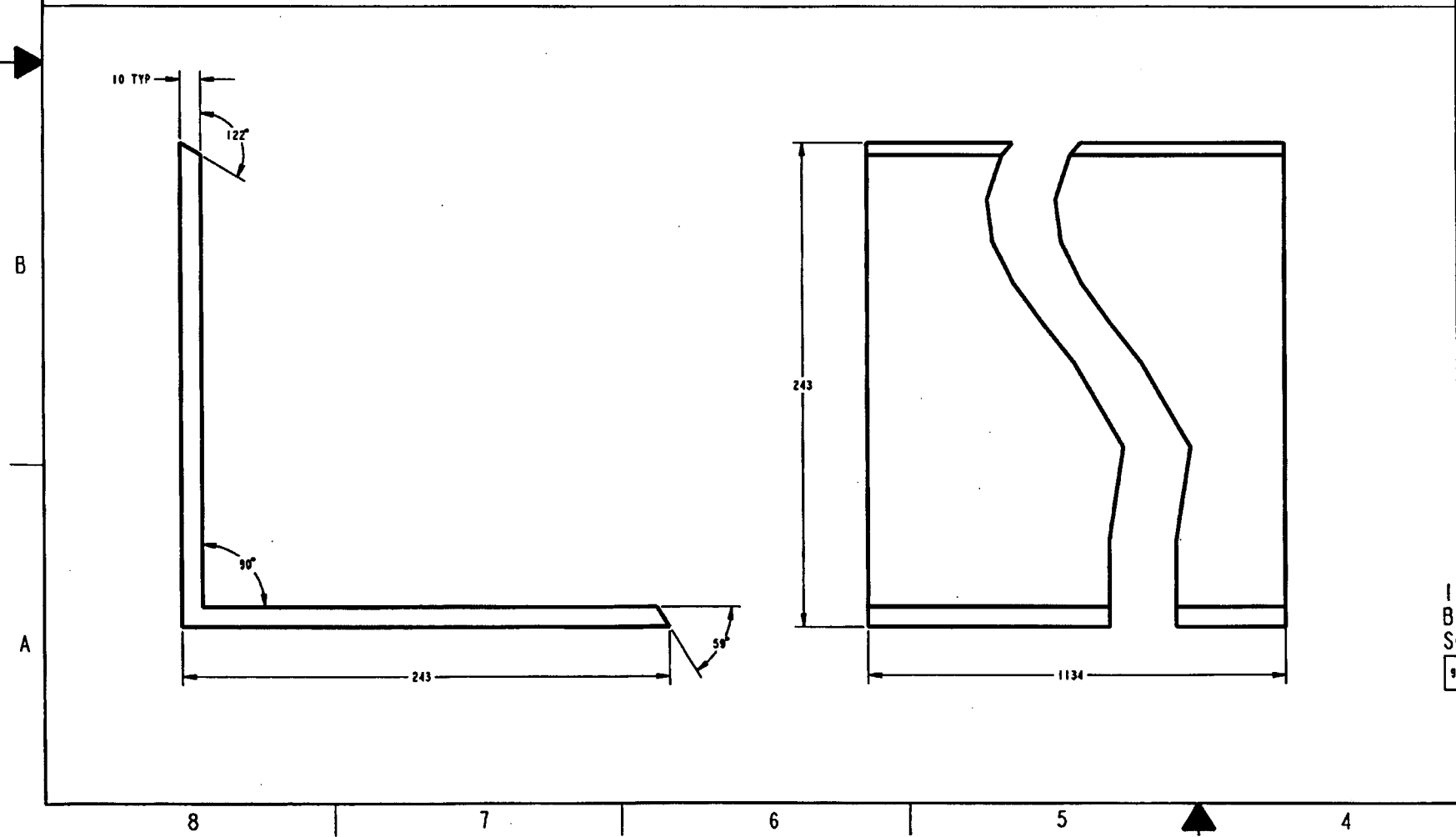
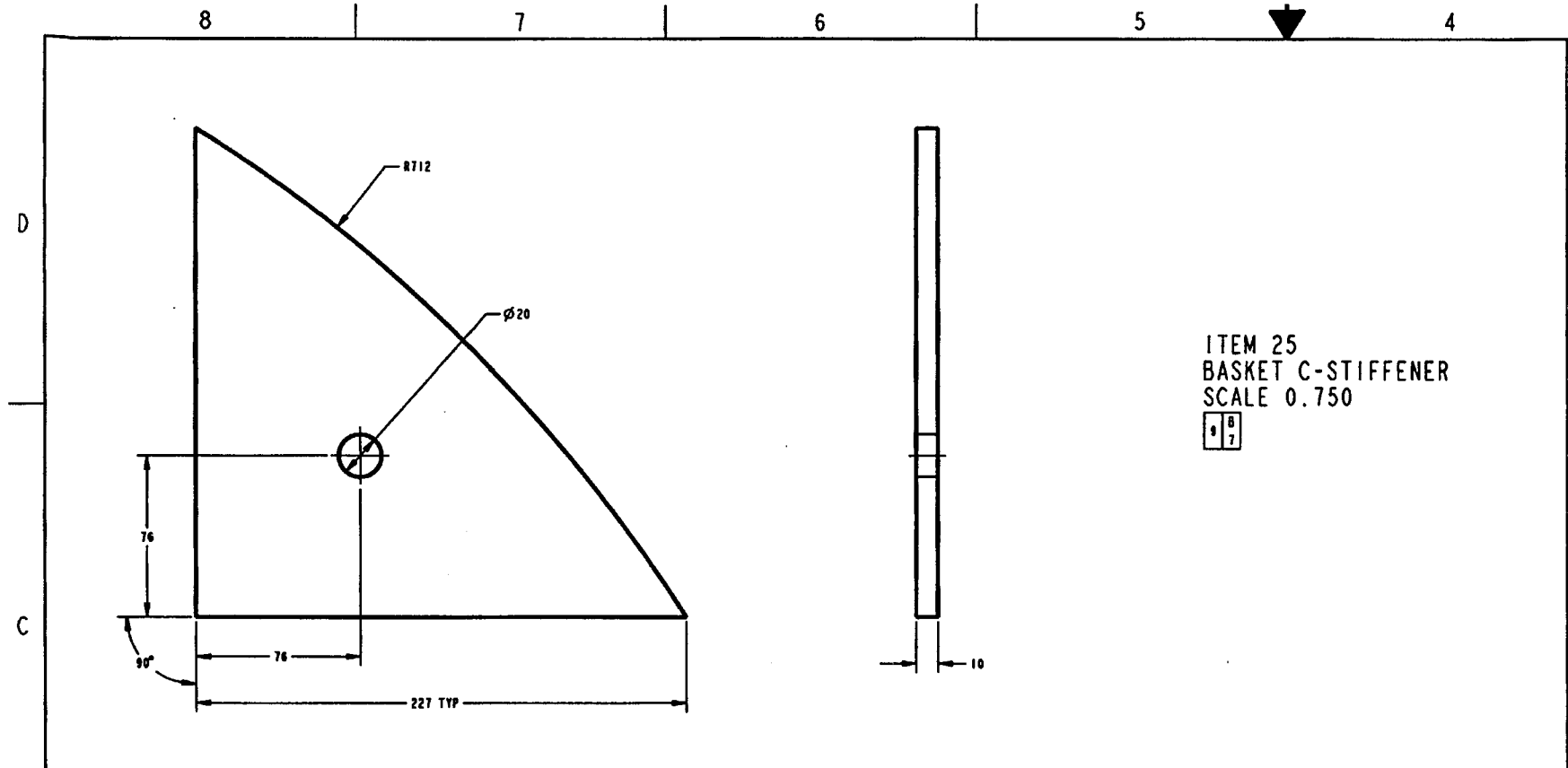
ITEM 20
 EVACUATION-BACKFILL PORT COVER PLATE
 SCALE 1.500
 8 B 3

ITEM 22
 BASKET A-STIFFENER
 SCALE 1.000
 9 D 6

ITEM 24
 BASKET B-STIFFENER
 SCALE 1.000
 9 C 7

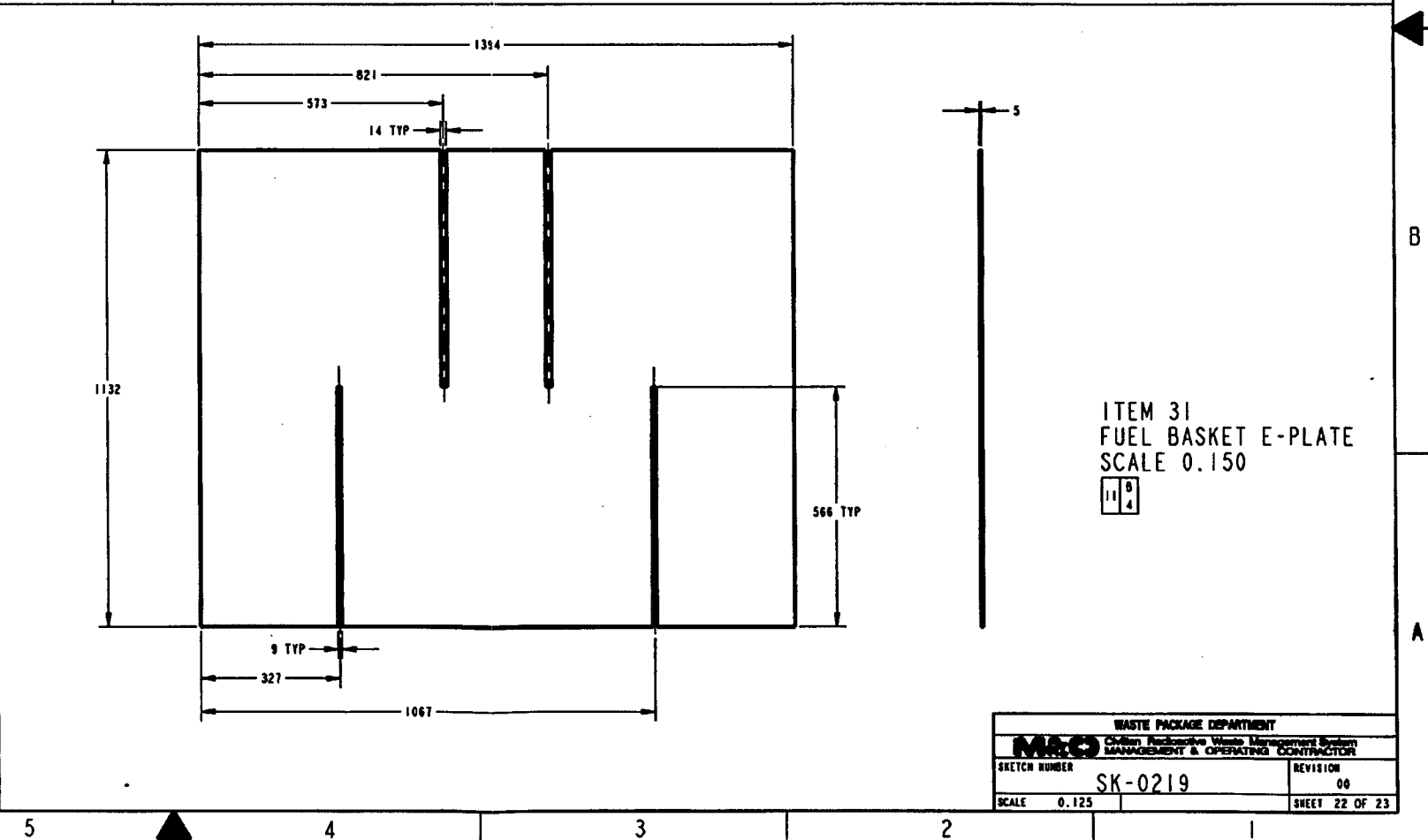
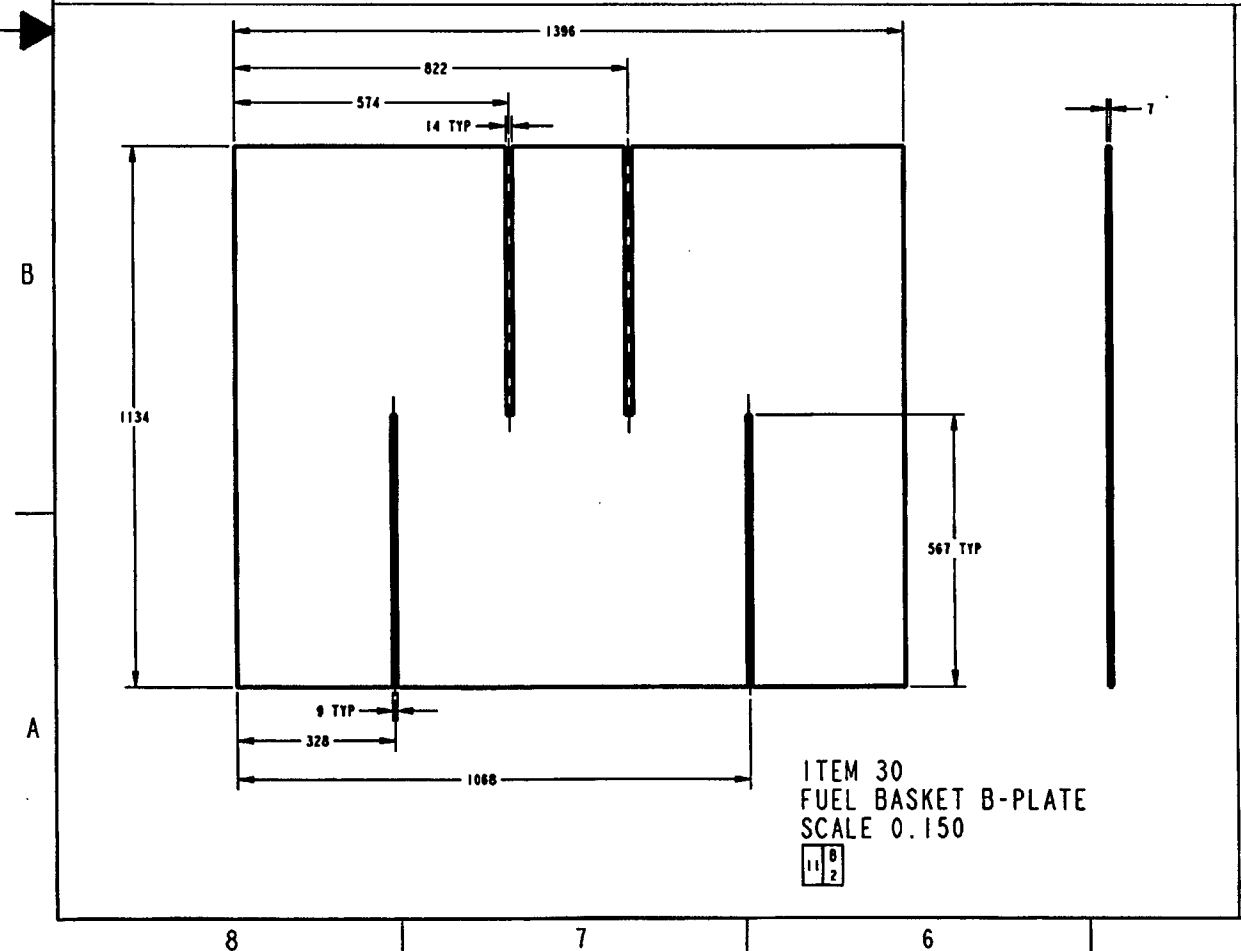
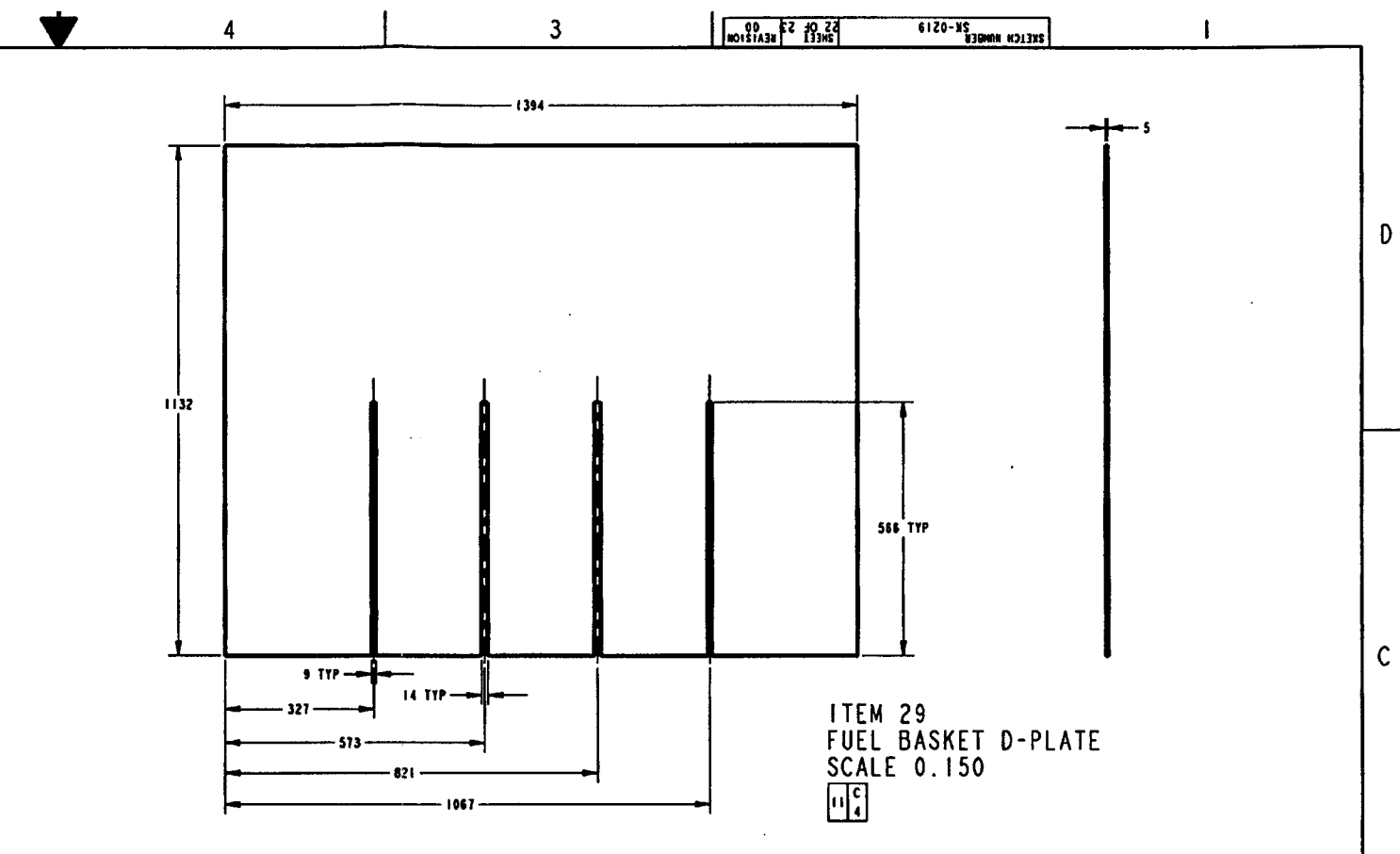
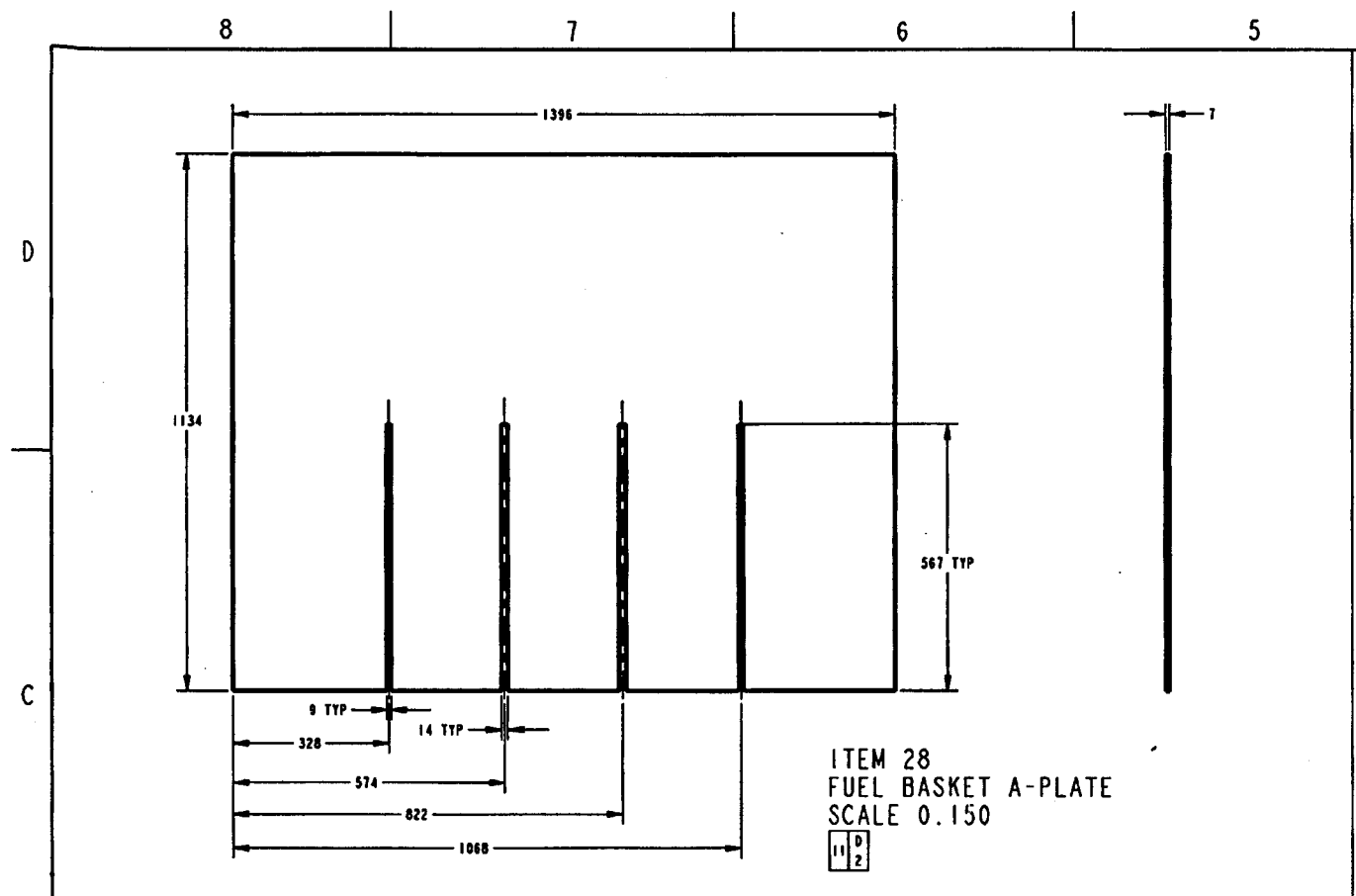
WASTE PACKAGE DEPARTMENT	
M&O Civilian Radioactive Waste Management System MANAGEMENT & OPERATING CONTRACTOR	
SKETCH NUMBER	SK-0219
REVISION	00
SCALE	0.125
SHEET 20 OF 23	

00	02	NO 12	6120-MS
NO121A2M	23	23	SK-0219



WASTE PACKAGE DEPARTMENT	
M&O Civilian Radioactive Waste Management System MANAGEMENT & OPERATING CONTRACTOR	
SKETCH NUMBER SK-0219	REVISION 00
SCALE 0.125	SHEET 21 OF 23

ITEM 26
BASKET CORNERGUIDE
SCALE 0.750



WASTE PACKAGE DEPARTMENT
M&O Calumet Nuclear Waste Management System
 MANAGEMENT & OPERATING CONTRACTOR

SKETCH NUMBER	SK-0219	REVISION	00
SCALE	0.125	SHEET 22 OF 23	

D

C

B

A

COMPONENT LIST								
ITEM NUMBER	ASSEMBLY	SUBASSEMBLY	SUBASSEMBLY	SUBASSEMBLY	COMPONENT NAME	MATERIAL	THICKNESS	QTY REQD
-1	21-PWR WASTE PACKAGE ASSEMBLY	-	-	-	-	-	-	24647
-2	-	OUTER SHELL ASSEMBLY	-	-	-	-	-	24671
1	-	-	-	-	OUTER SHELL	SB-575 N06022	20	4152
2	-	-	-	-	UPPER TRUNNION COLLAR SLEEVE	SB-575 N06022	40	446
3	-	-	-	-	LOWER TRUNNION COLLAR SLEEVE	SB-575 N06022	40	436
4	-	-	-	-	SHELL INTERFACE RING	SA-240 S31600	30	66
5	-	-	-	-	INNER SHELL SUPPORT RING	SB-575 N06022	40	47
6	-	-	-	-	OUTER SHELL FLAT BOTTOM LID	SB-575 N06022	25	416
-3	-	EXTENDED OUTER SHELL LID ASSEMBLY	-	-	-	-	-	718
7	-	-	-	-	EXTENDED OUTER SHELL LID	SB-575 N06022	25	133
8	-	-	-	-	EXTENDED OUTER SHELL LID BASE	SB-575 N06022	25	371
9	-	-	-	-	EXTENDED LID REINFORCEMENT RING	SB-575 N06022	50	98
10	-	-	-	-	SMALL REINFORCEMENT RING - TOP	SB-575 N06022	25	25
11	-	-	-	-	SMALL REINFORCEMENT RING - BOTTOM	SB-575 N06022	25	23
12	-	-	-	-	OUTER SHELL LID LIFTING FEATURE	SB-575 N06022	27	13
-4	-	OUTER SHELL FLAT CLOSURE LID ASSEMBLY	-	-	-	-	-	176
13	-	-	-	-	OUTER SHELL FLAT CLOSURE LID	SB-575 N06022	10	161
12	-	-	-	-	OUTER SHELL LID LIFTING FEATURE	SB-575 N06022	27	13
-5	-	INNER SHELL ASSEMBLY	-	-	-	-	-	18062
14	-	-	-	-	INNER SHELL	SA-240 S31600	50	8529
15	-	-	-	-	INNER SHELL BOTTOM LID	SA-240 S31600	50	708
16	-	-	-	-	FUEL BASKET TUBE	SA-516 K02700	5	164
-6	-	INNER SHELL TOP LID ASSEMBLY	-	-	-	-	-	646
17	-	-	-	-	INNER SHELL TOP LID	SA-240 S31600	50	632
18	-	-	-	-	INNER LID LIFTING FEATURE	SA-240 S31600	27	12
19	-	-	-	-	EVACUATION-BACKFILL QUICK RELEASE VALVE	SA-240 S31600	12.7	.06
20	-	-	-	-	EVACUATION-BACKFILL PORT COVER PLATE	SA-240 S31600	6.4	.84
-7	-	END SIDEGUIDE ASSEMBLY	-	-	-	-	-	29
21	-	-	-	-	BASKET A-SIDEGUIDE	SA-516 K02700	10	27
22	-	-	-	-	BASKET A-STIFFENER	SA-516 K02700	10	.72
-8	-	SIDEGUIDE ASSEMBLY	-	-	-	-	-	30
23	-	-	-	-	BASKET B-SIDEGUIDE	SA-516 K02700	10	36
24	-	-	-	-	BASKET B-STIFFENER	SA-516 K02700	10	1.5
-9	-	CORNERGUIDE ASSEMBLY	-	-	-	-	-	47
25	-	-	-	-	BASKET C-STIFFENER	SA-516 K02700	10	2.3
26	-	-	-	-	BASKET CORNERGUIDE	SA-516 K02700	10	42
-10	-	FUEL PLATE ASSEMBLY	-	-	-	-	-	599
27	-	-	-	-	FUEL BASKET C-PLATE	NEUTRONIT A 978	7	44
-11	-	FUEL PLATE A-D ASSEMBLY	-	-	-	SA-516 K02700	7	45
28	-	-	-	-	FUEL BASKET A-PLATE	NEUTRONIT A 978	7	85
29	-	-	-	-	FUEL BASKET D-PLATE	SA-516 K02700	7	86
-12	-	FUEL PLATE B-E ASSEMBLY	-	-	-	SB-209 A96061 T4	5	21
30	-	-	-	-	FUEL BASKET B-PLATE	NEUTRONIT A 978	7	85
31	-	-	-	-	FUEL BASKET E-PLATE	SA-516 K02700	7	86
-	-	-	-	-	TOTAL ALLOY 22 WELOS	SFA-5.14 N06022	-	183
-	-	-	-	-	TOTAL 316 WELOS	SFA-5.9 S31600	-	59
-	-	PWR FUEL ASSEMBLY	-	-	-	-	-	773.4
-	-	21-PWR WP ASSEMBLY WITH SNF	-	-	-	-	-	40889
-	-	-	-	-	-	-	-	40913

WELD LIST				
WELD NUMBER	WELD TYPE	MATERIAL	BASE PTH	QTY REQD
1	GROOVE	SFA-5.14 N06022	7.8	1
2	FILLET	SFA-5.14 N06022	35	1
3	FILLET	SFA-5.14 N06022	13	1
4	FILLET	SFA-5.14 N06022	12	1
5	FILLET	SFA-5.14 N06022	12	1
6	FILLET	SFA-5.14 N06022	11	1
7	FILLET	SFA-5.14 N06022	.20	2
8	FILLET	SFA-5.14 N06022	.98	2
9	GROOVE	SFA-5.14 N06022	3.2	2
10	FILLET	SFA-5.14 N06022	2.1	1
11	SQUARE	SFA-5.14 N06022	1.7	1
12	GROOVE	SFA-5.9 S31600	17	1
13	FILLET	SFA-5.9 S31600	.18	1
14	FILLET	SFA-5.9 S31600	.90	1
15	FILLET	SFA-5.9 S31600	.01	1
16	FILLET	SFA-5.9 S31600	.07	1
17	FILLET	SFA-5.14 N06022	14	2
18	GROOVE	SFA-5.9 S31600	40	1
19	GROOVE	SFA-5.14 N06022	1.9	1
20	FILLET	SFA-5.14 N06022	.81	1
21	GROOVE	SFA-5.14 N06022	13	1
22	FILLET	SFA-5.14 N06022	37	1
TOTAL ALLOY 22 WELOS		SFA-5.14 N06022	183	-
TOTAL 316 WELOS		SFA-5.9 S31600	59	-

- NOTES:
- ⚠ U-GROOVE WELD DIMENSIONS ARE TYPICAL FOR WELD 1, AND WELD 12.
 - ⚠ GEOMETRY FOR THE EVACUATION-BACKFILL VALVE IS TBD.
 - ⚠ THE 21-PWR WASTE PACKAGE CONFIGURATION WITH ABSORBER PLATES IS IDENTICAL TO THE 21-PWR WASTE PACKAGE CONFIGURATION WITH CONTROL RODS, EXCEPT FOR THE MATERIAL COMPOSITION OF THE FUEL BASKET A, B, AND C PLATES. ALL INFORMATION PROVIDED IN THIS TABLE IS FOR THE 21-PWR WASTE PACKAGE CONFIGURATION WITH ABSORBER PLATES, UNLESS OTHERWISE NOTED.
 - ⚠ INFORMATION FOR THE 21-PWR WASTE PACKAGE CONFIGURATION WITH CONTROL RODS.
 - ⚠ CRWMS M&O 1997, WASTE CONTAINER CAVITY SIZE DETERMINATION. BBA00000-01717-0200-00026 REV 00. LAS VEGAS, NV: CRWMS M&O. ACC. NO. 19960106.0061

WASTE PACKAGE DEPARTMENT	
M&O <small>Customer Radioactive Waste Management System</small>	
MANAGEMENT & OPERATING CONTRACTOR	
SKETCH NUMBER	REVISION
SK-0219	00
SCALE 0.125	SHEET 23 OF 23

Time = 0

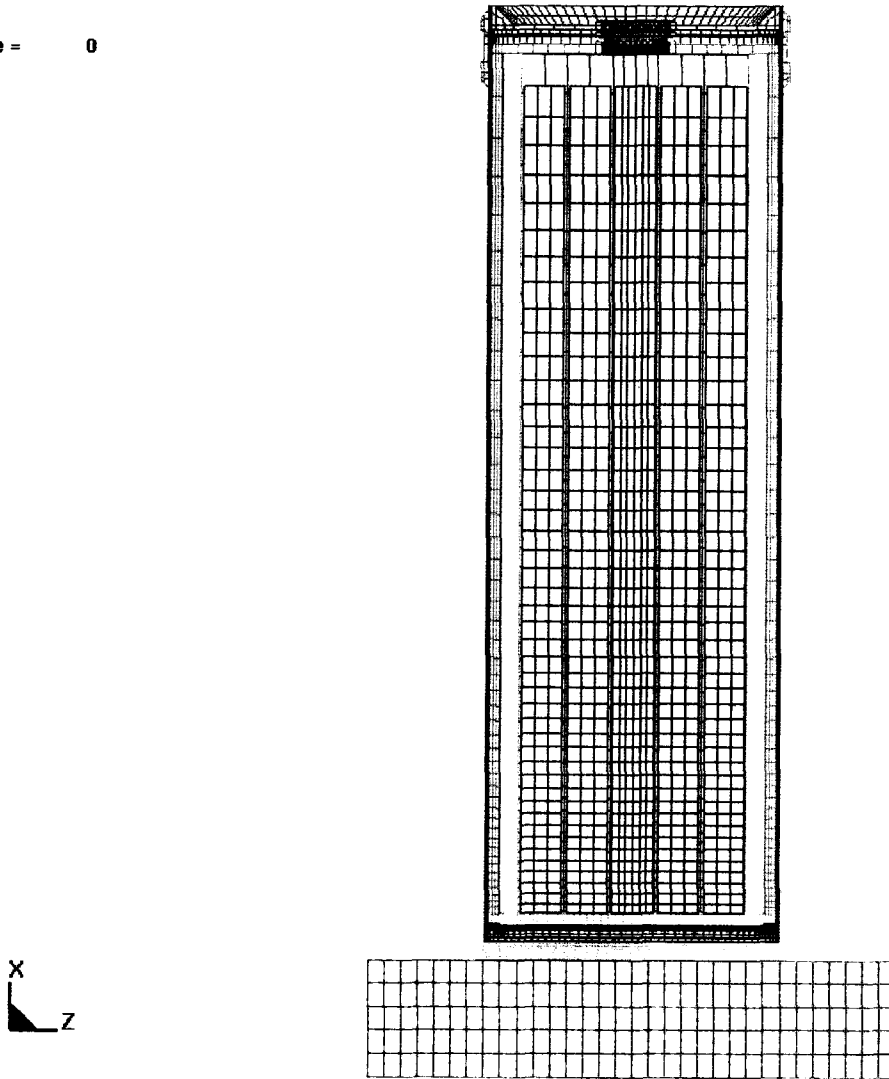


Figure II-1. Finite Element Representation of 21-PWR Waste Package and Unyielding Surface (Half Symmetry)

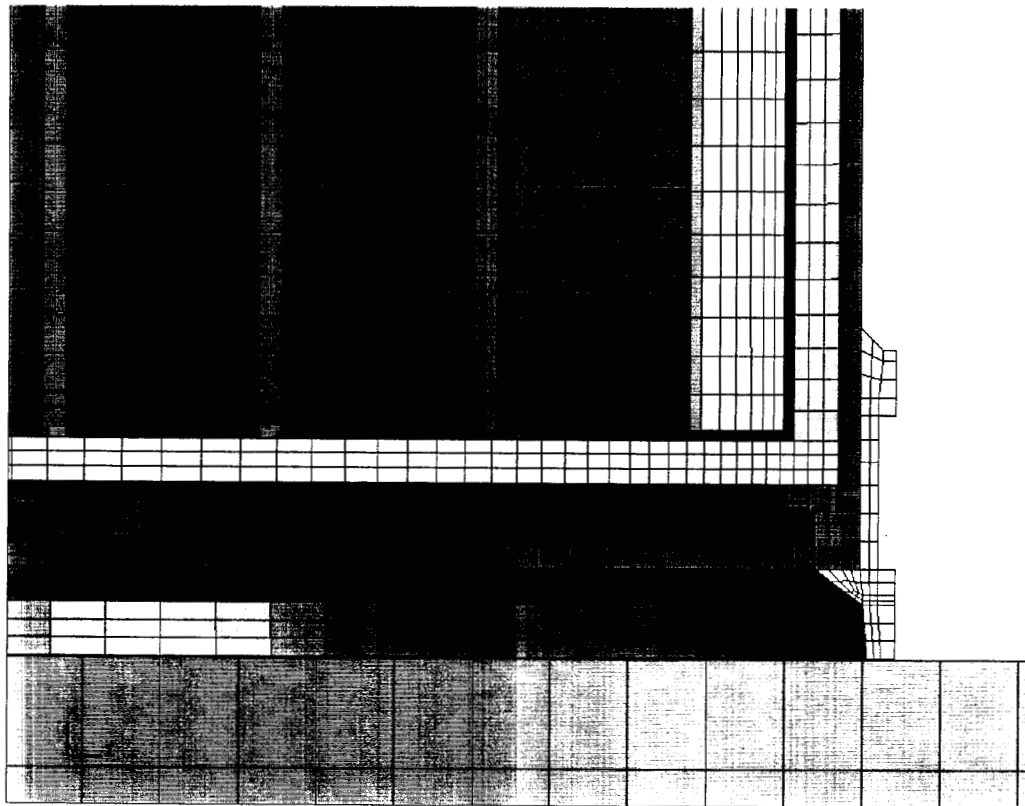


Figure II-2. Detailed View of Cross Section of 21-PWR WP and Unyielding Surface

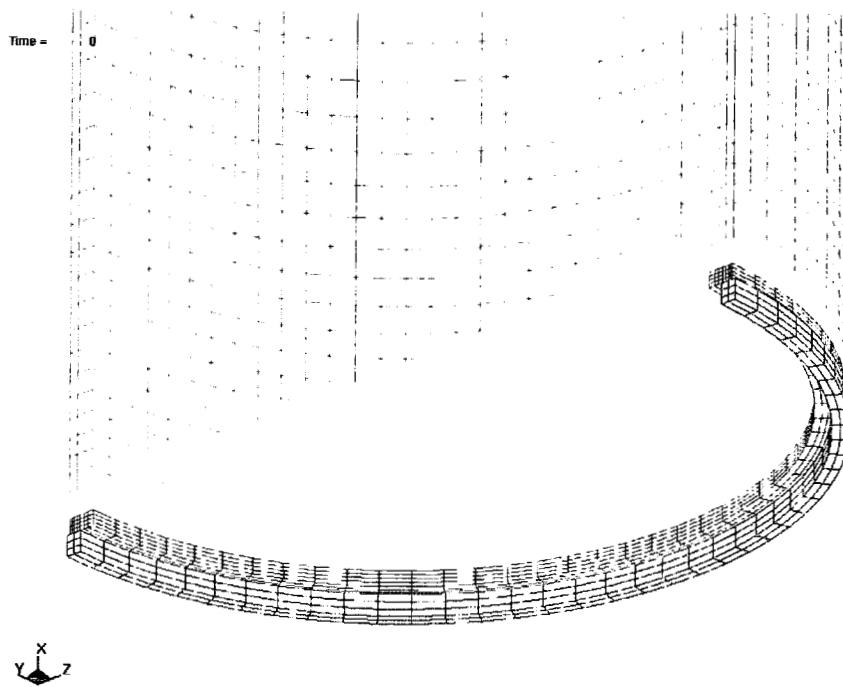


Figure II-3. Detailed View of Inner Shell, Inner Shell Bottom Lid, Interface Ring, and Inner Shell Support Ring

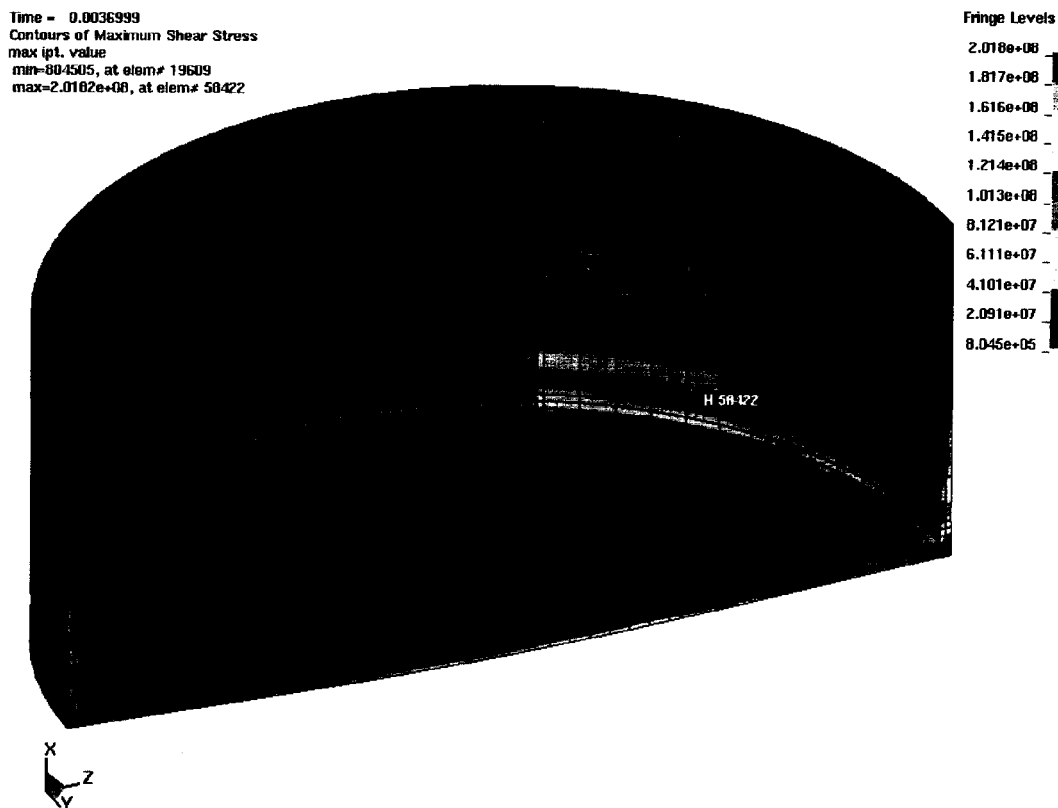


Figure II-4. Shear Stress in Outer Shell of 21-PWR WP (at Room Temperature)

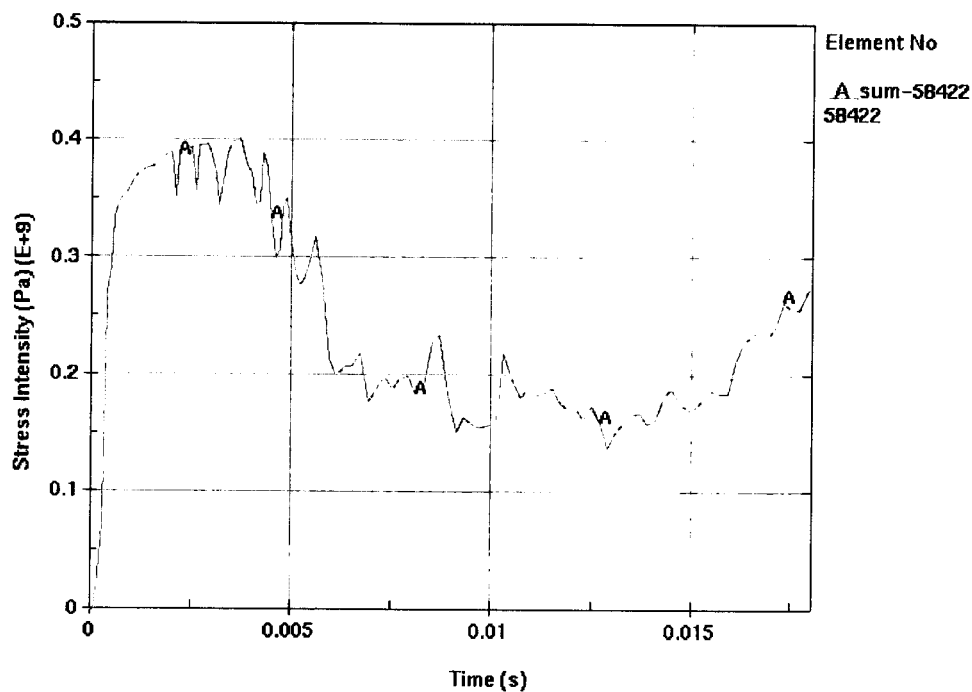


Figure II-5. Stress Intensity Plot for Element No. 58422 of Outer Shell (at Room Temperature)

Time = 0.0075434
 Contours of Maximum Shear Stress
 max (pt. value)
 min=336917, at elem# 7694
 max=1.75699e+08, at elem# 16454

Fringe Levels
 1.757e+08
 1.582e+08
 1.406e+08
 1.231e+08
 1.056e+08
 8.802e+07
 7.048e+07
 5.295e+07
 3.541e+07
 1.787e+07
 3.369e+05

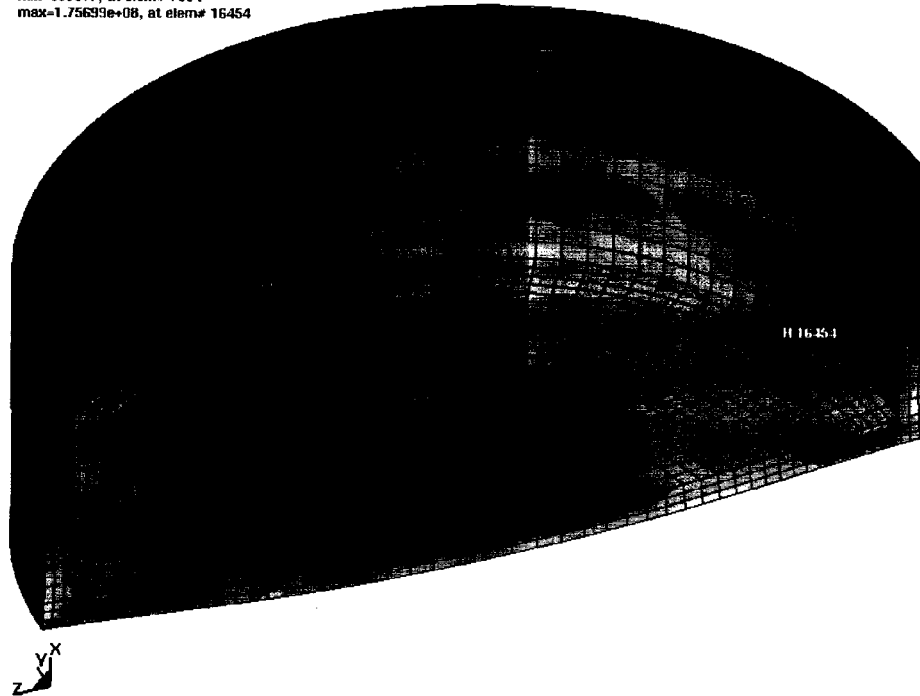


Figure II-6. Shear Stress in Inner Shell of 21-PWR WP (at Room Temperature)

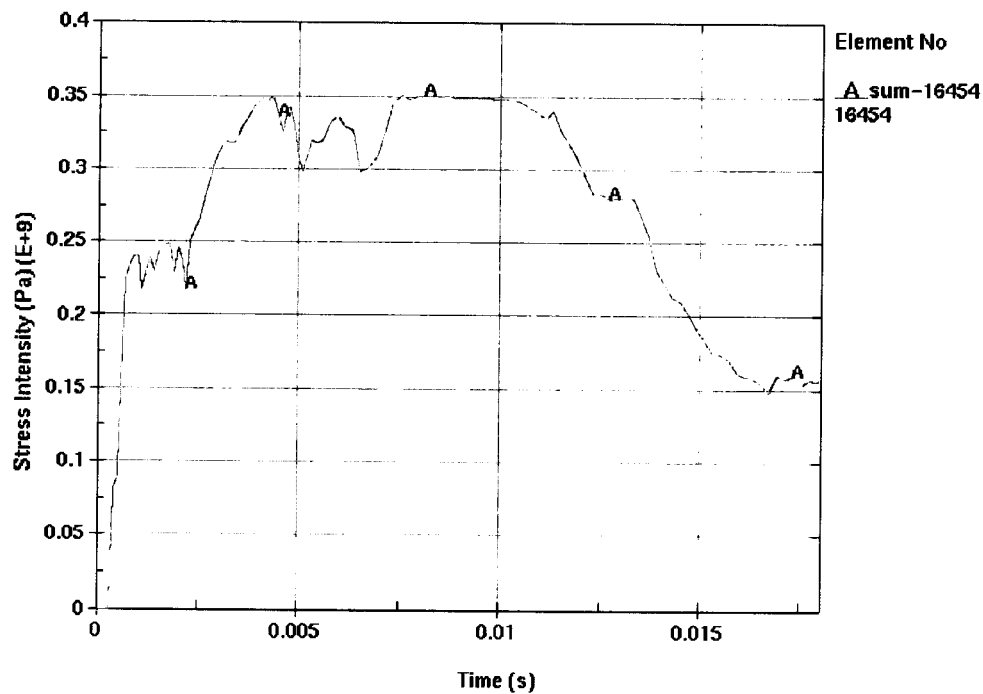


Figure II-7. Stress Intensity Plot for Element No. 16454 of Inner Shell (at Room Temperature)

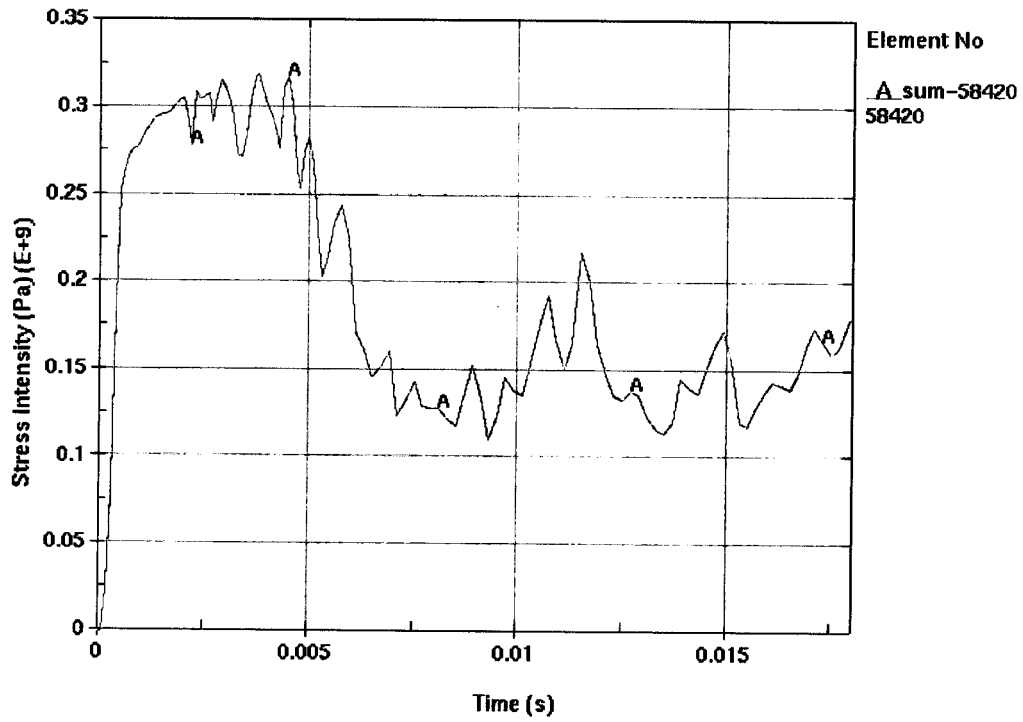


Figure II-8. Stress Intensity Plot for Element No. 58420 of Outer Shell (at $T = 204\text{ }^{\circ}\text{C}$)

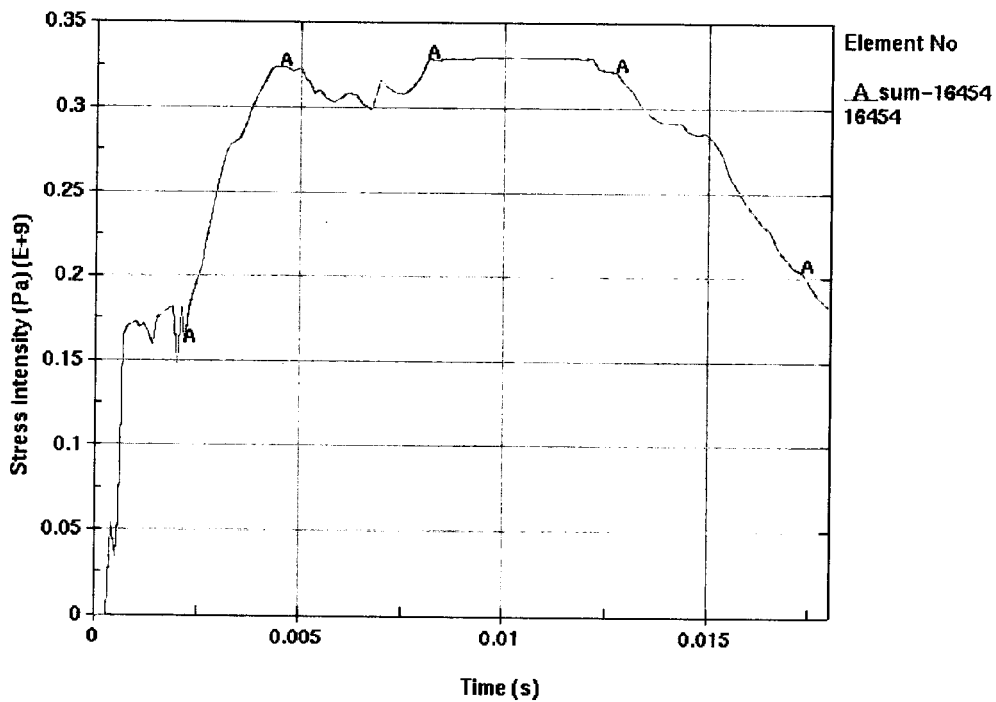


Figure II-9. Stress Intensity Plot for Element No. 16454 of Inner Shell (at $T = 204\text{ }^{\circ}\text{C}$)

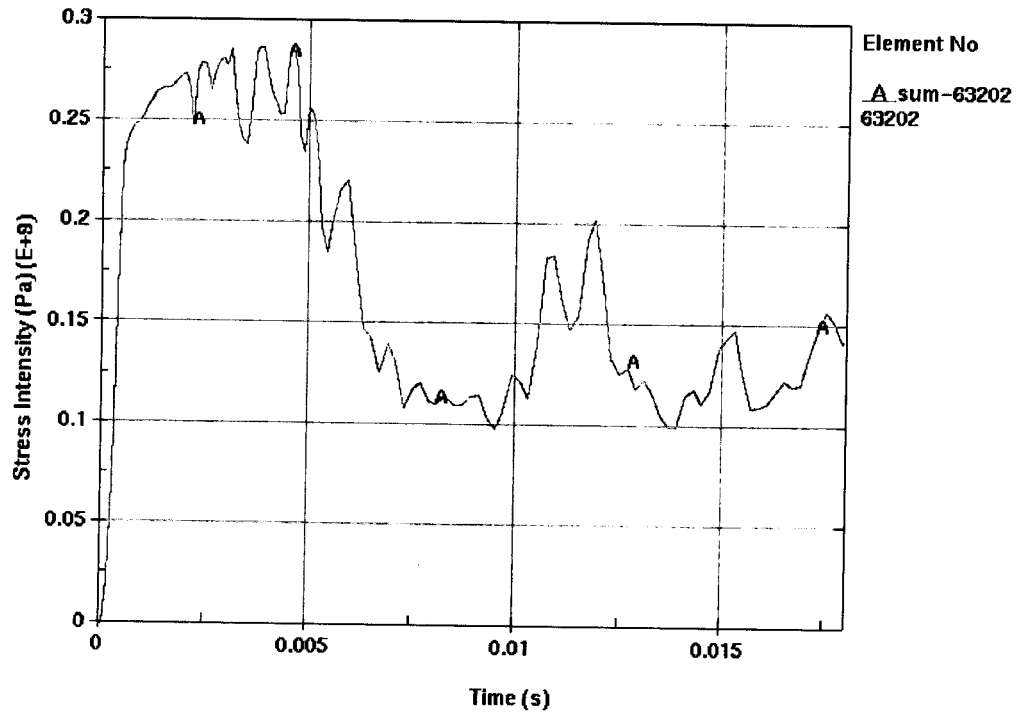


Figure II-10. Stress Intensity Plot for Element No. 63202 of Outer Shell (at $T = 316\text{ }^{\circ}\text{C}$)

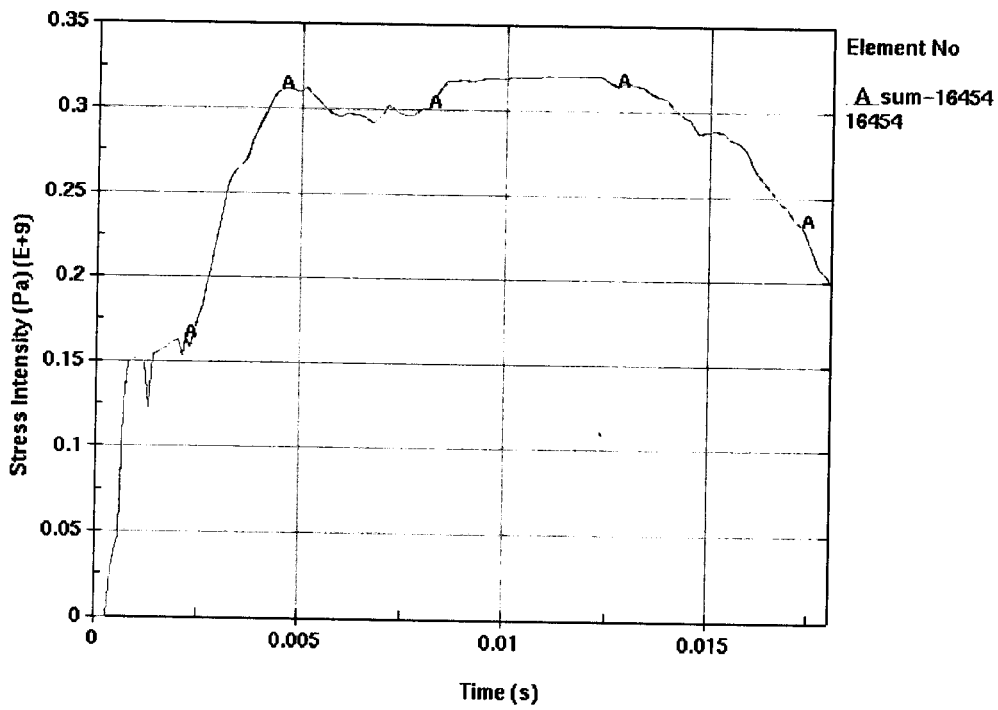


Figure II-11. Stress Intensity Plot for Element No. 16454 of Inner Shell (at $T = 316\text{ }^{\circ}\text{C}$)

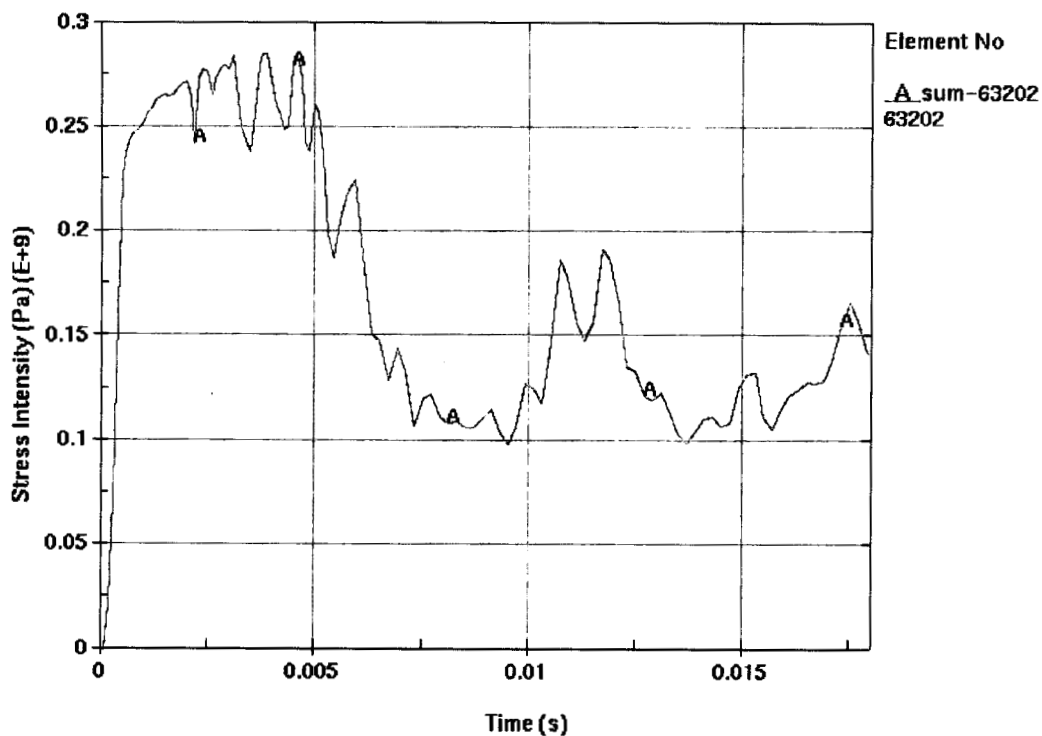


Figure II-12. Stress Intensity Plot for Element No. 63202 of Outer Shell for Temperature-Modified Elongation (at $T = 316\text{ }^{\circ}\text{C}$)

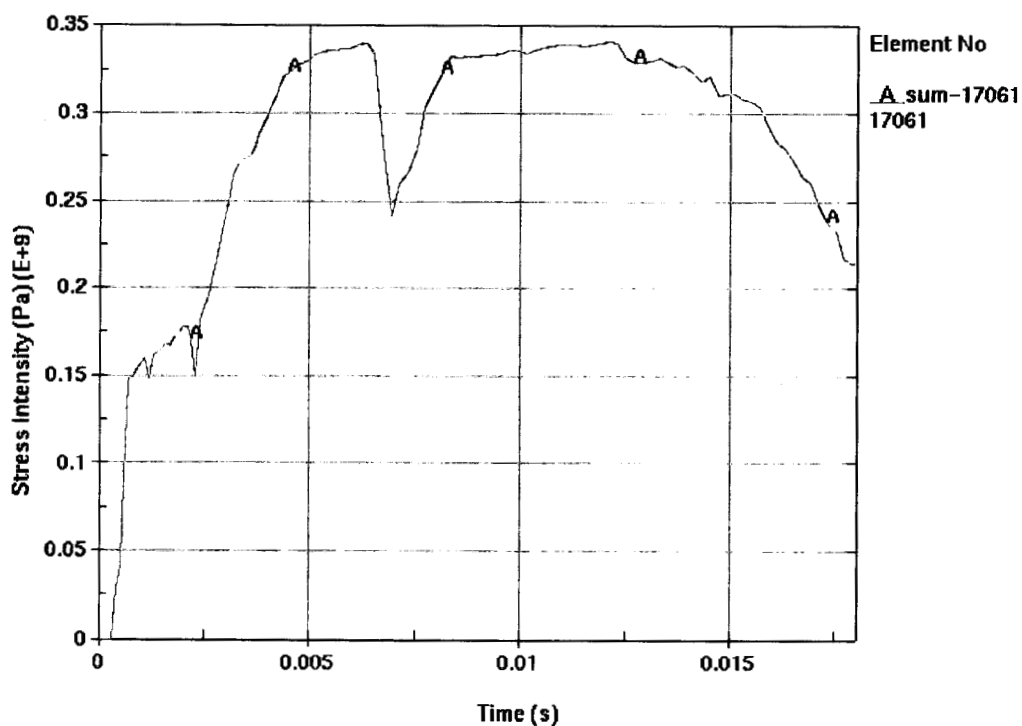


Figure II-13. Stress Intensity Plot for Element No. 17061 of Inner Shell for Temperature-Modified Elongation (at $T = 316\text{ }^{\circ}\text{C}$)

OFFICE OF CIVILIAN RADIOACTIVE WASTE MANAGEMENT
SPECIAL INSTRUCTION SHEET
Complete Only Applicable Items

1. QA: QA
Page: 1 of: 1

DR 2-21-01
MJC

This is a placeholder page for records that cannot be scanned or microfilmed

2. Record Date 01/29/2001	3. Accession Number <i>ATT-TO MOL. 20010220.0060</i>
4. Author Name(s) SRETEN MASTILOVIC	5. Author Organization N/A
6. Title VERTICAL DROP OF 21-PWR WASTE PACKAGE ON UNYIELDING SURFACE	
7. Document Number(s) CAL-UDC-ME-000012	8. Version 00
9. Document Type DATA	10. Medium CD-ROM
11. Access Control Code PUB	
12. Traceability Designator DC # 27043	

13. Comments *SPECIAL PROCESS*
~~THIS IS A ONE-OF-A-KIND DOCUMENT DUE TO THE CD-ROM ENCLOSED AS PART OF ATTACHMENT 1, AND CAN BE LOCATED THROUGH THE RPC~~ *(AB) 02-22-01*

NOTE: SEE ATTACHMENT OF ELECTRONIC SOURCE FILE VERIFICATION FORM PER AP-17.1Q/ICN 3, SECTION 5.1 (C), ELECTRONIC RECORDS.